Doxorubicin-induced vascular toxicity: Investigating the underlying mechanisms and its temporal relationship to cardiotoxicity

Proefschrift voorgelegd tot het behalen van de graad van doctor in de medische wetenschappen aan de Universiteit Antwerpen te verdedigen door:

Matthias BOSMAN

Promotoren
Prof. Dr. Pieter-Jan Guns
Prof. Dr. Emeline Van Craenenbroeck

Universiteit Antwerpen

Universiteit Antwerpen
Faculteit Geneeskunde en Gezondheidswetenschappen

Antwerpen, 2023

Cover and chapter front design by **Jannes De Koning,**
linkedin.com/in/jannes-de-koning-9b207b224

Book design and printing by **Ridderprint, www.ridderprint.nl**

The research described in the present doctoral dissertation was primarily performed at the Laboratory of Physiopharmacology at the University of Antwerp (Belgium). Proteomics experiments and clinical validation of SERPINA3 and THBS1 were conducted at Maastricht University (the Netherlands) and OLV Hospital Aalst (Belgium), respectively. This work was supported by the Fund for Scientific Research (FWO) Flanders to whom Matthias Bosman is predoctoral fellow (grant number: 1S33720N). Furthermore, the research is supported by a DOCPRO4 grant (BOF UAntwerp ID: 39984) and by the INSPIRE project, which has received funding from the European Union's Horizon 2020 Research and Innovation Program (H2020-MSCA-ITN program, Grant Agreement: No858070).

Doxorubicin-induced vascular toxicity: Investigating the underlying mechanisms and its temporal relationship to cardiotoxicity

Doxorubicine-geïnduceerde vasculaire toxiciteit: Het onderzoeken van de onderliggende mechanismen en de tijdsrelatie tot cardiotoxiciteit

Proefschrift voorgelegd tot het behalen van de graad van doctor in de medische wetenschappen aan de Universiteit Antwerpen te verdedigen door:

Matthias BOSMAN

Promotors:

Prof. Pieter-Jan D.F. Guns, Pharm.D.; Ph.D. &

Prof. Emeline M. Van Craenenbroeck, M.D.; Ph.D.

Members of the jury

Prof. An Wouters, Ph.D. (Chair of the jury)
Centre for Oncological Research (CORE) – University of Antwerp, Belgium

Prof. Aline Verstraeten, Ph.D. (Member)
Research Group Medical Genetics (MEDGEN) – University of Antwerp, Belgium

Prof. Pieter-Jan Guns, Pharm.D.; Ph.D. (Promotor)
Laboratory of Physiopharmacology (PHYSPHAR) – University of Antwerp, Belgium

Prof. Emeline Van Craenenbroeck, M.D.; Ph.D. (Promotor)
Research Group Cardiovascular Diseases (CARDIOVASC) – University of Antwerp, Belgium; Antwerp University Hospital, Belgium

Prof. Lucas Van Aelst, M.D.; Ph.D. (Member)
Department of Cardiology – KU Leuven, Belgium; University Hospital Leuven, Belgium

Prof. Volker Adams, Ph.D. (Member)
Research Group Experimental & Molecular Cardiology – Technical University of Dresden, Germany

Table of Content

CHAPTER I

General introduction

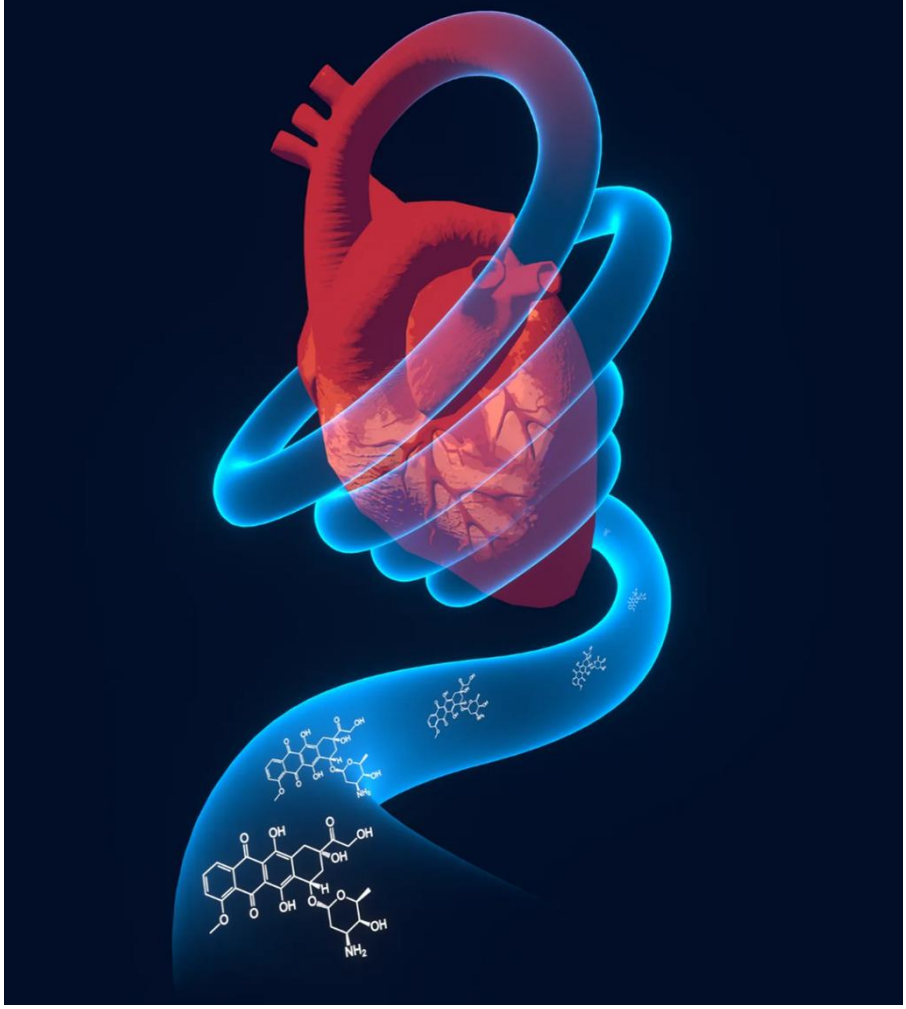

Over the course of the last decades, the discovery and development of novel anticancer therapies has substantially improved cancer patient survival [1]. In the USA alone for example, 17 million cancer patients survived in 2019, and it is projected that this number will grow to more than 22 million by the start of 2030 [2]. However, concomitant to the improved life expectancy, epidemiological data in cancer survivors reveal a higher incidence of hypertension [3], heart failure [4], stroke [5], cognitive impairment [6] and chronic kidney disease [7], contributing to overall patient mortality. Strikingly, childhood and adolescent cancer survivors show a 7-fold higher risk to die from cardiovascular disease compared to the general population [8]. Moreover, in 10-year adult breast cancer survivors, the risk for cardiovascular disease-related mortality even overtakes the likelihood to die from cancer [9]. It is therefore expected that the burden of cardiovascular disease in cancer survivors will continue to increase in the next decades, posing alarming prognostic and economic repercussions.

While continuously improving anticancer drugs have established a larger population of ageing survivors where cardiovascular events are relatively more common, the adverse impact of anticancer therapy itself on cardiovascular health cannot be disregarded. Growing, compelling evidence indicates that a broad spectrum of anticancer drugs directly contribute to cardiovascular disease [10, 11]. This recognition has led to the establishment of a multidisciplinary field called “cardio-oncology” that aims to understand the impact of anticancer therapy on the cardiovascular system, identify patients at risk early-on and introduce preventive management strategies [12].

1.1) Doxorubicin: a first-line anticancer agent despite cardiotoxic side effects

Among anticancer agents, the anthracycline doxorubicin (DOX) represents a chemotherapeutic drug that has gained substantial research attention in the field of cardio-oncology [13]. Originally discovered in the 1960's and isolated from *Streptomyces peucetius* and *Streptomyces caesius*, it is estimated that one third of breast cancer patients and more than half of lymphoma and childhood cancer patients receive a DOX-based treatment regimen today [14], placing this chemotherapeutic agent as a first-line and highly efficacious anticancer drug in the current oncology setting. However, despite its high efficacy in cancer treatment, DOX has been shown to provoke cardiotoxic side effects [13]. In fact, the incidence of left ventricular dysfunction has been estimated to be 3-5%, 7-26% and 18-48% for cumulative DOX doses of 400, 550 and 700 mg/m^2, respectively [15], yet also lower doses (100-300 mg/m^2) have been reported to provoke (subclinical) cardiotoxicity in patients, especially in children [16, 17]. The 2022 European Society of Cardiology (ESC) guidelines on cardio-oncology grade DOX-induced cardiotoxicity into three categories: (I) mild (i.e. left ventricular ejection fraction (LVEF) $\geq$ 50% but rise in cardiac damage biomarkers troponin and (N-terminal pro-)B-type natriuretic peptide, (II) moderate (i.e. 10% decline in LVEF to 40-49%), and (III) severe (i.e. LVEF reduction to < 40%) [13].

Given the cornerstone position of DOX in anticancer therapy [14], extensive research in the field of cardio-oncology has been undertaken over the past decades to elucidate the mechanisms involved in DOX-induced cardiotoxicity with the purpose to minimise cardiac risk without compromising its antitumour efficacy.

1.2) Mechanisms underlying doxorubicin-induced cardiotoxicity

In principle, DOX exerts its antitumour action by being converted into a semiquinone structure that forms reactive oxygen species (ROS) in the cellular cytoplasm and mitochondria, thereby causing DNA damage [18]. Additionally, DOX inhibits the DNA repair enzyme topoisomerase-IIα (TOP-IIα), which disrupts cancer cell replication [18]. In both cases, oxidative stress and DNA damage accumulate, eventually leading to cancer cell death [18].

Similar to the situation in cancer cells, DOX can be converted into a quinone moiety in the heart, thereby driving ROS formation and subsequently provoking oxidative damage. This oxidative damage ultimately compromises cardiac function [19, 20]. In more recent years, compelling evidence demonstrates that the ROS hypothesis does not fully account for DOX-induced cardiotoxicity and highlights an important role for topoisomerase-IIβ (TOP-IIβ), an isoform of TOP-IIα, in DOX-induced cardiac dysfunction. More specifically, Lyu et al. have shown that DOX induces DNA breaks in cardiomyocytes *in vitro* in a TOP-IIβ-dependent way [21]. Similarly, Zhang et al. showed that mice with depletion of TOP-IIβ showed no acute nor chronic cardiac injury following DOX exposure [22]. Finally, Jirkovsky et al. found that the antioxidant ADR-925, a metabolite of dexrazoxane (DEXRA), did not prevent cardiac dysfunction during DOX treatment in mice whereas the parent compound DEXRA itself effectively mitigated cardiotoxicity by depleting TOP-IIβ [23].

Apart from ROS and TOP-IIβ, DOX-induced cardiac dysfunction has also been ascribed to the formation of a so-called "senescence-associated secretory phenotype" (SASP) in cardiomyocytes [24]. Under these conditions, cardiomyocytes exhibit an active, metabolic and pro-inflammatory state where cytokines, proteases and growth factors are produced and released. Such SASP profile has been associated with abnormal patterns of troponin phosphorylation, leading to inefficient cardiac contraction, and has been particularly observed at low DOX doses [24, 25].

Collectively, DOX-induced cardiotoxicity results, at least in part, from ROS formation, TOP-IIβ inhibition and inflammatory responses. This is schematically illustrated in Figure 1.1.

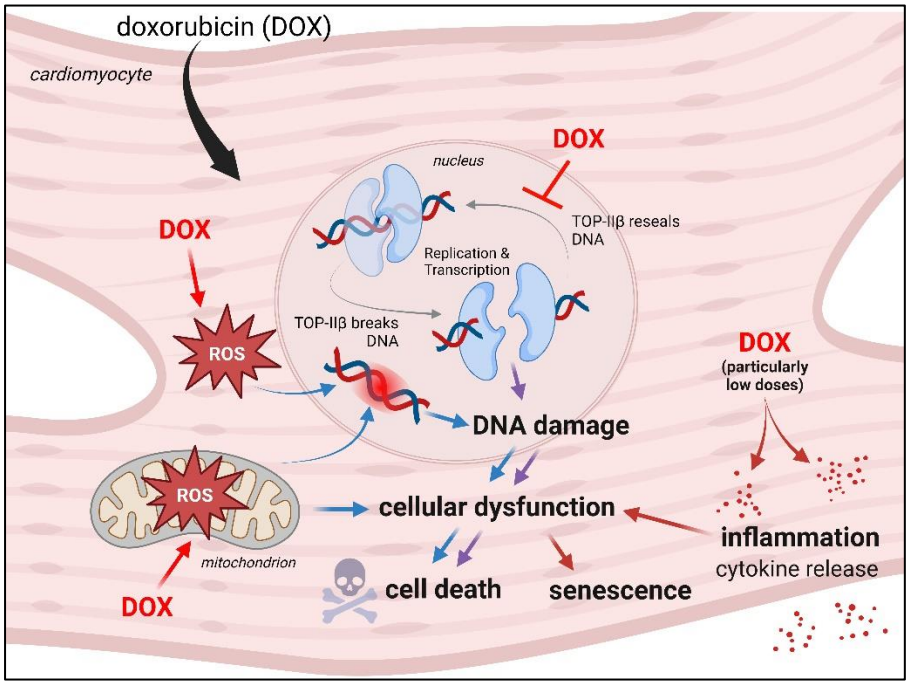

Figure 1.1: Key mechanisms underlying DOX-induced cardiotoxicity. *DOX treatment leads to formation of ROS, inhibition of TOP-IIβ and inflammation, which all adversely impact cardiac function.*

1.3) Current unmet clinical needs for doxorubicin-induced cardiotoxicity

Rapidly evolving ESC guidelines on cardio-oncology provide both oncologist and cardiologist with recommendations for management of DOX therapy-related cardiotoxicity [13]. For all patients, current guidelines advise evaluating cardiac function with echocardiography before commencing DOX treatment and within 12 months after therapy completion [13]. For patients at high cardiac risk (i.e. patients with prior history of cardiovascular disease), it is recommended to monitor cardiac function with echocardiography at baseline, every two treatment cycles and within 3 months after therapy completion, complemented by assessment of circulatory cardiotoxicity biomarkers, such as troponin and (N-terminal pro-)B-type natriuretic peptide [13]. Despite commendable effort, **the following major challenges remain**:

1. **Early detection of cardiac damage**: DOX-induced cardiotoxicity may not present with any noticeable symptoms until an advanced, symptomatic stage is reached. Early identification of (subclinical) cardiotoxicity is therefore paramount before it becomes symptomatic and/or irreversible.

2. **Identifying "at risk" patients**: Not every DOX-treated patient experiences cardiovascular complications. Moreover, some patients develop cardiac dysfunction years after DOX therapy completion whereas other subjects show acute impaired cardiac function. As such, it is important to improve cardiotoxicity risk stratification during and after DOX treatment, which requires a complete overview of lifestyle patient characteristics, investigation of possible genetic predisposition and a

broadening of the functional and molecular diagnostic biomarker panel.

3. **Developing effective cardioprotective strategies**: Further study is required to develop therapeutic drugs or strategies that prevent, or at least mitigate, DOX-induced cardiotoxicity.

1.4) Apart from cardiotoxicity, doxorubicin induces vascular toxicity

Apart from cardiotoxicity, DOX has been shown to induce vascular toxicity as well. In fact, epidemiological data in childhood cancer survivors reveal a higher incidence of systemic hypertension and coronary artery disease compared to control siblings, years after anthracycline therapy completion [26]. Moreover, DOX has been shown to increase arterial stiffness and endothelial dysfunction in patients [27-32]. On average, DOX-treated patients show a 1.2-fold increase in pulse-wave velocity (PWV), the clinical gold-standard measure of arterial stiffness, and a 2- to 4-fold decrease in endothelium-dependent flow-mediated vasodilation (i.e. endothelial dysfunction), typically within 1 to 6 months of treatment (cumulative dose 50-400 mg/m^2) [27-32]. In the next paragraphs, we elaborate on "arterial stiffness" and "endothelial dysfunction".

What is "arterial stiffness"?

Under physiological conditions, the heart ejects blood from the left ventricle into the aorta at high velocity. Upon ejection, the aorta distends during systole and subsequently recoils during diastole. The aortic distension mitigates the increase in pressure resulting from blood ejection, thereby preventing excessive pressure from damaging more distal blood vessels [33], while gradual elastic recoil further supports blood flow [34]. This process is primarily facilitated by the passive

vascular wall components collagen and elastin, which provide tensile strength and flexibility, respectively.

With ageing, the dampening capacity of the aorta attenuates, at least in part, due to ROS-mediated overproduction of collagen [35, 36], collagen cross-linking [37, 38] and elastin degradation [35, 36], ultimately resulting in less compliant or "stiffer" arteries [39-41]. This decline in arterial compliance is typically referred to as "arterial stiffness".

What is "endothelial dysfunction"?

Although passive components, like collagen and elastin, play an important role in large artery compliance, arterial stiffness is also modulated by active elements [42, 43]. The endothelial monolayer fulfils a crucial role in this regard. Specifically, in endothelial cells (ECs), endothelial nitric oxide synthase (eNOS) produces nitric oxide (NO) [44], which diffuses to vascular smooth muscle cells (VSMCs) upon secretion where it promotes vasodilation [42, 43]. When NO production is impeded, vascular tone consequently increases, thereby augmenting arterial stiffness [42, 43].

Decreased NO bio-availability and resulting enhanced vascular tone are important hallmarks of so-called "endothelial dysfunction". However, apart from promoting vasodilation, NO exerts anti-inflammatory effects as well [45]. In the case of lower NO levels, the endothelium thus displays also an "activated" state, characterised by a pro-inflammatory and pro-coagulatory environment [46]. This inflammatory state is a characteristic hallmark of endothelial dysfunction as well [46]. Endothelial dysfunction therefore encompasses both altered vascular tone and endothelial inflammation.

Based on the location of endothelial dysfunction in the vasculature, a distinction can be made between "micro

endothelial dysfunction", i.e. endothelial dysfunction in the microvasculature, and "macro endothelial dysfunction", i.e. endothelial dysfunction in large elastic arteries.

1.5) Arterial stiffness and endothelial dysfunction are associated with increased risk for cardiovascular events in the general population

Interestingly, in the general population, enhanced arterial stiffness and endothelial dysfunction have previously been shown to independently predict future cardiovascular events, and have been demonstrated to play an important initiating role in systemic hypertension, coronary artery disease and heart failure [47-52]. Here, we discuss how these parameters contribute to cardiovascular disease.

As mentioned above, the aorta fulfils a crucial role in mitigating the increase in pulse pressure resulting from left ventricular blood ejection [33]. In the case of arterial stiffness, this dampening capacity is impeded, which leads to continuous augmented pressure [39-41]. Persistently increased pressure can result in systemic hypertension and/or damage end-organs, such as the heart, brain and kidneys, thereby increasing the risk for cardiac, brain and kidney disease [53-55].

With regards to how endothelial dysfunction contributes to cardiovascular disease, micro endothelial dysfunction in small resistance arteries enhances, at least in part, blood flow and blood pressure [56, 57]. When persistent in nature, elevated blood pressure leads to systemic hypertension [58]. Furthermore, micro endothelial dysfunction in the coronary vasculature promotes inflammation-based platelet adherence and leukocyte infiltration, an important hallmark of early atherosclerotic plaque formation [59]. Excessive plaque build-up in coronary microvessels leads to coronary heart disease where blood vessels become narrow and blood flow and oxygen supply to the heart is limited [59].

Macro endothelial dysfunction in large elastic arteries is accompanied by decreased arterial distensibility and compliance over time [39, 43], leading to arterial stiffness, which, as mentioned above, poses risk for heart failure, dementia and renal disease [53-55]. When macro endothelial function is impaired in the carotid and peripheral arteries, atherosclerotic plaque formation is enhanced, thereby reducing blood vessel diameter, which can lead to peripheral artery disease and/or ischemic stroke [59].

1.6) Doxorubicin-induced arterial stiffness and endothelial dysfunction: Are they contributors to and predictors of future cardiotoxicity?

Given that arterial stiffness and endothelial dysfunction represent early contributors to cardiovascular disease [47-52], and since these representations of vascular toxicity manifest during DOX therapy [27-32], it is conceivable that arterial stiffness and endothelial dysfunction possibly precede and potentiate cardiovascular disease in DOX-treated patients. Hence, the present **doctoral dissertation hypothesised** that:

1. **DOX-induced arterial stiffness and endothelial dysfunction contribute to cardiotoxicity, systemic hypertension and atherosclerosis.**
2. **Arterial stiffness and endothelial dysfunction precede cardiotoxicity and could thus serve as early, functional markers to identify DOX-treated patients at risk.**

A schematic overview of the rationale for these main hypotheses is illustrated in Figure 1.2.

If DOX-induced arterial stiffness and endothelial dysfunction contribute to cardiovascular disease, it is important to comprehend the underlying mechanisms to allow timely (therapeutic) intervention. However, at present, it remains poorly

understood how arterial stiffness and endothelial dysfunction develop in DOX-treated patients. While preclinical work suggests that low DOX doses induce endothelial dysfunction [60] and high doses provoke vascular inflammation and remodelling [61], it remains unclear whether arterial stiffness in DOX-treated patients is caused by altered vascular tone or structural changes. Furthermore, the direct impact of DOX on VSMCs, and how this influences arterial stiffness remains debatable as well. For example, DOX has been shown to stimulate Ca^{2+}-release from the sarcoplasmic reticulum and Ca^{2+}-entry in VSMCs that result in increased VSMC contraction [62], yet the opposite has been reported as well, that is, that DOX decreases VSMC contraction through attenuating Ca^{2+}-release and -entry [63, 64]. Finally, although inhibition of TOP-IIβ constitutes an important mechanism involved in DOX-induced cardiotoxicity [19, 20, 23], it remains to be elucidated whether TOP-IIβ is also involved in DOX-induced vascular toxicity.

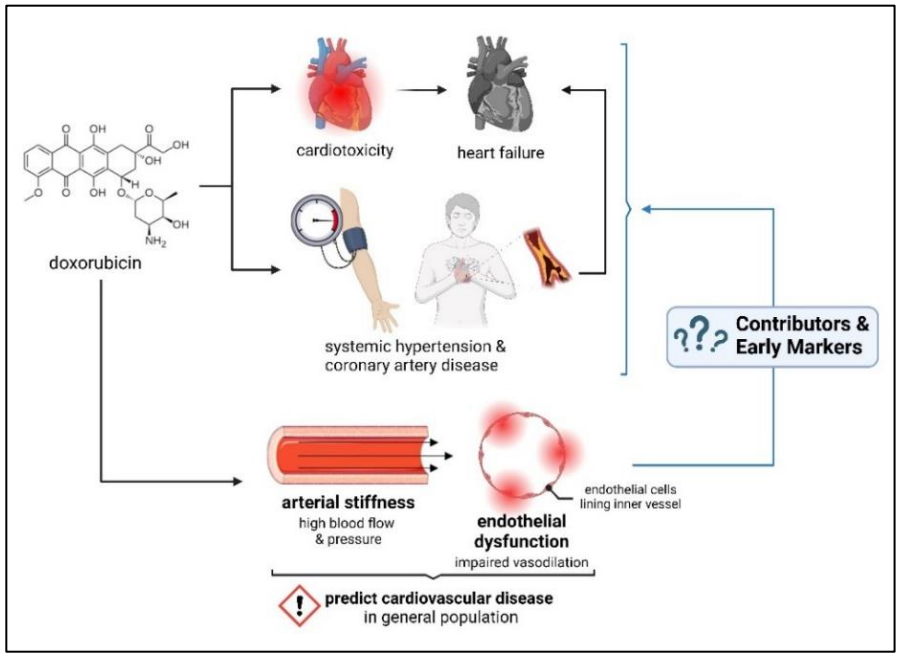

Figure 1.2: Rationale for the main research hypotheses of the present doctoral dissertation.

CHAPTER II

Aims of the doctoral dissertation

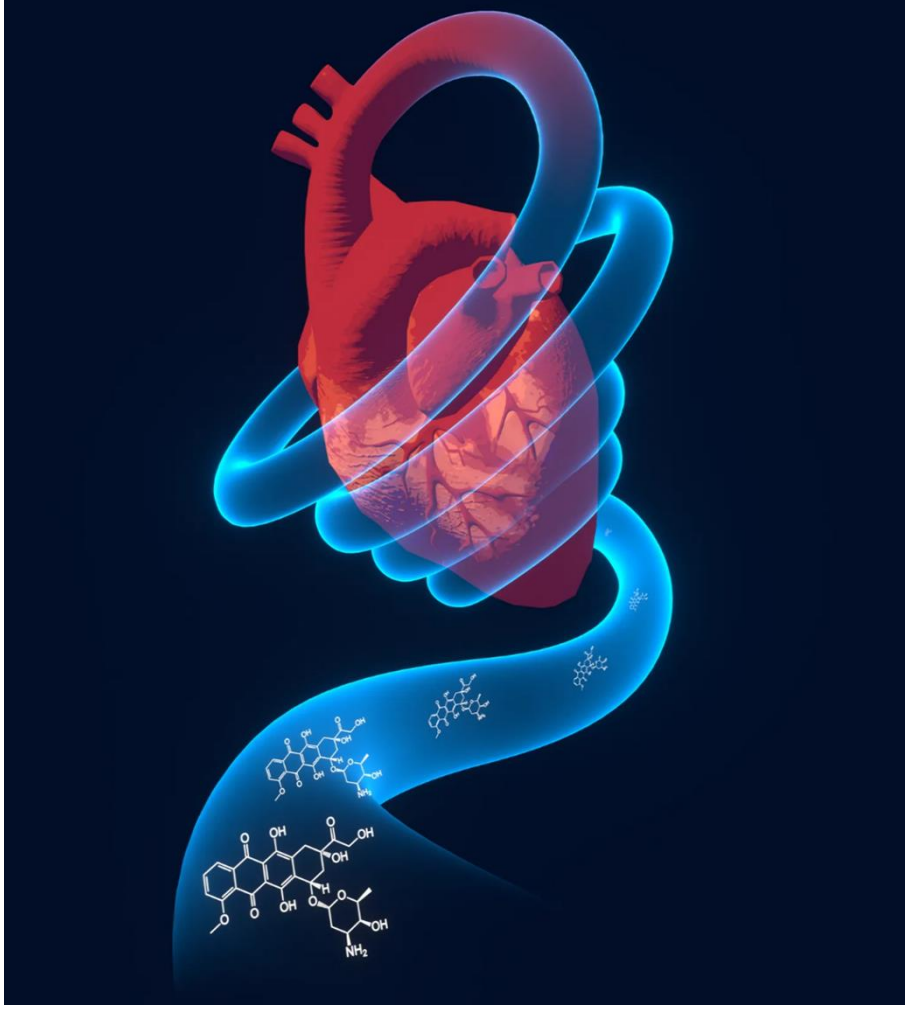

To address the research gaps concerning DOX-induced vascular toxicity, **this doctoral dissertation aimed to**:

1. **Delineate the mechanisms of DOX-induced arterial stiffness in a preclinical model**

In order to delineate the mechanisms involved in DOX-induced arterial stiffness, we first aimed to **establish a preclinical, murine model.**

In preclinical research, DOX is administered either as a single (high) bolus of 20-25 mg/kg that is associated with a severe decline in left ventricular ejection fraction (LVEF) [65, 66], or with repeated lower doses (5 mg/kg) over time [22]. To avoid the impact of impaired left ventricular systolic function on arterial stiffness, we specifically aimed to use a DOX dose and treatment regimen that would not result in severe cardiotoxicity. Based on a study by Zhang et al. that reported a 10% decrease in LVEF after 5 weeks of DOX treatment (5 mg/kg/week) [22], we chose a DOX dose of 4 mg/kg to be administered once per week.

After establishing a preclinical DOX model, we subsequently **investigated** the **mechanisms underlying DOX-induced arterial stiffness**. This new mechanistic insight is discussed in **Chapter III**.

2. **Investigate the impact of DOX on VSMC reactivity**

Since conflicting findings have been reported regarding the role of DOX in VSMC function alteration [62-64], we **hypothesised** that the **effects of DOX on modulation of VSMC function depend on the dose or treatment protocol**. To test this hypothesis, VSMC reactivity was evaluated 16 hours after DOX administration, and these data were compared to our vascular reactivity results reported in Chapter III. The findings of this study are discussed in **Chapter IV**.

3. **Determine the contribution of TOP-IIβ to DOX-induced vascular toxicity and discern the possible protective capability of DEXRA hereto**

In an *ex vivo* DOX model of acute vascular toxicity, the **contribution of TOP-IIβ to DOX-induced vascular toxicity was determined in Chapter V**. In addition, the potential **protective effect** of **DEXRA** hereto was discerned.

4. **Evaluate arterial stiffness and endothelial dysfunction as possible early markers for and contributors to DOX-induced cardiotoxicity, complemented by a proteomics approach**

The temporal relationship between DOX-induced arterial stiffness, endothelial dysfunction and cardiotoxicity has not been characterised. It also remains unclear whether vascular toxicity is reversible after therapy cessation. Finally, contemporary biomarkers, such as circulating troponin and (N-terminal pro-)B-type natriuretic peptide prove insufficient to detect early cardiac damage in every DOX-treated patient [67, 68]. Hence, a broadening of the biomarker panel is recommended.

In order to evaluate arterial stiffness and endothelial dysfunction as potential early markers for cardiotoxicity, we characterised the time-course of DOX-induced cardiovascular toxicity by assessing arterial stiffness, endothelial function and cardiac function during and after DOX therapy. In addition, a **proteomics approach** was implemented to **identify new potential biomarkers**, which were further **clinically validated.** Finally, we **elucidated** whether **DOX-induced arterial stiffness and endothelial dysfunction contribute to cardiac dysfunction** and **systemic hypertension**. The findings of this study are discussed in **Chapter VI**.

5. **Assess the impact of DOX on atherosclerotic plaque formation.**

Although a higher incidence of coronary artery disease has been reported in DOX-treated cancer survivors [26], it remains unclear whether DOX, and more specifically DOX-induced arterial stiffness and endothelial dysfunction, directly accelerate or exacerbate atherosclerotic plaque formation.

In **Chapter VII**, the **impact of DOX** on **atherosclerosis** is **assessed** in apolipoprotein-E deficient (**ApoE**$^{-/-}$) mice that were fed a high-fat diet.

The aims of this doctoral dissertation are schematically summarised in Figure 2.1.

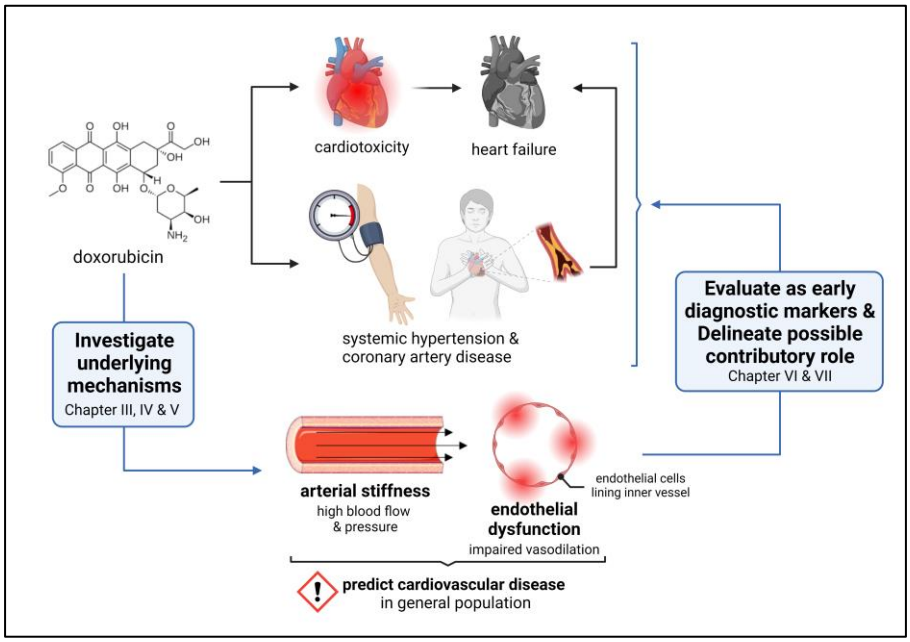

Figure 2.1: Research aims of the present doctoral dissertation.

CHAPTER III

Doxorubicin-induced arterial stiffness is driven by endothelial dysfunction-mediated enhancement of vascular tone

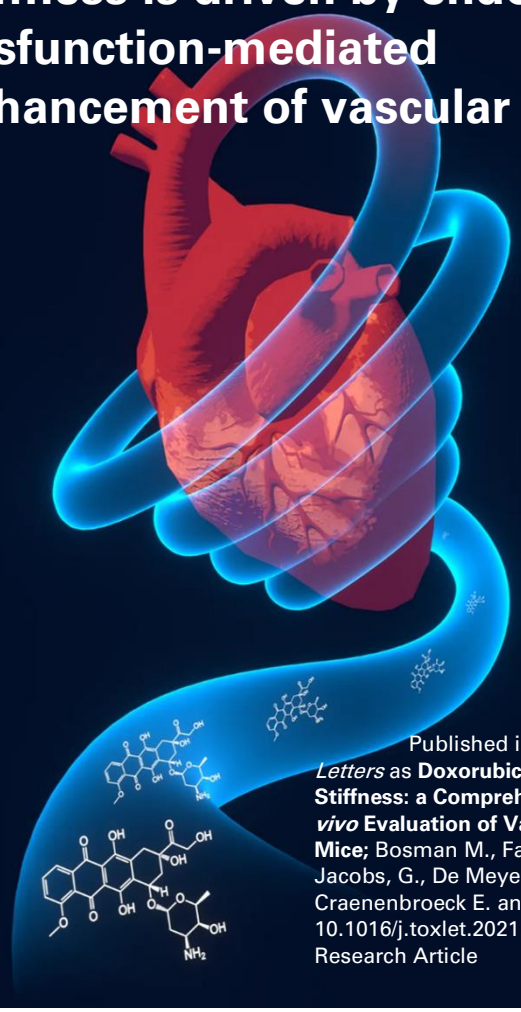

Published in 2021 in *Toxicology Letters* as **Doxorubicin Induces Arterial Stiffness: a Comprehensive *in vivo* and *ex vivo* Evaluation of Vascular Toxicity in Mice;** Bosman M., Favere K., Neutel C., Jacobs, G., De Meyer G., Martinet W., Van Craenenbroeck E. and Guns P.-J.; DOI: 10.1016/j.toxlet.2021.04.015; Original Research Article

Abstract

Arterial stiffness is an important predictor of cardiovascular risk. Clinical studies have demonstrated that arterial stiffness increases in cancer patients treated with the chemotherapeutic doxorubicin (DOX). However, the mechanisms of DOX-induced arterial stiffness remain largely unknown. This study aimed to evaluate artery stiffening in DOX-treated mice using *in vivo* and *ex vivo* techniques. Male C57BL/6J mice were treated for 2 weeks with 2 mg/kg (low dose) or 4 mg/kg (high dose) of DOX weekly. Arterial stiffness was assessed *in vivo* with ultrasound imaging (abdominal aorta pulse wave velocity (aaPWV)) and applanation tonometry (carotid-femoral PWV) combined with *ex vivo* vascular stiffness and reactivity evaluation. The high dose increased aaPWV, while cfPWV did not reach statistical significance. Phenylephrine (PE)-contracted aortic segments showed a higher Peterson's modulus (Ep) in the high dose group, while Ep did not differ when vascular smooth muscle cells (VSMCs) were relaxed by a NO donor (DEANO). In addition, aortic rings of DOX-treated mice showed increased PE contraction, decreased basal nitric oxide (NO) index and impaired acetylcholine-induced endothelium-dependent relaxation. DOX treatment contributed to endothelial cell loss and reduced endothelial nitric oxide synthase (eNOS) expression in the aorta. In conclusion, we have replicated DOX-induced arterial stiffness in a murine model and this aortic stiffness is driven by impaired endothelial function, contributing to increased vascular tone.

3.1) Introduction

Large artery stiffening is an important feature in the process of vascular ageing [33, 69]. Under physiological conditions, the heart ejects blood from the left ventricle into the aorta at high velocity [33]. The distensibility of the aorta during systole will mitigate the increase in aortic pressure, while the elastic recoil during diastole supports blood flow [34, 70, 71]. In contrast, arterial stiffening impairs the dampening capacity of the aorta, which, in turn, leads to increased afterload on the heart and increased pulsatility in highly perfused organs, such as the kidneys, brain and heart, potentially damaging them [40]. In previous studies, stiffening of the aorta has been associated with increased risk of developing coronary artery disease, atrial fibrillation, stroke and heart failure [72-74]. Hence, arterial stiffness, measured non-invasively by pulse wave velocity (PWV), is an early and predictive marker of future cardiovascular events [75].

For a long time, research has mainly focussed on structural changes contributing to arterial stiffness, such as the balance between collagen synthesis and elastin degradation within the vascular wall [76-78]. Although structural remodelling is an important contributor to vascular ageing, there is emerging evidence that artery stiffening is regulated by active components as well. More specifically, endothelial cells (ECs) and vascular smooth muscle cells (VSMCs) have been reported to contribute to arterial stiffness by dysregulating vascular tone [79, 80]. For example, decreased nitric oxide (NO) bioavailability and elevated contraction are associated with increased aortic stiffness [42, 81]. Therefore, large artery stiffening depends on a delicate, not mutually exclusive, balance between these active and passive elements.

In humans, carotid-femoral pulse wave velocity (cfPWV) assessed by tonometry is the gold-standard method for evaluating arterial stiffness, but in mice ultrasound imaging is more frequently used [82, 83]. Ultrasound imaging offers a local determination of aorta PWV, such as abdominal aorta PWV (aaPWV) [84], while tonometry focusses more on regional determination of PWV [85]. These *in vivo* techniques offer a high translational value, but do not provide insight about the underlying active and passive mechanisms that are involved. In addition, *in vivo* measurements are dependent on heart rate and blood pressure [86]. Therefore, we have established a unique in-house developed organ bath set-up, called the Rodent Oscillatory Tension Set-up to study Arterial Compliance (ROTSAC), to assess arterial stiffness *ex vivo*, independent from confounding factors, such as heart rate and blood pressure [42, 87, 88].

Here, we present a preclinical study investigating arterial stiffness in mice treated with DOX. Dose-dependent cardiotoxicity limits the clinical use of DOX, which has been intensively investigated (reviewed elsewhere) [89], yet the effects on the vascular system have been less considered. Clinical studies have shown increased arterial stiffness after DOX-therapy. Moreover, some childhood cancer survivors show signs of accelerated cardiovascular ageing as well [26, 27, 90, 91]. In murine models, DOX contributes to EC and VSMC dysfunction [63, 64]. More specifically, DOX mediates excessive reactive oxygen species (ROS) production, which might impair NO signalling, thereby disturbing endothelium-dependent vasodilation *ex vivo* [92]. Furthermore, low doses of DOX induce senescence of VSMCs *in vitro*, contributing to vascular damage [93]. However, it remains unclear whether increased arterial stiffness in DOX-treated patients is caused by an altered vascular tone or by structural remodelling. Therefore, the current study aimed to replicate DOX-

induced arterial stiffening in a preclinical murine model and to delineate the mechanisms involved herein.

3.2) Materials & methods

Animals & Ethical approval

24 male C57BL/6J mice (Charles River, France) between an age of 10 and 12 weeks and with a body weight between 26 and 30 g were housed in the animal facility of the University of Antwerp in standard cages with 12-12 hours light-dark cycles with access to regular chow and water *ad libitum*. Male mice were chosen to avoid the influence of female hormone confounding factors. The experiments were approved by the Ethical Committee of the University of Antwerp and were conform to the ARRIVE guidelines and to the Guide for the Care and Use of Laboratory Animals published by the US National Institutes of Health (NIH Publication no.85-23, revised 1996).

DOX treatment and experimental workflow

Mice were randomly divided into three groups: vehicle (n = 8), low dose DOX (2 mg/kg; n = 8) and high dose DOX (4 mg/kg; n = 8). DOX was injected intraperitoneally once per week for a total of two weeks. DOX (Adriamycin®, 2 mg/mL) was diluted in a 0.9% NaCl solution (B. Braun, Belgium) on the day of injection. The vehicle group received an intraperitoneal injection (10 mL/kg) of a 0.9% NaCl solution. Ultrasound imaging was performed before (day -1) and 4, 7 and 11 days after the start of DOX treatment. The time points were selected based on a pilot study where mice were measured daily after treatment with a high dose of DOX (data not shown). Applanation tonometry and blood pressure were evaluated on day 5 and 10, respectively, after starting DOX treatment. Mice were sacrificed between 12 and 13 days after the start of treatment for *ex vivo* measurements with

ROTSAC and organ baths. Supplementary Figure 3.1 provides an overview of the experimental design and workflow.

High-frequency ultrasound imaging

Ultrasound imaging was performed in anaesthetised mice under 1.5 - 2.5% (v/v) isoflurane (Forene; Abbvie, Belgium) using a high-frequency ultrasound system (Vevo2100, VisualSonics). Images were only acquired when heart rate and body temperature met the inclusion criteria, i.e. 550 ± 50 beats/min and 37 ± 1 °C, respectively. M-mode images were obtained for determination of cardiac parameters using a 24-MHz transducer. Left ventricular ejection fraction (LVEF), left ventricular internal diameter (LVID), stroke volume, left ventricular anterior wall (LVAW) and left ventricular posterior wall (LVPW) thickness were subsequently calculated using measurements of three consecutive M-mode cycles with Vevo LAB Software (Version 3.2.0, VisualSonics). In the same session, abdominal aorta PWV (aaPWV) was determined according to the method developed by Di Lascio et al. with a 24-MHz transducer [84]. Briefly, pulse wave Doppler tracing was used to measure aortic flow velocity (V). Immediately thereafter, aortic diameter (D) was measured on 700 frames-per-second B-mode images of the abdominal aorta in EKV imaging mode. The ln(D)-V loop method was then applied to calculate aaPWV, using MathLab v2014 software (MathWorks).

Applanation tonometry

Carotid-femoral PWV (cfPWV) was determined in anaesthetised mice (4 - 6% sevoflurane (v/v) (Sevorane; Abbvie, Belgium), as previously described by our research group [85]. In brief, two pulse tonometers (SPT-301, Millar Instruments) were applied on the skin using a micromanipulator. Carotid–femoral transit time (Δt) was determined using the time difference between the foot of carotid and femoral artery pulses (foot-to-foot method). The foot of the pressure wave was defined as the

second derivative maximum. Fifty consecutive pulses with sufficient amplitude and a reproducible waveform were analysed; pulses that interfered with respiratory movement peaks were excluded.

Blood pressure evaluation

Systolic and diastolic blood pressure were determined at day 10 non-invasively in restrained, awake mice using a tail-cuff system with programmed electrosphygmomanometer (Coda, Kent Scientific Corporation). To reduce stress and variability during the procedure, animals were trained for two days prior to the actual measurements.

***Ex vivo* evaluation of aortic stiffness and vascular reactivity**

Mice were intraperitoneally injected with sodium pentobarbital (75 mg/kg; Sanofi, Belgium), followed by perforation of the diaphragm (when under deep anaesthesia). The thoracic aorta was carefully dissected and cut into six segments of 2 mm length (i.e. TA0 to TA5) with the crossing of the diaphragm as the reference point for the sixth segment (TA5). Next, segments were mounted between two hooks of an *ex vivo* organ bath set-up (10 mL) filled with Krebs Ringer solution (37°C, 95% O2/5% CO2, pH 7.4) containing (in mmol/L): NaCl 118, KCl 4.7, CaCl2 2.5, KH2PO4 1.2, MgSO4 1.2, NaHCO3 25, CaEDTA 0.025, and glucose 11.1.

For ROTSAC: *Ex vivo* assessment of arterial stiffness was performed as previously described [87]. In brief, segments (TA2 and TA3) were continuously stretched between alternating preloads corresponding to "systolic" and "diastolic" transmural pressures and at a physiological frequency of 10 Hz to mimic the physiological heart rate in mice (600 beats/ min). The set-up is calibrated by acquiring photographs of each aorta segment at different tensions (10 to 60 mN), from which the diameter and

width of the segment are determined. Subsequently, these parameter serve as input in the LaPlace's equation to calculate in real-time the "systolic" and "diastolic" pressure and the Peterson's modulus (Ep), a measure for arterial stiffness. Ep was calculated as follows: $Ep = D_0 * \Delta P/\Delta D$ with ΔP = difference in pressure (kept constant at 40 mmHg), D_0 = "diastolic" diameter and ΔD = the change in diameter between "diastolic" and "systolic" pressure.

The ROTSAC protocol included the evaluation of arterial stiffness (Ep) at different pressures (i.e. 60-100, 80-120, 100-140 and 120-160 mmHg). Furthermore, the contribution of VSMC tonus was investigated by adding a high concentration (2 µM) of the α1-adrenergic receptor agonist phenylephrine (PE), while the contribution of ECs was evaluated by blocking endothelial nitric oxide synthase (eNOS) with Nω-nitro-L-arginine methyl ester (L-NAME, 300 µM). Conversely, a high concentration (2 µM) of the NO-donor diethylamine NONOate (DEANO) was added to completely relax VSMCs to remove vascular tonus, which allows the evaluation of passive stiffness of the vessel wall. The detailed protocol for the ROTSAC experiments is provided in Supplementary Figure 3.2.

For organ baths with isometric transducer: aortic segments (TA4 and TA5) were mounted at a preload of 20 mN. Since we have previously shown that basal NO declines over time [94], the experimental protocol was started 70 minutes after puncture of the diaphragm to minimise time-dependent biases. VSMC contraction was evaluated by adding cumulative concentrations of PE (3 nM – 10 µM). Additionally, the basal NO index was calculated as follows: PE was first added to induce VSMC contraction (PE contraction). Once the contraction was stable, the eNOS blocker L-NAME (PE + L-NAME contraction) was subsequently added, further increasing contraction. By substracting the PE contraction from the PE + L-NAME

contraction, the amount of contraction that is solely due to L-NAME (eNOS inhibition) can be acquired, which provides an estimate of basal NO. Endothelium-dependent relaxation was investigated by addition of cumulative concentrations of acetylcholine (ACh), a muscarinic receptor agonist. The involvement of Ca^{2+}-channels was determined by adding a single, high concentration (35 µM) of diltiazem, a voltage-gated Ca^{2+}-channel blocker. The detailed protocol for the organ bath experiments and the method for basal NO index calculation is illustrated in Supplementary Figure 3.3.

Chemical compounds

DOX (Adriamycin®, 2 mg/mL) was purchased from Pfizer (Belgium). PE, L-NAME, ACh, DEANO and diltiazem were purchased from Sigma-Aldrich (Belgium).

Histology

Aortic segments were fixed in 4% formalin for 24 h, dehydrated overnight in 60% isopropanol and then embedded in paraffin. Transversal sections were stained with orcein or immunohistochemically stained with a primary antibody against collagen type I (1:500; ab21286, Abcam) to determine elastin and collagen type I content, respectively. The EC layer continuity was evaluated with immunohistochemical staining with a primary antibody against CD31 (1:100; D8V9E, Cell Signalling Technology) and visualised with EnVision+ (Dako). Images were acquired with Universal Graph 6.1 software using an Olympus BX40 microscope and quantified with ImageJ software. Elastin and collagen type I content were quantified by calculating the signal-to-wall area ratio (expressed as percentage). CD31 was quantified by determining the length of CD31 positive cells along the luminal border divided by the total aortic lumen circumference (expressed as percentage).

Western blotting

Aortic samples were lysed in Laemmli sample buffer (Bio-Rad) containing 5% β-mercaptoethanol (Sigma-Aldrich) and subsequently heat-denatured for 5 minutes at 100 °C. Next, samples were loaded on Bolt 4–12% Bis-Tris gels (Invitrogen) and after electrophoresis transferred to Immobilon-FL PVDF membranes (Millipore) according to standard procedures. Thereafter, membranes were immediately blocked for 1 hour in Odyssey Li-COR blocking buffer. After blocking, membranes were probed with primary antibodies, diluted in Odyssey Li-COR blocking buffer, overnight at 4 °C. The following primary antibodies were used: mouse anti-eNOS (1:500; ab76198, Abcam) and mouse anti-β-actin (1:5000; ab8226, Abcam). The next day, membranes were incubated with IRDye-labeled secondary antibodies (goat anti-rabbit IgG926-32211; goat anti-mouse IgG926-68070, both purchased from Li-COR Biosciences) for 1 hour at room temperature. Membranes were visualised with an Odyssey SA infrared imaging system (Li-COR Biosciences). Western blot data was quantified using ImageJ software. Signal intensity of the protein of interest (eNOS) was normalised to the β-actin signal intensity and expressed as the fold change (compared to vehicle).

Statistical analysis

All results were expressed as the mean ± standard error of the mean (SEM). Statistical analyses were performed using GraphPad Software (Prism 8 - Version 8.4.2, Graphpad, USA). Repeated measures two-way ANOVA, one-way ANOVA and Kruskal-Wallis tests were performed for comparison between groups. A Dunnett's post hoc test was used to correct for multiple comparisons. A Bland-Altman plot was used to evaluate concordance between aaPWV (day 4 and 7) and cfPWV (day 5)

values. A p-value < 0.05 was considered to be statistically significant.

3.3) Results

Doxorubicin (high dose) increased aaPWV *in vivo*

A significant and consistent increase in aaPWV was observed for the high dose group at 4, 7 and 11 days after the start of DOX treatment (Figure 3.1A). More specifically, at 4, 7 and 11 days, aaPWV was 5.67 ± 0.32 m/s, 5.36 ± 0.30 m/s and 5.03 ± 0.25 m/s in the high dose group compared to 4.36 ± 0.31 m/s, 4.00 ± 0.24 m/s and 4.13 ± 0.20 m/s in the vehicle group, respectively (Figure 3.1A). LVEF did not differ among treatment groups (Figure 3.1B). Additional evaluated cardiovascular parameters, including LVAW, LVID, LVPW, stroke volume, heart mass and body weight (measured at day 11) are provided in Table 3.1. These parameters did not change between the different treatment groups after DOX treatment (Table 3.1), except pulse pressure. Pulse pressure, the difference between systolic and diastolic blood pressure, was significantly elevated in the high dose group (Table 3.1).

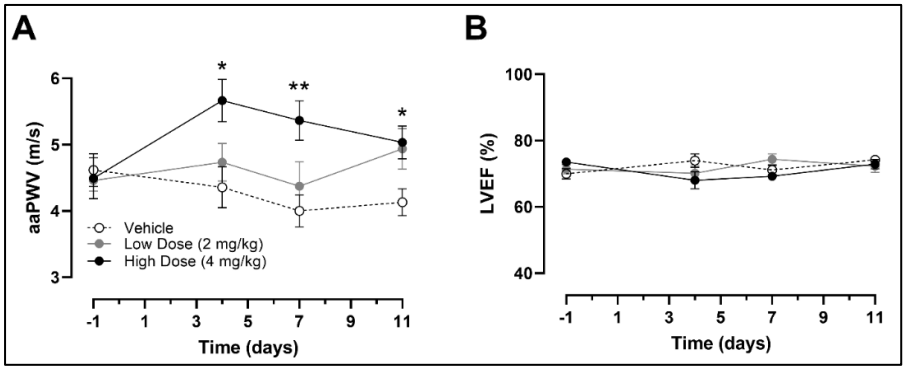

Figure 3.1: In vivo measurement of aaPWV and LVEF in vehicle-, low dose- and high dose-treated mice. *High dose treatment of DOX increased aaPWV significantly compared to the vehicle group at 4, 7 and 11 days after the start of DOX treatment (A). LVEF did not change during treatment among all groups (B). For vehicle: n = 8, low dose: n = 8 and high dose: n = 8. For A & B: Repeated measures two-way ANOVA with Dunnett's multiple comparisons test. *, ** p < 0.05, 0.01*

Table 3.1: Additional cardiovascular parameters and body weight.

	Vehicle	Low Dose (2 mg/kg)	High Dose (4 mg/kg)
LVAW thickness systole (mm)	1.20 ± 0.07	1.20 ± 0.05	1.19 ± 0.04
LVAW thickness diastole (mm)	0.78 ± 0.03	0.76 ± 0.03	0.77 ± 0.03
LVID systole (mm)	1.86 ± 0.06	1.90 ± 0.12	2.05 ± 0.06
LVID diastole (mm)	3.33 ± 0.07	3.18 ± 0.13	3.48 ± 0.06
LVPW thickness systole (mm)	1.50 ± 0.07	1.46 ± 0.03	1.53 ± 0.04
LVPW thickness diastole (mm)	0.91 ± 0.05	0.96 ± 0.08	0.90 ± 0.03
Stroke volume (µL)	33.8 ± 1.73	29.3 ± 2.27	36.65 ± 1.64
Heart mass (mg)	143.2 ± 6.1	139.9 ± 1.9	133.7 ± 4.4
Body weight (g)	27.8 ± 0.8	27.2 ± 0.9	25.8 ± 0.8
Systolic blood pressure (mmHg)	103 ± 4	104 ± 4	105 ± 3
Diastolic blood pressure (mmHg)	77 ± 3	74 ± 5	72 ± 3
Pulse pressure (mmHg)	26 ± 2	30 ± 1	33 ± 2 *

*Abbreviations: LVAW, left ventricular anterior wall; LVID, left ventricular internal diameter; LVPW, left ventricular posterior wall. * $p < 0.05$ compared to vehicle. For vehicle: n = 8, low dose: n = 8 and high dose: n = 8. (2-column fitting table)*

Measurement with tonometry, only performed at day 5 for logistical reasons, showed a trend ($p = 0.0547$) of increased cfPWV in the high dose group (Figure 3.2A). Individual aaPWV-values for all time points are presented in Figure 3.2B to illustrate inter-animal variability. To evaluate the agreement between aaPWV and cfPWV measurement techniques a Bland-Altman plot was created. Bland-Altman analysis revealed that aaPWV values were systematically higher than cfPWV values (bias = 1.372) (Figure 3.2C). In addition, the bias tended to be higher with increasing PWV values (Figure 3.2C).

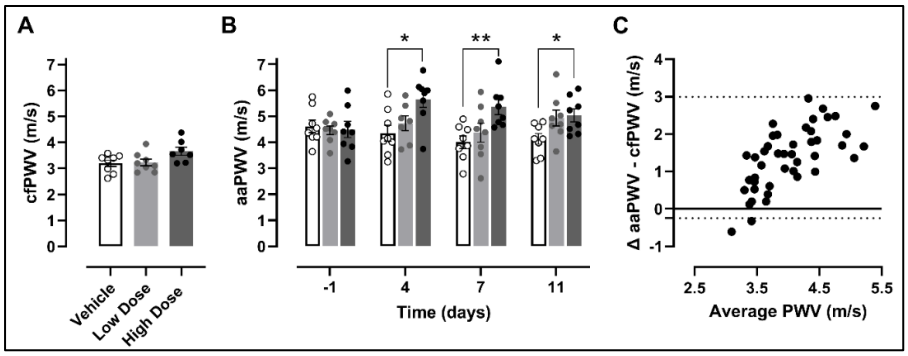

Figure 3.2: In vivo measurement of cfPWV in vehicle-, low dose- and high dose-treated mice and comparison of aaPWV and cfPWV. *cfPWV in the high dose group did not significantly increase compared to the vehicle group (p = 0.0547) (A). aaPWV values were systematically higher than cfPWV values after Bland-Altman analysis (bias = 1.372) (B & C). For vehicle: n = 8, low dose: n = 8 and high dose: n = 8. For A: One-way ANOVA with Dunnett's multiple comparisons test. For B: Repeated measures two-way ANOVA with Dunnett's multiple comparisons test. For C: Bland-Altman graph (dotted lines represent 95% limits of agreement) *, ** p < 0.05, 0.01*

Doxorubicin (high dose) increased aortic stiffness *ex vivo*

The "diastolic" and "systolic" diameters (at 80 –120 mmHg) in Krebs Ringer and PE conditions, determined in the *ex vivo* ROTSAC set-up, are presented in Figure 3.3A and 3.3B, respectively. The change (Δ) in "systolic" and "diastolic" diameter after PE-addition as compared with Krebs Ringer conditions was calculated (Figure 3.3C). This Δ diameter corresponds with the magnitude of contraction. In the high dose group, the change in "systolic" and "diastolic" diameter increased significantly, reflecting higher PE-induced contractions. Low dose-treated animals showed a non-significant trend towards elevated contraction (Figure 3.3C).

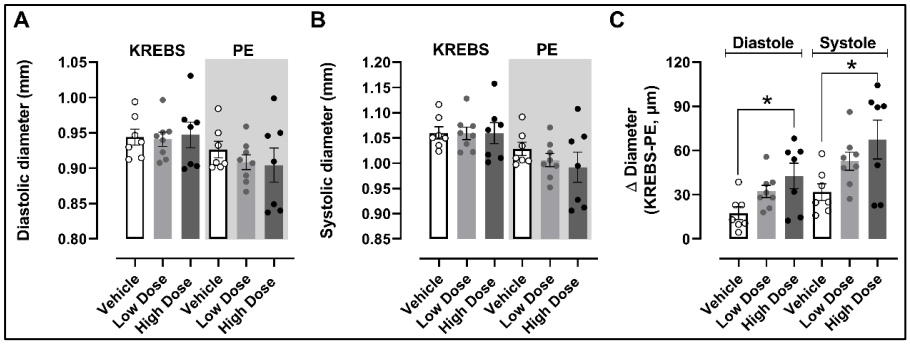

Figure 3.3: Evaluation of "diastolic" and "systolic" diameters in the ex vivo ROTSAC set-up. *Diastolic and systolic diameter in Krebs Ringer and PE conditions at 80-120 mmHg (A & B). Δ Diameter (Krebs - PE) was significantly increased in high dose-treated mice during systole and diastole (C). For vehicle: n = 8, low dose: n = 8 and high dose: n = 7. For C: One-way ANOVA with Dunnett's multiple comparisons test. * p < 0.05*

Ep, a measure of arterial stiffness, showed a pressure-dependent increase in all groups. Under Krebs Ringer conditions, there was no significant difference in Ep between vehicle- and DOX-treated mice, both in the absence and presence of L-NAME (300 µM) (Figure 3.4A & 3.4B). Similarly, in the presence of DEANO (2 µM), a NO-donor that removes vascular tonus, there were no differences in Ep between the vehicle and DOX-treated groups (Figure 3.4C), indicating no alteration in passive stiffness. However, Ep was significantly increased in the high dose-treated mice as compared with the vehicle-treated mice when aortic rings were stimulated with PE (2 µM) (Figure 3.4D). Mice treated with the low dose of DOX did not exhibit a higher Ep value in the presence of PE (Figure 3.4D). Remarkably, the high dose of DOX did not show a pressure-dependent increase in Ep in the combined presence of PE and L-NAME. More specifically, mice treated with the high dose of DOX exhibited a lower Ep value at 120 - 160 mmHg compared to the vehicle group (Figure 3.4E).

Furthermore, we determined the basal NO index by calculating the increase in Ep due to inhibition of eNOS with L-NAME (Supplementary Figure 3.2). The basal NO index (at 80-120 mmHg) was significantly decreased in the high dose group as compared with the vehicle group (Figure 3.4F).

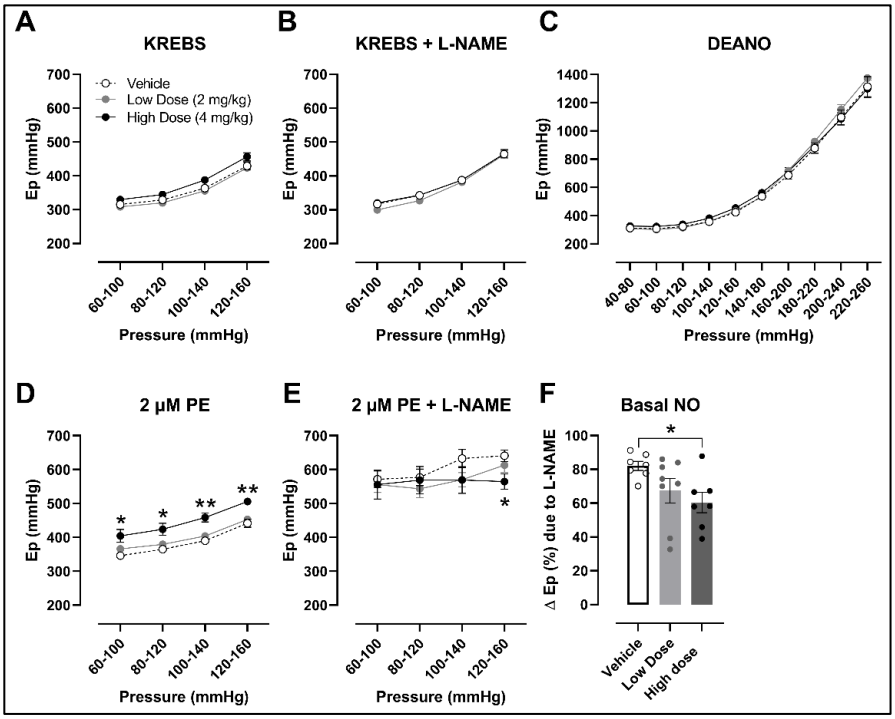

Figure 3.4: Assessment of aortic stiffness in mice treated with vehicle, low and high dose of DOX at different pressures with the ex vivo ROTSAC set-up. *Peterson's modulus (Ep), a measure for aortic stiffness, did not significantly differ between vehicle- and DOX-treated mice in Krebs conditions in the absence and presence of L-NAME (A &B). Ep was similar in all treatment groups in the presence of DEANO (C). Addition of 2 µM PE increased Ep in the high dose group compared to the vehicle group (D). In the presence of PE (2 µM) combined with L-NAME (300 µM), the high dose group showed no pressure-dependency of Ep, resulting in a lower Ep at 120–160 mmHg (E). Basal NO index was significantly reduced the high dose group (F). For vehicle: n = 8, low dose: n = 8 and high dose: n = 7. For A-E: Repeated measures two-way ANOVA with Dunnett's multiple comparisons test. For F : One-way ANOVA with Dunnett's multiple comparisons test. *, ** p < 0.05, < 0.01*

Finally, histological staining for elastin and collagen type I visualisation in aorta samples was performed to investigate potential structural remodelling (Figure 3.5). Elastin (Figure 3.5A) and collagen type I (Figure 3.5B) content did not differ between the treatment groups.

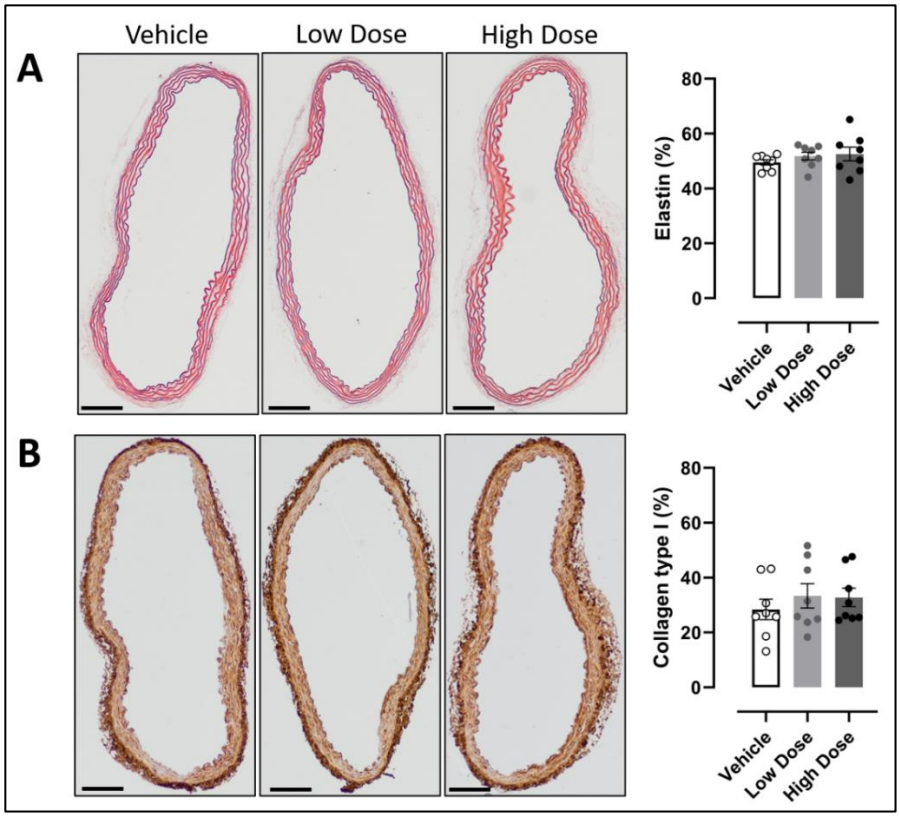

Figure 3.5: Evaluation of elastin and collagen type I content in the aortic wall of mice treated with vehicle, low and high dose of DOX. *The elastin (A) and collagen type I (B) amount were not altered in the different treatment groups. For vehicle: n = 8, low dose: n = 8 and high dose: n = 8. For A and B: One-way ANOVA with Dunnett's multiple comparisons test (p > 0.05 for low and high dose compared to vehicle). Scale bar: 100 µm.*

Doxorubicin impaired endothelium-dependent relaxation, basal NO index and increased contraction

The high dose group exhibited increased PE-induced contractions compared to the vehicle, while the low dose did not (Figure 3.6A). This difference disappeared in the presence of L-NAME (Figure 3.6A). The sensitivity of VSMCs for PE (defined by the EC_{50}) was significantly elevated in animals treated with the high dose of DOX (Figure 3.6B). More specifically, the mean EC_{50}-values (logarithmic) were -7.014 ± 0.050 M and -6.796 ± 0.052 M for the high dose and vehicle groups, respectively.

We further determined the basal NO index by calculating the change in isometric force due to eNOS-inhibition with L-NAME (Supplementary Figure 3.3). The basal NO index was significantly decreased in the high dose group as compared with the vehicle group (Figure 3.6C).

ACh-induced endothelium-dependent relaxation was impaired (Figure 3.6D). Both the maximal relaxation and the sensitivity for ACh was significantly reduced in the high dose-treated mice (Figure 3.6D & 3.6E). More specifically, the mean EC_{50}-values (logarithmic) were -7.454 ± 0.073 M and -7.751 ± 0.086 M for the high dose and vehicle groups, respectively. In addition, there was no difference in DEANO-induced endothelium-independent relaxation between vehicle and DOX-treated mice nor in the sensitivity of VSMCs for DEANO (Figure 3.6D). For diltiazem (35 μM), no differences in the magnitude of relaxation were present between the different groups (Figure 3.6F).

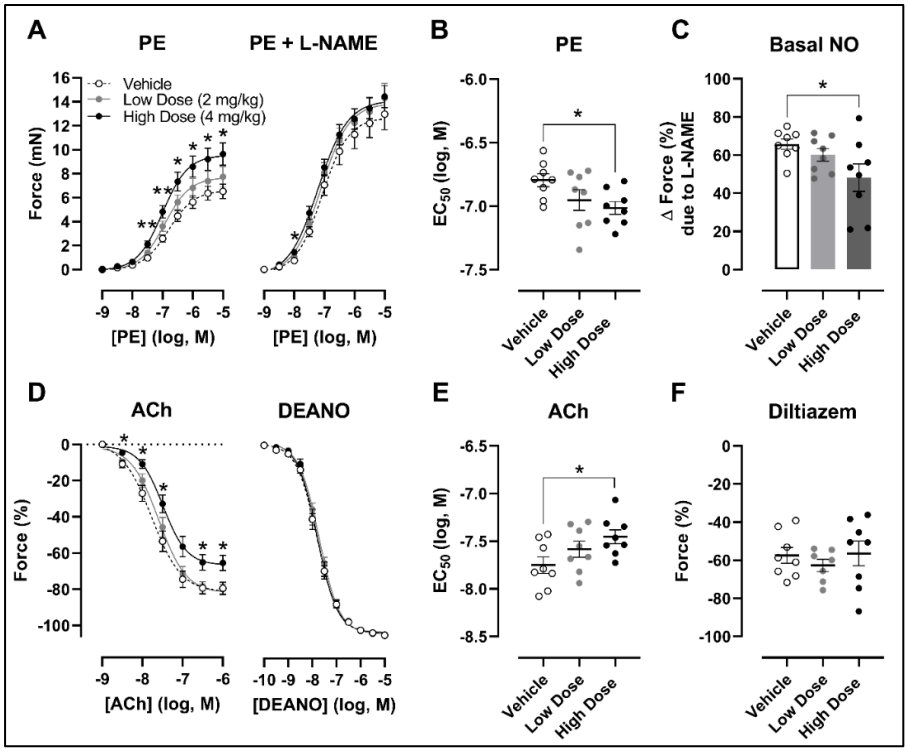

Figure 3.6: VSMC and EC function in mice treated with vehicle, low and high dose of DOX determined in organ baths with isometric force transducer. *Concentration-response curves for mice treated with vehicle, low and high dose of DOX under PE-stimulation in the absence and presence of L-NAME (A), ACh (D) and DEANO (D). Contraction and VSMC-sensitivity for PE increased significantly in high dose-treated mice compared to vehicle group (A & B), but not after addition of L-NAME (A). Basal NO index, calculated from panel A, was significantly reduced in high-dose treated mice (C). No changes were present in the magnitude of DEANO-induced relaxation (D). ACh-induced relaxation and sensitivity of the endothelium for ACh decreased significantly in the high dose group (D & E). Diltiazem-induced relaxation did not differ between treatment groups (F). For vehicle: n = 8, low dose: n = 8 and high dose: n = 8. For A and D: Repeated measures two-way ANOVA with Dunnett's multiple comparisons test. For B, C, E and F: One-way ANOVA with Dunnett's multiple comparisons test. *, ** p < 0.05, < 0.01*

Doxorubicin disrupted EC layer continuity and decreased eNOS-expression

Endothelial layer continuity and eNOS-expression in the aorta were further investigated. The EC layer was evaluated with an immunohistochemical stain against CD31, a marker for ECs. CD31 positivity was significantly decreased in the high dose group compared to the vehicle in a dose-dependent way, revealing gaps in the EC monolayer (Figure 3.7A). In addition, eNOS-expression was reduced in the high dose group as well (Figure 3.7B).

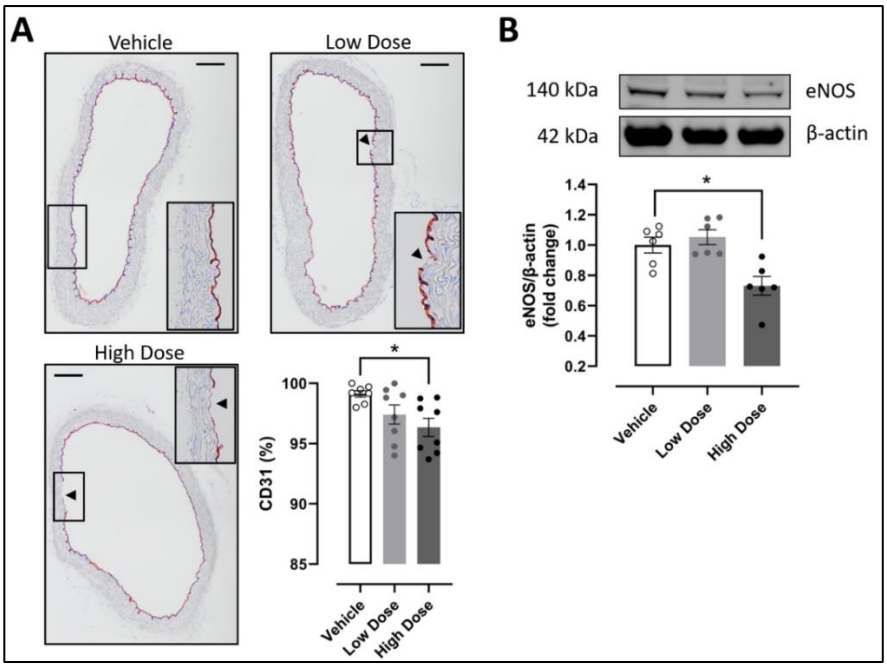

Figure 3.7: Evaluation of EC layer continuity with CD31 staining and eNOS-expression in mice treated with vehicle, low and high dose of DOX. *CD31 staining revealed a significant dose-dependent decrease in EC layer continuity in the high dose group compared to the vehicle (A). In addition, high dose treatment with DOX reduced eNOS-expression (B). Panel A: Black arrows show discontinuity of the endothelial monolayer; For vehicle: n = 7, low dose: n = 8 and high dose: n = 8. Panel B: For vehicle: n = 6, low dose: n = 6 and high dose: n = 6. For A: One-way ANOVA with Dunnett's multiple comparisons test. For B: Kruskal-Wallis with Dunn's multiple comparisons test. * p < 0.05; Scale bar: 100 µm*

3.4) Discussion

Arterial stiffness is considered as an important predictor of cardiovascular disease [75]. While clinical studies have demonstrated an increase in arterial stiffness after DOX treatment, the exact mechanism remains elusive [26, 27, 90, 91]. Here we present a study where DOX-induced arterial stiffness was investigated in mice, using both *in vivo* and *ex vivo* techniques.

The current study revealed a consistent increase in aaPWV after DOX treatment, while LVEF function remained unaffected. Previously, studies in mice demonstrated LVEF decline after DOX treatment, but these studies used high doses (20-25 mg/kg) [22, 66]. We used lower doses of DOX (8 mg/kg cumulative), since we did not aim to induce severe cardiotoxicity. Body weight and cardiac parameters were not altered after DOX treatment. The observation of DOX-induced arterial stiffness in the absence of cardiac dysfunction is an important finding. Not only does this indicate that the observed vascular toxicity during DOX treatment was independent of cardiac parameters, but this also suggests that DOX-induced arterial stiffness either precedes DOX-cardiotoxicity, or occurs at lower doses. In both cases, arterial stiffness holds potential as a clinical marker for identifying patients at risk. Additionally, systolic and diastolic blood pressure did not significantly differ, but pulse pressure was elevated in the high dose group, which may point to increased arterial stiffness [95]. The high dose (4 mg/kg) corresponds approximately with 160 mg/m^2 in patients, which is below the maximal recommended dose of 450 mg/m^2 [15, 96]. Furthermore, dosing schedules of DOX for breast cancer [97], non-Hodgkin lymphoma [98] and small cell lung cancer [99] typically involve multiple DOX-infusions every 2 – 3 weeks. The doses used in our preclinical study are also in line with epidemiological studies that have

reported accelerated cardiovascular ageing (i.e. increased vascular stiffness), especially in childhood cancer survivors [26].

In patients, regional cfPWV measured by applanation tonometry is the gold standard. In mice, cfPWV measurements are feasible [85], but aaPWV by ultrasound imaging, is more frequently used. Although not the primary objective of our study, we included a comparison between both methods. Bland-Altman analysis showed that aaPWV in mice was consistently higher than cfPWV. aaPWV was more sensitive to detect DOX-induced aortic stiffness *in vivo* in mice, although different timing of the methods and the use of a different anaesthetic do not allow a direct head-to-head comparison. The absolute difference between the aaPWV and cfPWV values can be attributed to variation in geometry and structure of the vessel wall along the arterial tree, which affects the speed of the propagating pulse wave. Previous studies in humans have reported PWV values of 4.4 m/s, 6 m/s and 9 m/s at the aortic root, abdominal aorta and femoral artery, respectively [100, 101]. In this respect, cfPWV represents an integrated average PWV of the different parts of the artery system [100, 101]. In addition, cfPWV measurement depends on determination of the external carotid-femoral distance, which may be prone to a measurement error, particularly in mice [85]. Taken together, these factors might explain the lower cfPWV values and the observation of cfPWV not reaching statistical significance in the high dose group.

The *in vivo* data were confirmed in the *ex vivo* ROTSAC set-up. Aortic rings of high dose-treated mice showed significantly increased aortic stiffness, yet only in the presence of a contractile stimulus (PE). Hence, this finding suggests that a contractile stimulus, provided for example by catecholamines, is essential in the modulation of vascular tone after DOX treatment *in vivo*. Remarkably, in the presence of PE combined with L-NAME, high dose-treated animals showed no pressure-

dependency of Ep compared to vehicle-treated animals. More specifically, half of the high dose-treated animals exhibited a decrease in Ep with increasing pressure (data not shown), resulting in an apparent flattening of the Ep-pressure curve. The exact mechanism remains elusive, although DOX has been shown to induce VSMC death and senescence *in vitro* [102, 103]. Another possible explanation may be the interaction of DOX with the extracellular environment or focal adhesion complexes, which are required for maintaining vascular tonus [104]. Finally, DOX-related structural alterations were evaluated by adding a high dose of DEANO (2 μM), an exogenous NO donor, which relaxes VSMCs and removes vascular tone. In the absence of VSMC tonus, no difference in Ep was observed, which suggests unaltered passive stiffness of the aortic wall. These findings were corroborated by histological stains for elastin and collagen type I, showing no changes in elastin and collagen type I content. Hence, our results point towards active mechanisms contributing to DOX-induced aortic stiffness.

Treatment with the high dose of DOX resulted in increased contraction force in response to PE, an α1-adrenergic receptor agonist. In order to delineate the specific mechanisms involved herein, different aspects of vascular function were further investigated. A dose response of DEANO was used to investigate endothelium-independent relaxation of VSMCs. DEANO causes relaxation of VSMCs through a cyclic guanosine monophosphate (cGMP)-mediated pathway, which results in a reduction in free intracellular Ca^{2+}, thus mediating relaxation of VSMCs [105]. DEANO-induced relaxation did not differ between treatment groups, indicating unaltered guanylate cyclase and cGMP-signalling. This suggests that the sensitivity of VSMCs for NO and the VSMC relaxation capacity remain unaffected after DOX treatment. We previously showed that PE causes an increase in intracellular Ca^{2+} through, in part, voltage-gated Ca^{2+}- channels,

thus mediating contraction of VSMCs [106]. Therefore, using diltiazem, a voltage-gated Ca^{2+}-channel blocker, can provide useful insight about potential disturbed Ca^{2+}-homeostasis involved in impaired VSMC contraction. Diltiazem-induced relaxation did not differ between the vehicle- and DOX-treated groups. This indicates that Ca^{2+}-influx through voltage-gated calcium channels in VSMCs is not perturbed in response to DOX-administration. Taken together, these findings show that VSMC-specific mechanisms involved in VSMC contraction and relaxation are not impaired. Hence, VSMC function remains intact after DOX treatment.

The endothelial cell layer of the aorta plays a crucial role in regulating VSMC contraction and relaxation [107]. Low levels of basal NO are associated with endothelial dysfunction and, consequently, with increased VSMC contraction, contributing to aortic stiffness [81]. The basal NO index (percentage increase in PE-contraction upon addition of the eNOS blocker L-NAME) provides an estimate about basal NO production and thus is a useful marker for endothelial function. Previous work from our lab has demonstrated that in wild-type C57BL6 mice approximately 80% of maximal contraction (PE + L-NAME) is attributable to basal NO [94]. Contraction force was higher in the DOX-treated group upon PE-stimulation, but contraction force was similar between all treatment groups after addition of L-NAME. Consequently, the index of basal NO was reduced in DOX-treated animals, indicating that DOX potentially impairs NO production or NO bioavailability.

DOX treatment resulted in reduced CD31 positivity, reflecting gaps in the EC monolayer. This finding indicates that DOX causes EC loss, probably through EC death. In addition, eNOS protein expression was decreased in the high dose group. Both EC loss and reduced eNOS-expression may contribute to the observed decrease in basal NO index, which, in turn, could result

in endothelial dysfunction. The observed results are in line with a study of He et al. (2019) in mice, that reported decreased EC viability and reduced eNOS-expression after 3 weeks of DOX treatment (15 mg/kg cumulative) [60]. The authors identified excess ROS-accumulation after DOX treatment as the primary cause of EC death and reduced eNOS expression, which resulted in decreased NO content [60]. DOX-induced ROS generation is mainly caused by the conversion of DOX in a superoxide radical via an intermediate semiquinone structure at the reductase domain of eNOS [108]. Paradoxically, other studies have reported that eNOS expression is upregulated in response to DOX due to ROS-accumulation [64, 109]. Moreover, DOX interferes with eNOS function, resulting in uncoupling of eNOS [64, 109]. In this case, eNOS no longer produces NO, but instead, contributes to superoxide formation, thereby exacerbating ROS-generation. However, these studies were performed using a single high dose of doxorubicin (20 mg/kg) or were performed *in vitro,* which might explain the difference between our results and these other studies.

Similarly, aortic rings of DOX-treated mice exhibited reduced endothelium-dependent relaxation. Previous work from our research group has demonstrated that endothelial dysfunction increases vascular tone and thereby actively augments arterial stiffness [42, 43, 87]. For instance, aortic segments of mice without eNOS expression ($eNOS^{-/-}$) showed no endothelium-dependent relaxation, increased contraction and augmented arterial stiffness [43]. Another recent study demonstrated reduced ACh-induced relaxation after DOX treatment (10 mg/kg cumulative) in mice without altering relaxation in response to an exogenous NO-donor [92]. This is in agreement with our results. However, impaired endothelium-independent relaxation by a NO-donor in mice after DOX treatment (15 mg/kg cumulative) has also been reported [60].

While inactivation of NO by ROS has been proposed as a possible mechanism [110], this concept is not supported by our DEANO relaxation curves, which were identical for the three groups. Possibly, the mechanism of interference with NO signalling depends on the dose of DOX. Our findings suggest that lower doses of DOX (< 15 mg/kg) decrease NO content by decreasing eNOS expression, rather than inactivating NO with excess ROS.

In conclusion, we report a consistent increase in aaPWV in DOX treated mice, which was confirmed *ex vivo*. Moreover, the *ex vivo* ROTSAC and organ bath experiments, revealed that exclusively active components are involved in aortic stiffening in response to DOX. More specifically, DOX impaired endothelial function, resulting in reduced endothelium-dependent relaxation and increased contraction, thereby augmenting arterial stiffness. This endothelial dysfunction could be attributable to EC loss and reduced eNOS-expression. The experimental DOX model and the methods presented in this study, offer the opportunity for further navigating the mechanisms of arterial stiffening in DOX-treated patients.

Supplementary Figures

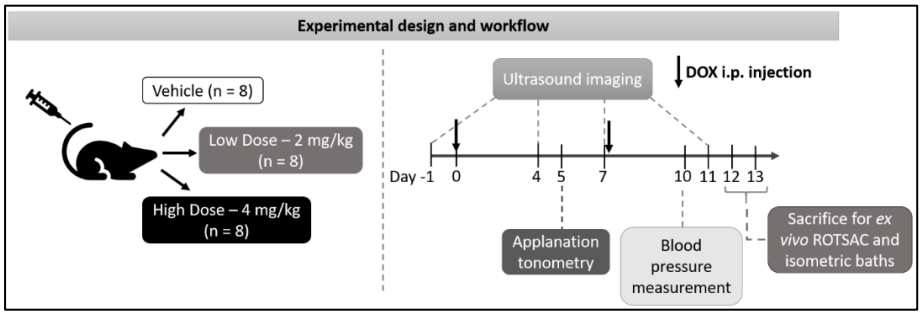

Supplementary Figure 3.1: Experimental design and workflow.

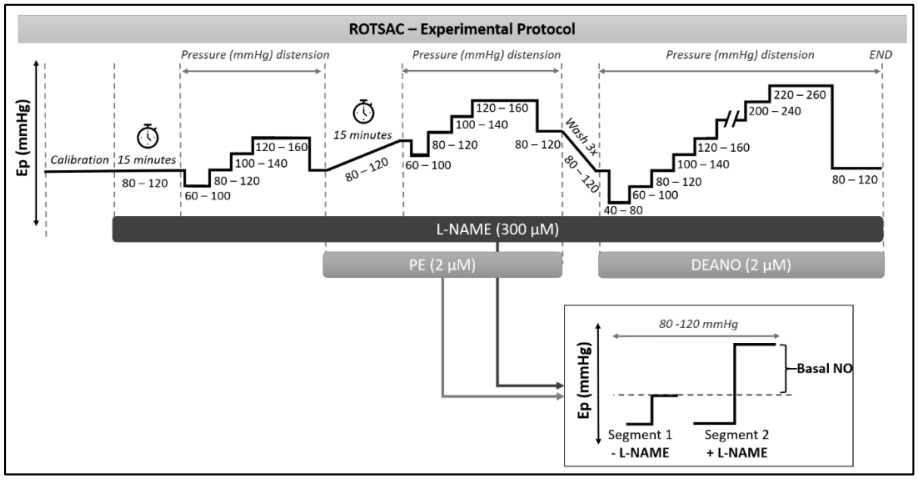

Supplementary Figure 3.2: Experimental protocol for aortic stiffness evaluation in ROTSAC set-up.

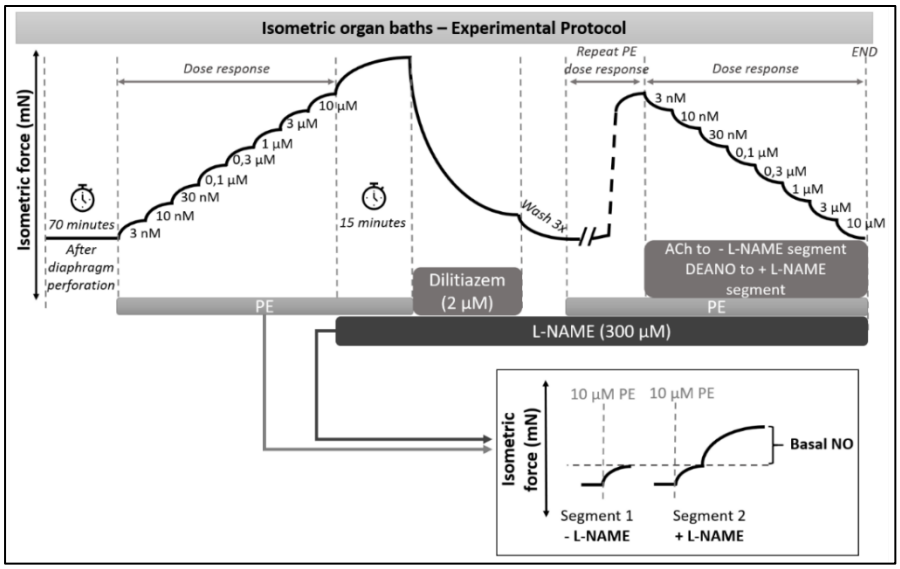

Supplementary Figure 3.3: Experimental protocol for vascular reactivity assessment in isometric organ baths.

CHAPTER IV

Doxorubicin impairs vascular smooth muscle cell contraction yet only shortly after administration

Published in 2021 in *International Journal of Molecular Sciences* as **Doxorubicin Impairs Smooth Muscle Cell Contraction: Novel Insights in Vascular Toxicity;** Bosman M., Krüger D., Favere K., Wesley C., Neutel C., Van Asbroeck B., Diebels O., Faes B., Schenk T., Martinet W., De Meyer G., Van Craenenbroeck E. and Guns P.-J.; DOI: 10.3390/ijms222312812; Original Research Article

Abstract

Clinical and animal studies have demonstrated that the chemotherapeutic doxorubicin (DOX) increases arterial stiffness, a predictor of cardiovascular risk. Despite consensus about DOX-impaired endothelium-dependent vasodilation as a contributing mechanism, some studies have reported conflicting results on vascular smooth muscle cell (VSMC) function after DOX treatment. The present study aimed to investigate the effects of DOX on VSMC function. To this end, mice received a single injection of 4 mg DOX/kg, or mouse aortic segments were treated *ex vivo* with 1 μM DOX, followed by vascular reactivity evaluation 16 hours later. Phenylephrine (PE)-induced VSMC contraction was decreased after DOX treatment. DOX did not affect the transient PE contraction dependent on Ca^{2+}-release from the sarcoplasmic reticulum (0 mM Ca^{2+}), but reduced the subsequent tonic phase characterised by Ca^{2+}-influx. These findings were supported by similar angiotensin II and attenuated endothelin-1 contractions. The involvement of voltage-gated Ca^{2+}-channels in DOX-decreased contraction was excluded by using levcromakalim and diltiazem in PE-induced contraction, and corroborated by similar K^+ and serotonin contractions. Despite the evaluation of multiple blockers of transient receptor potential channels, the exact mechanism for DOX-decreased VSMC contraction remains elusive. Surprisingly, DOX reduced *ex vivo,* but not *in vivo* arterial stiffness, highlighting the importance of appropriate timing for evaluating arterial stiffness in DOX-treated patients.

4.1) Introduction

The anthracycline doxorubicin (DOX) is one of the most efficacious chemotherapeutic drugs for the treatment of a wide array of cancers [18]. However, DOX treatment has been associated with development of cardiotoxicity and eventually heart failure, which limits its clinical use [111-115]. While DOX-induced cardiotoxicity has been extensively investigated (reviewed elsewhere) [89], the toxic effects of DOX on the vasculature have been less considered. Epidemiological studies point towards accelerated vascular ageing in childhood cancer survivors, as evidenced by a higher incidence of atherosclerosis and hypertension [26, 116, 117]. Moreover, several studies have demonstrated that DOX increases arterial stiffness in cancer patients, both during and after treatment [27, 30, 90, 118]. Arterial stiffness is associated with an increased risk of cardiovascular events and mortality, as it impacts arterial pressure, cardiac performance and perfusion [72-74].

Previously, it was shown that DOX impairs flow-mediated vasodilation in the brachial artery in patients shortly after DOX treatment, often referred to as endothelial dysfunction [119]. In addition, our research group demonstrated that 2 weeks of DOX administration to mice (4 mg/kg/week) acutely impaired endothelium-dependent vasodilation and consequently increased vascular tone, thereby actively augmenting arterial stiffness [120]. We, and others, identified endothelial cell loss and reduced endothelial nitric oxide synthase (eNOS) levels as potential mechanisms contributing to impaired endothelial function after DOX treatment [60, 120].

Apart from the demonstrated toxic impact of DOX on endothelial function, DOX also affects vascular smooth muscle cell (VSMC) function [62-64]. However, conflicting findings have been reported about the role of DOX in the alteration of VSMC

reactivity. Gibson et al. reported decreased VSMC contraction in rat thoracic aorta rings 24 hours after DOX treatment (15 mg/kg) [63]. Similarly, Olukman et al. demonstrated that DOX (20 mg/kg) attenuated VSMC contraction in rat aortic segments 1 week after administration [64]. Conversely, Shen et al. described increased VSMC contraction in mouse aortic rings after *ex vivo* DOX treatment (100 μM), which was attributable to increased Ca^{2+}-release from the sarcoplasmic reticulum and Ca^{2+}-entry in VSMCs [62]. In our previous study, we did not observe any direct effects of 2 weeks DOX treatment on VSMC contraction [120]. Hence, the exact effects of DOX on modulation of VSMC function remain unclear and may be dependent upon the dose or treatment protocol.

In the present study, we aimed to investigate the effects of a single dose of DOX on VSMC function, including its contribution to arterial stiffness. A secondary goal was to evaluate whether the acute effects of DOX could be studied *ex vivo* in aortic rings. Such an *ex vivo* platform holds potential for mechanistic studies, as well as for future drug screening.

4.2) Materials and Methods

Animals and ethical approval

Male C57BL/6J mice (Charles River, France) with an age of 10 to 12 weeks and a body weight between 26 and 30 g were used for all experiments. Mice were housed in the animal facility of the University of Antwerp in standard cages with 12-12 hours light-dark cycles with access to regular chow and water *ad libitum*. To avoid the influence of female hormone confounding factors, male mice were chosen. All experiments in this work were approved by the Ethical Committee of the University of Antwerp (dossier 2019-34) and were conform to the ARRIVE guidelines, to the Guide for the Care and Use of Laboratory Animals published by the US National Institutes of Health (NIH Publication no.85-23, revised 1996) and to the Belgian Royal Decree of 2013.

DOX treatment and experimental workflow

The current study composes two distinct experimental parts, namely a part where DOX was administered to mice (*in vivo* DOX treatment), and a second part where aortic segments were first isolated from mice and subsequently either treated with vehicle or DOX (*ex vivo* DOX treatment).

For *in vivo* DOX treatment: C57BL/6J mice received a single intraperitoneal injection of 4 mg/kg DOX (Adriamycin®, 2 mg/mL) or 10 mL/kg of a 0.9% NaCl solution (B. Braun, Belgium) as vehicle. DOX was diluted in a 0.9% NaCl solution on the day of injection. Based on other studies that investigated acute DOX effects [63, 64, 93, 121], mice were sacrificed 16 hours later for vascular reactivity evaluation in organ baths with isometric transducer. To this end, mice were intraperitoneally injected with sodium pentobarbital (100 mg/kg; Sanofi, Belgium), followed by perforation of the diaphragm (when under deep anaesthesia). The thoracic aorta was carefully dissected and cut into six segments

of 2 mm length (i.e. TA0 to TA5) with the crossing of the diaphragm as the reference point for the sixth segment (TA5). Next, TA3, TA4 and TA5 segments were mounted between two hooks of an organ bath set-up (10 mL) filled with Krebs Ringer solution (37°C, 95% O2/5% CO2, pH 7.4) for vascular reactivity and arterial stiffness evaluation. The Krebs Ringer solution contained (in mmol/L): NaCl 118, KCl 4.7, $CaCl_2$ 2.5, KH_2PO_4 1.2, $MgSO_4$ 1.2, $NaHCO_3$ 25, CaEDTA 0.025, and glucose 11.1.

For ex *vivo* DOX treatment: Healthy wild-type C57BL/6J mice were first sacrificed and the aorta was subsequently isolated, as described above. Following dissection, aortic segments were immediately transferred to Dulbecco's Modified Eagle Medium (DMEM) medium (ThermoFisher Scientific), supplemented with 1% penicillin/streptomycin. Aortic segments were randomly divided and received either phosphate buffer saline solution (PBS) as vehicle (1:100) or DOX (1 μM) for 16 hours. DOX was diluted in PBS on the day of the experiment. After 16 hours, aortic segments were mounted between two hooks of an organ bath set-up (10 mL) filled with Krebs Ringer solution (37°C, 95% O2/5% CO2, pH 7.4) for vascular reactivity evaluation.

High-frequency ultrasound imaging

Ultrasound imaging was performed in anaesthetised mice under 1.5 - 2.5% (v/v) isoflurane (Forene; Abbvie, Belgium) using a high-frequency ultrasound system (Vevo2100, VisualSonics). Images were only acquired when heart rate and body temperature met the inclusion criteria, i.e. 550 ± 50 beats/min and 37 ± 1 °C, respectively. M-mode images were obtained for determination of cardiac parameters using a 24-MHz transducer. LVEF was subsequently calculated using measurements of three consecutive M-mode cycles with Vevo LAB Software (Version 3.2.0, VisualSonics). In the same session, abdominal aorta PWV (aaPWV) was determined according to the method developed by

Di Lascio et al. with a 24-MHz transducer [84]. Briefly, pulse wave Doppler tracing was used to measure aortic flow velocity (V). Immediately thereafter, aortic diameter (D) was measured on 700 frames-per-second B-mode images of the abdominal aorta in EKV imaging mode. The ln(D)-V loop method was then applied to calculate aaPWV, using MathLab v2014 software (MathWorks).

Applanation tonometry

Carotid femoral PWV (cfPWV) was determined in anaesthetised mice under 1.5 - 2.5% (v/v) isoflurane (Forene; Abbvie, Belgium), as previously described by our research group [85]. In brief, two pulse tonometers (SPT-301, Millar Instruments) were applied on the skin using a micromanipulator. Carotid–femoral transit time (Δt) was determined using the time difference between the foot of carotid and femoral artery pulses (foot-to-foot method). The foot of the pressure wave was defined as the second derivative maximum. Twenty consecutive pulses with sufficient amplitude and a reproducible waveform were analysed; pulses that interfered with respiratory movement peaks were excluded.

Blood pressure evaluation

Systolic and diastolic blood pressure were determined non-invasively in restrained, awake mice using a tail-cuff system with programmed electrosphygmomanometer (Coda, Kent Scientific Corporation). To reduce stress and variability during the procedure, animals were trained for two days prior to the actual measurements.

Evaluation of vascular reactivity

For clarity, the standard experimental protocol for the *in vivo* and *ex vivo* DOX treatment experiments is illustrated in Supplementary Figure 4.1 and Figure 4.2, respectively. Aortic segments were mounted at a preload of 20 mN. Since we have

previously shown that basal nitric oxide (NO) declines over time [94], the experimental protocol for *in vivo* DOX-treated aortic segments was started exactly 70 minutes after puncture of the diaphragm to minimise time-dependent biases. *Ex vivo* DOX-treated aortic segments were also mounted at a preload of 20 mN, and the experimental protocol was started 20 minutes thereafter to allow optimal stabilisation. VSMC contraction was evaluated by adding cumulative concentrations of phenylephrine (PE; 3 nM – 3 μM), an α1-adrenergic receptor agonist. Next, endothelium-dependent relaxation was investigated by addition of cumulative concentrations of acetylcholine (ACh; 3 nM – 10 μM), a muscarinic receptor agonist.

The PE-elicited contraction response was further investigated by incubating the aortic segments in the organ bath with a single PE-dose of 2 μM for 15 minutes. Once the contraction was stable after 15 minutes, Nω-nitro-L-arginine methyl ester (L-NAME; 300 μM) was added, further increasing contraction (PE + L-NAME contraction). L-NAME is an eNOS blocker, which inhibits NO production and allows to evaluate the involvement of the endothelial cell layer in regulating VSMC contraction and tone. After 20 minutes, cumulative concentrations of the exogenous NO-donor diethylamine NONOate (DEANO; 0.3 nM – 10 μM) were added to the organ bath to evaluate endothelium-independent relaxation of VSMCs through the cyclic guanosine monophosphate (cGMP)-mediated pathway.

The contraction via inositol-triphosphate (IP_3)-mediated Ca^{2+}-release from the sarcoplasmic reticulum was investigated by incubating aortic segments with Ca^{2+}-free Krebs Ringer solution (0 mM Ca^{2+}) for three minutes, followed by addition of PE (2 μM) for three minutes. 0 mM Ca^{2+} Krebs Ringer solution contained (in mmol/L): NaCl 118, KCl 4.7, $CaCl_2$ 0, KH_2PO_4 1.2, $MgSO_4$ 1.2, $NaHCO_3$ 25, CaEDTA 0.025, EGTA 1.0 and glucose 11.1. An

extracellular 0 mM Ca^{2+}-environment will prevent Ca^{2+}-influx during PE contraction, which will shift contraction to solely Ca^{2+}-release from the sarcoplasmic reticulum [106]. Next, $CaCl_2$ (3.5 mM) was added to restore Ca^{2+}-containing Krebs, which results in contraction in a similar way as the PE-elicited contraction response [106]. Finally, the involvement of voltage-gated Ca^{2+} channels (VGCCs) was determined by adding a single, high concentration (35 μM) of diltiazem, a voltage-gated Ca^{2+}-channel blocker. This results in relaxation, which offers an estimate of the amount of contraction that is attributable to VGCCs.

To determine the role of VSMC membrane potential in modulating contraction, a dose-response of K^+ (10 mM, 20 mM, 30 mM, 40 mM and 50 mM) was performed in the organ bath. A high dose of K^+ causes depolarisation of the membrane potential, thereby activating VGCC-mediated Ca^{2+}-influx, which eventually results in contraction [106, 122]. Finally, the VGCC blockers levcromakalim (1 μM) and diltiazem (35 μM), and the non-selective cation channel (NSCC) blockers tranilast (100 μM), SKF-96365 (10 μM), 2-aminoethoxydiphenyl borinate (2-APB; 20 μM) and 9-phenantrol (1 μM) were used to delineate the involvement of NSCCs in the PE-elicited contraction response. Levcromakalim hyperpolarises the VSMC membrane potential, thereby deactivating VGCCs, which will consequently inhibit Ca^{2+}-influx via these channels [106, 123]. These experiments were performed in the presence of L-NAME to exclude the influence of NO on VGCCs and NSCCs. Prior to the addition of a NSCC blocker, PE-contraction was elicited in the presence of diltiazem, thereby promoting Ca^{2+}-influx through NSCCs. The protocol for investigation of NSCCs in modulating contraction is illustrated in Supplementary Figure 4.3.

Evaluation of arterial stiffness in ROTSAC

Ex vivo assessment of arterial stiffness was performed, using the Rodent Oscillatory Tension Set-up to assess Arterial Compliance (ROTSAC), as previously described [87, 120]. In brief, segments (TA3) were continuously stretched between alternating preloads corresponding to "systolic" and "diastolic" transmural pressures. Calibration of the set-up allows to calculate in real-time the "systolic" and "diastolic" pressure and the Peterson's modulus (Ep), a measure for arterial stiffness, based on LaPlace's equation. Ep was calculated as follows: $Ep = D_0 * \Delta P/\Delta D$ with ΔP = difference in pressure (kept constant at 40 mmHg), D_0 = "diastolic" diameter and ΔD = the change in diameter between "diastolic" and "systolic" pressure. The ROTSAC protocol included the evaluation of arterial stiffness (Ep) at different pressures (i.e. 60-100 until 220-260 mmHg with 20 mmHg intervals). The contribution of VSMC tonus was investigated by adding a high concentration (2 µM) of PE combined with L-NAME (300 µM).

Chemical compounds

DOX (Adriamycin®, 2 mg/mL) was purchased from Pfizer (Belgium). PE, L-NAME, ACh, DEANO, diltiazem, tranilast, SKF-96365, 9-phenantrol, serotonin hydrochloride and angiotensin II (human) were obtained from Sigma-Aldrich (Belgium). Levcromakalim and 2-APB were purchased from TOCRIS (United Kingdom). Finally, endothelin-1 was supplied by Alexis® Biochemicals.

Statistical analysis

All results were expressed as the mean ± standard error of the mean (SEM). Statistical analyses were performed using GraphPad Software (Prism 9 - Version 9.2.0, Graphpad, USA). A p-value < 0.05 was considered to be statistically significant.

4.3) Results

A single dose of DOX impairs VSMC contraction and endothelial-dependent vasodilation

There was a decrease in PE-induced contraction, 16 hours after *in vivo* DOX administration (Figure 4.1A). The PE-elicited contraction response, which comprises an initial transient and a subsequent tonic phase [106], was further investigated. DOX reduced the tonic, but not the transient contraction in aortic segments after addition of 2 μM PE (Figure 4.1B).

Since the tonic contraction phase is dependent on Ca^{2+}-influx [106], determining the increase in contraction force (Δ) at different time points offers an estimate of the effectiveness of Ca^{2+}-influx in VSMCs. Here, we calculated the increase in force (Δ) by subtracting the force at 800 seconds (s) from the force at 100s during the PE-elicited contraction response. This increase in contraction force (Δ) was lower in the DOX-treated group compared to the vehicle-treated group (Figure 4.1C), which suggests that DOX impairs Ca^{2+}-influx.

The contraction force remained lower in the DOX-treated group in the presence of L-NAME (Figure 4.1D). Of note, the PE contraction in panel D is the maximal amplitude of panel B, and these contraction amplitudes are higher than in panel A due to a decrease of basal nitric oxide (NO) over time [94]. Further, impaired acetylcholine (ACh)-induced endothelium-dependent relaxation was observed after DOX, while DEANO-induced endothelium-independent relaxation was not affected (Figure 4.1E). These results suggest that DOX decreases VSMC-contraction through a VSMC-specific mechanism.

Ex vivo incubation of aortic rings with DOX leads to reduced VSMC contraction and impaired endothelium-dependent relaxation

To develop a drug testing platform for studying the acute vascular effects of DOX in depth and to corroborate the *in vivo* findings, isolated aortic segments were isolated from mice, and subsequently treated with DOX (1 μM) *ex vivo* for 16 hours. Similar results were obtained under these experimental conditions. More specifically, PE-induced contraction was reduced after DOX treatment in a PE concentration response curve (Figure 4.2A) and contraction-over-time curve (Figure 4.2B). The increase in force (Δ) was lower for DOX-treated aortic segments compared to the vehicle group (Figure 4.2C). Under L-NAME conditions, the contraction remained decreased in the DOX group (Figure 4.2D), and there was impaired ACh-induced relaxation and unaltered DEANO-induced relaxation (Figure 4.2E).

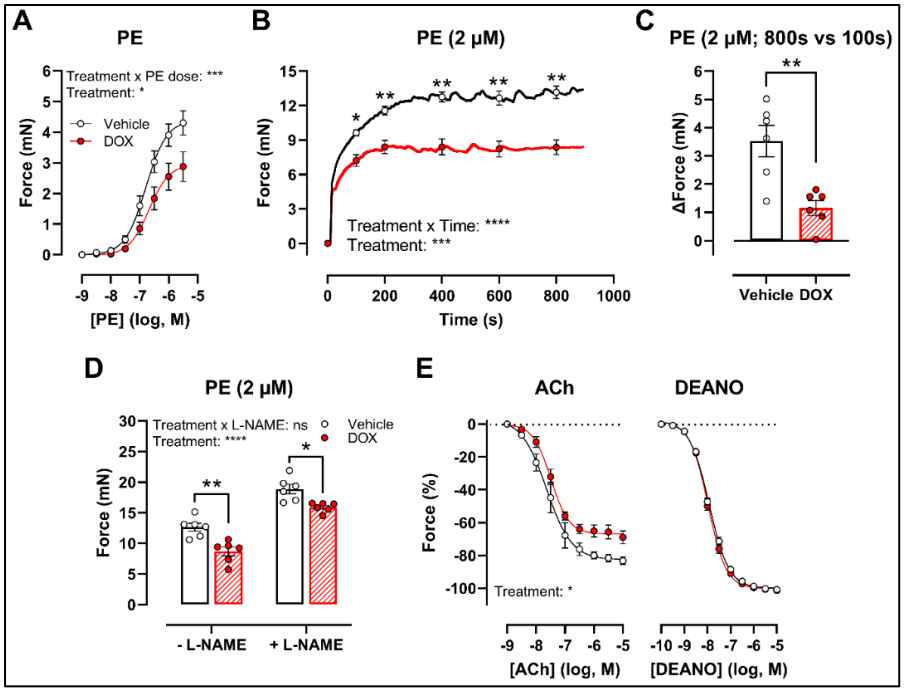

Figure 4.1: VSMC contraction and relaxation in aortic segments, 16 hours after in vivo DOX administration. *PE-induced contraction was decreased in aortic segments after in vivo DOX treatment (A). The PE-elicited contraction response was reduced after DOX treatment, which suggests perturbed tonic contraction (B). The increase in force between 800s and 100s was lower in the DOX group, indicating that DOX impairs Ca^{2+}-influx (C). The DOX-induced reduction in contraction persisted under L-NAME conditions (D). DOX impaired ACh-induced relaxation, but relaxation of aortic segments in response to DEANO did not change (E). For A, B and E: Repeated measures two-way ANOVA with Šidàk's multiple comparisons test. For C: Unpaired t-test. For D: Two-way ANOVA with Tukey's multiple comparisons test. *, **, ***, **** $p < 0.05$, 0.01, 0.001, 0.0001; n = 6 for each group.*

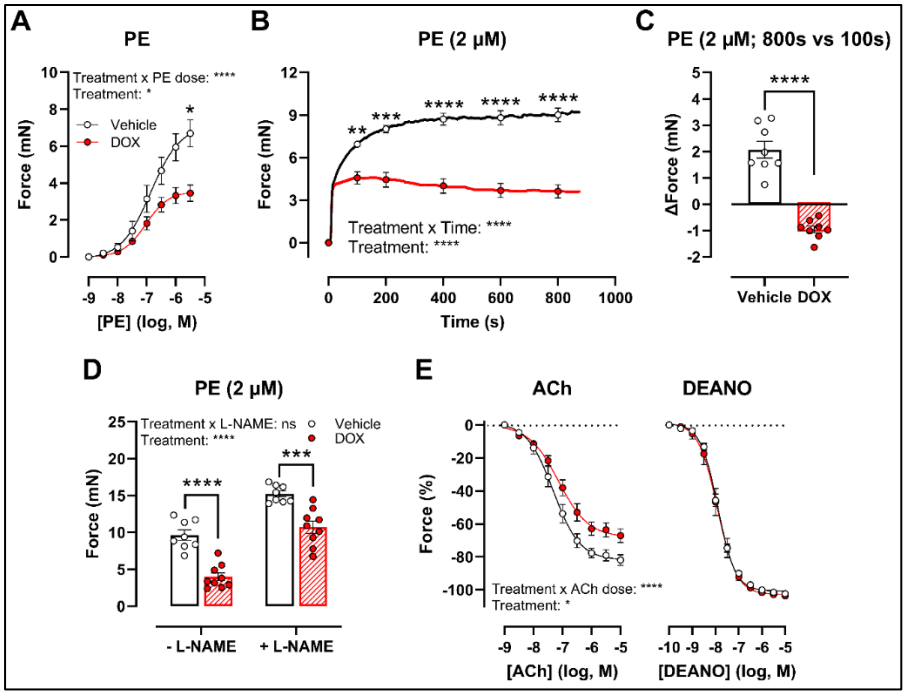

Figure 4.2: VSMC contraction and relaxation in aortic segments after 16 hours of ex vivo DOX treatment. *Following 16 hours of ex vivo DOX-treatment, VSMC contraction was decreased in response to PE (A & B). In the DOX-treated aortic segments, there was a lower increase in force between 800s and 100s (C). The DOX-induced decrease in contraction was still observed in the presence of L-NAME (D). ACh-induced relaxation, but not DEANO-induced relaxation, was impaired in response to DOX (E). For A, B and E: Repeated measures two-way ANOVA with Šidàk's multiple comparisons test. For C: Unpaired t-test. For D: Two-way ANOVA with Tukey's multiple comparisons test. *, **, ***, **** p < 0.05, 0.01, 0.001, 0.0001; n = 8 for vehicle group and n = 9 for DOX group.*

DOX does not modulate Ca^{2+}-release from the sarcoplasmic reticulum or Ca^{2+}-influx through voltage-gated calcium channels

To further investigate the molecular mechanisms of DOX-reduced VSMC contraction, the PE contraction (2 μM) was repeated under 0 mM Ca^{2+} Krebs Ringer and $CaCl_2$ (3.5 mM Ca^{2+}) conditions to specifically evaluate the transient contraction phase caused by Ca^{2+}-release from the sarcoplasmic reticulum, and the tonic contraction phase characterised by VGCC- and NSCC-mediated Ca^{2+}-entry, respectively. To avoid the possible influence of NO, experiments were performed under L-NAME conditions. Contraction mediated by Ca^{2+}-release from the sarcoplasmic reticulum and decline in contraction due to Ca^{2+}-uptake and Ca^{2+}-efflux, were not altered in response to DOX (Figure 4.3A). Upon addition of 3.5 mM Ca^{2+}, thereby promoting Ca^{2+}-entry through VGCCs and NSCCs, the resulting VSMC contraction was lower in the DOX-treated group compared to the vehicle group (Figure 4.3B). Subsequent addition of the VGCC blocker diltiazem (35 μM) revealed similar relaxation between the vehicle- and DOX-treated aortic segments (Figure 4.3C). VSMC contraction, elicited by different doses of K^+ (10, 20, 30, 40 and 50 mM), was not altered after DOX treatment (Figure 4.3D & 4.3E). Moreover, incubation of aortic segments with the VGCC deactivator levcromakalim (1 μM), prior to addition of PE, resulted again in decreased tonic contraction in the DOX-treated group compared to the vehicle group (Figure 4.3E). These results suggest that DOX does not decrease VSMC contraction through molecular mechanisms responsible for intracellular Ca^{2+}-release or Ca^{2+}-uptake, Ca^{2+}-efflux and VGCC-mediated Ca^{2+}-entry.

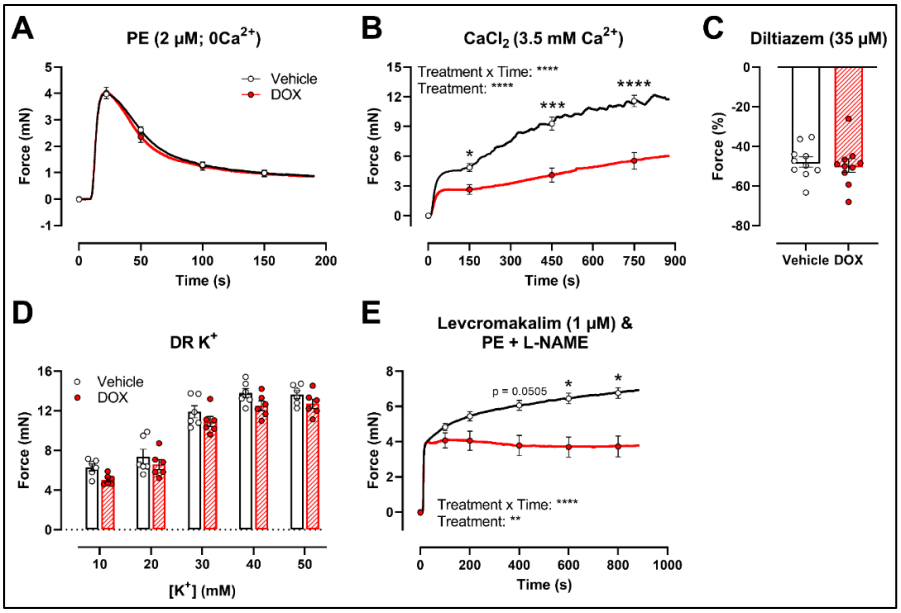

Figure 4.3: Contraction of aortic segments mediated by Ca^{2+}-release from the sarcoplasmic reticulum and Ca^{2+}-entry through VGCCs and NSCCs after 16 hours of ex vivo DOX treatment. *Panel A: Contraction through Ca^{2+}-release from the sarcoplasmic reticulum in response to PE (2 µM) in the absence of extracellular Ca^{2+} (0 mM Ca^{2+}) Panel B: Addition of 3.5 mM Ca^{2+} after 0 mM Ca^{2+} PE-elicited contraction. Panel C: Addition of 35 µM diltiazem following stable $CaCl_2$-mediated contraction. Panel D: Dose response of K^+-elicited contraction (10, 20, 30, 40 and 50 mM). Panel E: PE-induced contraction (with L-NAME) under levcromakalim (1 µM). DOX did not change contraction through Ca^{2+}-release from the sarcoplasmic reticulum, nor Ca^{2+}-uptake and Ca^{2+}-efflux after 16 hours of ex vivo DOX treatment (A), but VSMC contraction was decreased in the DOX-treated group after $CaCl_2$ addition (B). There was no difference in VSMC relaxation between the groups after blocking of VGCCs with diltiazem (C), nor in the contraction magnitude in response to different K^+ doses (D). DOX decreased PE-induced contraction (with L-NAME) in the presence of levcromakalim (E). For A, B, D & E: Repeated measures two-way ANOVA with Šidàk's multiple comparisons test. For C: Unpaired t-test. *, ***, **** $p < 0.05$, 0.001, 0.0001; $p > 0.05$ in A, C & D; Panel A, B & C: n = 10 in each group; Panel D & E: n = 6 in each group.*

Another possibility is that DOX affects NSCC-mediated contraction instead. Accordingly, further experiments were performed using several pharmacological agents blocking a variety of NSCCs, such as tranilast, SKF-96365, 2-APB and 9-phenantrol. To avoid any possible inhibitory effect of NO on VGCCs and NSCCs, the following experiments were performed under L-NAME conditions.

Similar to the decrease in PE-elicited contraction (with L-NAME) under levcromakalim, DOX reduced the PE-induced VSMC contraction (2 μM) in aortic segments, pre-incubated with diltiazem (35 μM) (Figure 4.4A). Subsequent addition of tranilast (100 μM), SKF-96365 (10 μM), 2-APB (20 μM) or 9-phenantrol (1 μM) resulted in a decline in VSMC contraction, which did not differ in absolute values (Figure 4.4B), but was higher in the DOX-treated group when expressed relative to its preceding contraction (Figure 4.4C).

Finally, to evaluate whether the decrease in VSMC contraction after DOX treatment was specific for the PE-elicited response, additional contraction agonists were used. DOX-treated aortic segments showed decreased VSMC contraction in response to 0.25 μM endothelin-1 (Figure 4.5A), but not after 2 μM angiotensin II (Figure 4.5B), 2 μM serotonin (Figure 4.5C) and 50 mM K^+ (Figure 4.5D) stimulation.

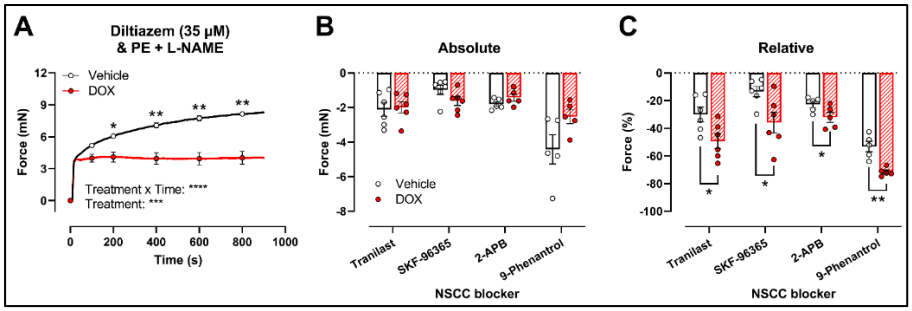

Figure 4.4: Evaluation of the involvement of members of the NSCC family in decreased PE-induced contraction in aortic segments after 16 hours of ex vivo DOX treatment. *Panel A: PE-induced contraction (2 µM, with L-NAME) under diltiazem (35 µM). Panel B & C: Absolute and relative decline in PE-induced contraction (with L-NAME and diltiazem) under, from left to right, tranislast, SKF-96365, 2-APB and 9-phenantrol. DOX decreased PE-induced contraction (with L-NAME) in the presence of diltiazem (A). In addition, the DOX-treated group did not display a significant change in VSMC contraction in absolute values (B), but showed a greater decline in VSMC contraction when expressed relative to its preceding contraction magnitude under tranilast (100 µM), SKF-96365 (10 µM), 2-APB (20 µM) and 9-phenantrol (1 µM) (E). For A: Repeated measures two-way ANOVA with Šidàk's multiple comparisons test. For B & C: Unpaired t-test for each NSCC blocking condition. *, **, ***, **** p < 0.05, 0.01, 0.001, 0.0001; n = 6 in each group.*

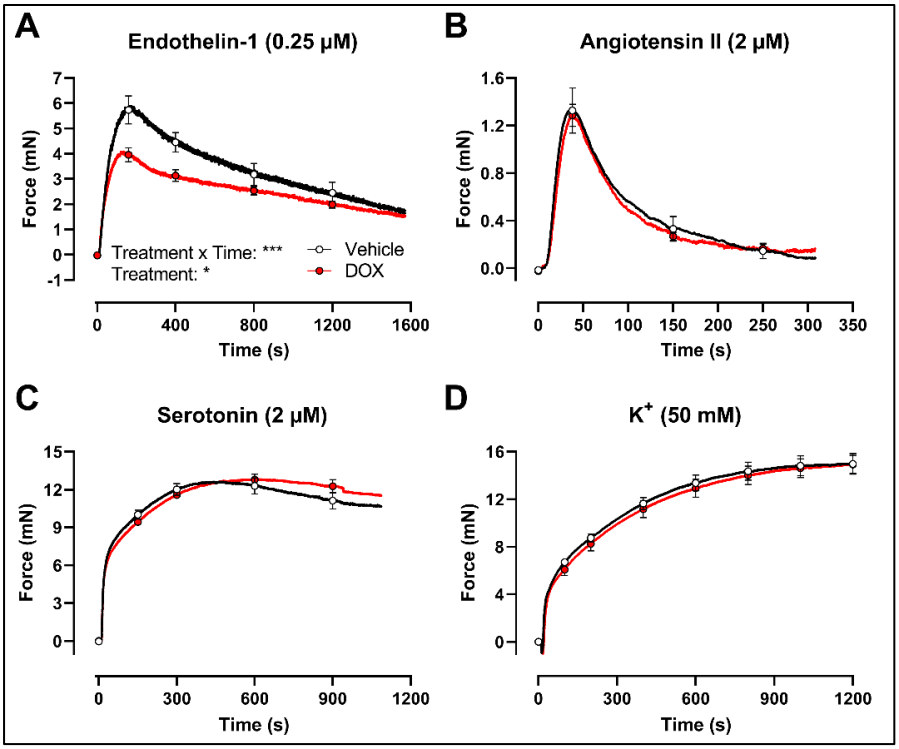

Figure 4.5: Contraction of aortic segments with endothelin-1, angiotensin II, serotonin and K⁺ after 16 hours of ex vivo DOX treatment. *DOX decreased VSMC contraction in response to 0.25 µM endothelin-1 (A), but not after stimulation with 2 µM angiotensin II (B), 2 µM serotonin (C) and 50 mM K⁺ (D). For A-D: Repeated measures two-way ANOVA with Šidàk's multiple comparisons test. *, *** $p < 0.05, 0.001$; $p > 0.05$ in B, C & D; For panel A-C: n = 6 in each group; for panel D: n = 10 in each group.*

A single dose of DOX decreases *ex vivo* arterial stiffness, but not *in vivo* arterial stiffness and blood pressure

The possible translation of the aforementioned findings to arterial stiffness was investigated by evaluation of *ex vivo* and *in vivo* arterial stiffness.

The ROTSAC set-up was used for *ex vivo* evaluation of arterial stiffness, 16 hours after *in vivo* DOX administration (4 mg/kg). Under Krebs Ringer conditions, the Peterson's modulus (Ep), a measure for arterial stiffness, was pressure-dependently lower in the DOX group, especially at higher pressures (Figure 4.6A). This effect was less pronounced in the presence of PE combined with L-NAME (Figure 4.6B). In the presence of DEANO, which removes VSMC tonus, DOX decreased Ep (Figure 4.6C) in a pressure-dependent way.

In vivo arterial stiffness was investigated by measuring aaPWV with ultrasound imaging as well as cfPWV with tonometry, 16 hours after injecting a single DOX dose. Blood pressure and left ventricular ejection fraction (LVEF) were measured as well. DOX did not change aaPWV (Figure 4.6D), cfPWV (Figure 4.6E), blood pressure (Figure 4.6F & 4.6G) and LVEF (Figure 4.6H).

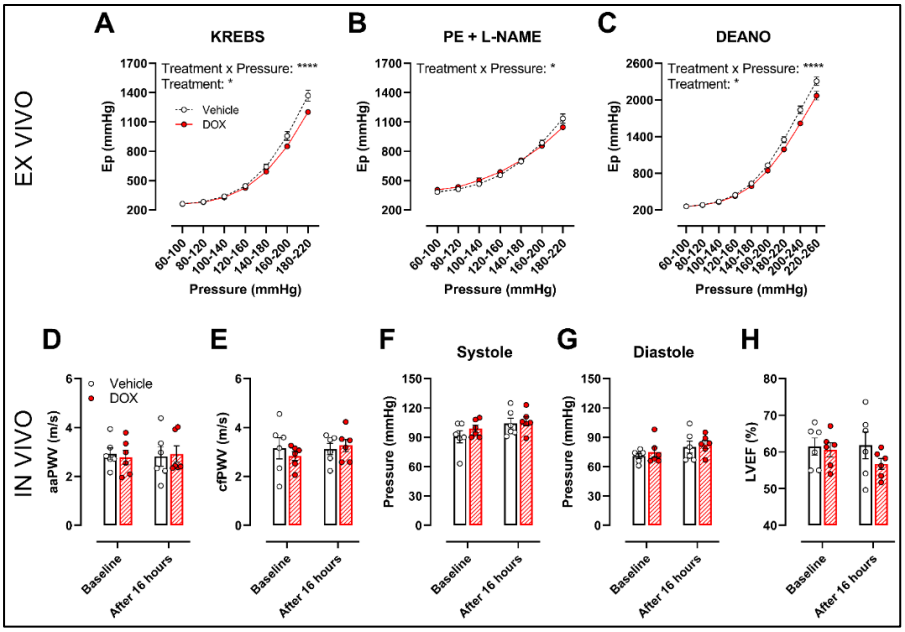

Figure 4.6: Evaluation of in and ex vivo aortic stiffness, 16 hours after in vivo DOX administration. *Panel A - C: Ex vivo evaluation of arterial stiffness with ROTSAC set-up. Panel D & E: In vivo evaluation of arterial stiffness with ultrasound imaging (D) and tonometry (E). Panel F: Systolic blood pressure measurements. Panel G: Diastolic blood pressure measurements. Panel H: Evaluation of LVEF with ultrasound imaging. Ep was lower in the DOX-treated group in a pressure-dependent way under Krebs Ringer conditions (A), but the effect was less pronounced in the presence of PE with L-NAME (B). Ep in response to DEANO was lower after DOX treatment (C). aaPWV (D), cfPWV (E), systolic blood pressure (F), diastolic blood pressure (G) and LVEF (H) were not affected after DOX treatment. For A-H: Repeated measures two-way ANOVA with Šidàk's multiple comparisons test. *, **** $p < 0.05, 0.0001$; $n = 6$ for each group.*

4.4) Discussion

It has been recently recognised that DOX impairs vascular function [27, 30, 90, 118, 120], yet the exact mechanisms are not fully elucidated yet. While there is consensus about the detrimental effects of DOX on endothelium-dependent vasodilation [60, 109, 120, 121], several studies have reported conflicting results on VSMC contraction [62-64]. The present study therefore aimed to investigate VSMC function after a single DOX dose in mice, and how it contributes to arterial stiffness.

DOX decreased PE-induced VSMC contraction and impaired ACh-induced endothelium-dependent relaxation in both the *in vivo* and *ex vivo* treatment setting. Impaired ACh-induced relaxation is in line with previous reports [60, 120, 121]. Endothelial cell loss and reduced eNOS-expression contribute to DOX-induced endothelial dysfunction [60, 120, 121], which leads to decreased NO bioavailability [81]. This, in turn, results in increased vascular tone and augmented arterial stiffness [42, 43]. Contradictory, in the present study, we observed a reduction in VSMC contraction following DOX treatment, even after L-NAME addition. L-NAME inhibits eNOS function, thereby excluding the influence of NO in modulating vascular tone. Accordingly, our data suggest that DOX impairs VSMC contraction through a VSMC-specific mechanism.

For the convenience of the reader, Figure 4.7 illustrates the different mechanisms involved in PE-elicited contraction. Moreover, the different experimental conditions and compounds that were used to elucidate the contributing mechanisms to DOX-induced decrease in VSMC contraction are schematically illustrated in Figure 4.7 [106].

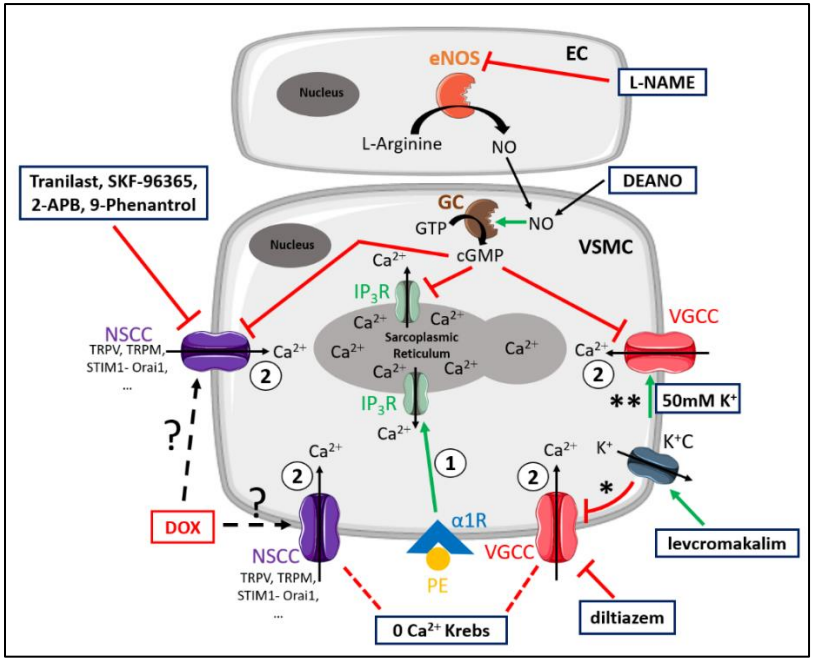

Figure 4.7: Schematic representation of the PE-elicited VSMC contraction response, including the compounds used to delineate the mechanisms of reduced VSMC contraction after DOX treatment. *VSMC contraction through stimulation of α1-adrenergic receptors (α1R) with PE is characterised by two components, namely a fast transient contraction (event 1) and a concomitant tonic contraction (event 2) [106]. Event 1: The fast transient contraction is determined by inositol trisphosphate (IP_3)-mediated release of Ca^{2+} from the sarcoplasmic reticulum through IP_3-receptors (IP_3R) [106]. Event 2: The concomitant tonic contraction is determined by Ca^{2+}-influx via VGCCs and NSCCs [106]. In both phases, cytoplasmic Ca^{2+}-content increases, thereby forming a Ca^{2+}-calmodulin complex [124], which activates the myosin light chain kinase, promotes the binding of actin to myosin and thus initiates contraction [124]. Production of NO in ECs inhibits Ca^{2+}-release from the sarcoplasmic reticulum, and VGCC- and NSCC-mediated Ca^{2+}-influx in a cyclic guanosine monophosphate (cGMP)-dependent way, thereby continuously diminishing contraction [42]. This eNOS-mediated NO production can be inhibited by L-NAME. A 0 mM Ca^{2+} Krebs environment prevents Ca^{2+}-influx, which results in exclusively IP_3-mediated contraction. Diltiazem actively inhibits VGCCs, thereby inhibiting VGCC-mediated Ca^{2+}-influx. Levcromakalim activates ATP-dependent K^+-channels (K^+C), resulting in K^+-efflux, thereby causing a hyperpolarisation (event *) of the resting membrane potential and consequently deactivates VGCCs. In the presence of 50 mM K^+, depolarisation will occur (event **), which will promote VGCC-mediated Ca^{2+}-influx and subsequently leads to VSMC contraction. DEANO acts as an exogenous NO-donor and inhibits VGCCs and NSCCs similarly as NO. Members of the diverse family of NSCCs are TRPV, TRPM, STIM1-Orai1, ... channels, which can be inhibited with tranilast, SKF-96365, 2-APB and 9-phenantrol. DOX may interfere with these channels through an unclear mechanism. Red lines represent inhibition or deactivation, while green lines correspond to activation or stimulation.*

VSMC sensitivity for NO was not affected by DOX, as evidenced by similar endothelium-independent relaxation with DEANO. It is thus most likely that the cGMP pathway is not targeted by DOX.

Further experiments demonstrated that DOX did not alter the initial IP_3-mediated contraction under 0 mM Ca^{2+}-conditions, suggesting that DOX does not affect Ca^{2+}-release from the sarcoplasmic reticulum. Moreover, the subsequent decline in force was similar in the vehicle- and DOX-treated groups. This indicates that DOX does not affect Ca^{2+}-uptake and Ca^{2}-efflux, mediated, for example, by the sarco-endoplasmic reticulum and plasmalemma Ca^{2+}-ATPase pumps, respectively. However, we observed that DOX particularly reduced the tonic contraction phase, which may point to altered Ca^{2+}-influx, either through VGCCs or NSCCs. Relative relaxation of PE-contracted aortic segments with diltiazem, a VGCC-blocker, was not altered after DOX treatment. Under 10-50 mM K^{+}-conditions, depolarisation of the membrane potential will promote VGCC-mediated contraction. VSMC contraction with different doses of K^{+} (10, 20, 30, 40 and 50 mM)$^{+}$ was similar between the vehicle- and DOX-treated group. Moreover, after pre-incubation of aortic segments with levcromakalim and diltiazem, tonic VSMC contraction was lower in the DOX-treated group compared to the vehicle-treated group. These findings indicate that VGCCs are not the molecular mechanism explaining the reduced contractions in the presence of DOX. The attenuated VSMC contraction is therefore possibly attributable to DOX-induced alteration of NSCC function.

Recently, it was found that DOX can inhibit the transient receptor potential vanilloid 2 (TRPV2) channel, a member of the extensive family of NSCCs, in cancer cells by permeating into the channel pore, thereby blocking it [125, 126]. Transient receptor potential (TRP) channels are involved in tumorigenesis, tumour proliferation and tumour migration [125, 127-130]. Since the

discovery that Ca^{2+}-influx plays a crucial role in cancer development [131], targeting corresponding mediators, such as TRP channels, has proven to be an effective strategy in cancer treatment [128, 130, 132]. Importantly, TRP channels play a pivotal role in VSMC contraction where they participate in Ca^{2+}-influx and Ca^{2+}-homeostasis [133]. Therefore, it is conceivable that DOX, as a chemotherapeutic drug, also inhibits TRP channels in aortic VSMCs, similar to tumour cells, thereby contributing to reduced VSMC contraction and vascular toxicity.

To investigate the possible role of DOX in targeting members of the NSCC family, several NSCC blockers, such as tranilast, SKF-96365, 2-APB and 9-phenantrol were evaluated. We limited our selection of NSCC blockers to inhibitors of TRP channels, which have been proven to be involved in VSMC contraction [133]. One should be cautious to interpret the data from the experiments evaluating the role of DOX in NSCC function, because high molecular structure homology between the different subtypes of TRP channels limits the specificity of corresponding NSCC blockers [133]. Accordingly, we selected two specific TRPV2 inhibitors, namely tranilast and SKF-96365 (as stated by literature) [134, 135], and the rather general TRP inhibitor 2-APB. Finally, the TRPM4 blocker 9-phenantrol was also used due to a recently identified role of TRPM4 in breast cancer [136].

Surprisingly, DOX treatment resulted in a greater decline in VSMC contraction in the presence of tranilast, SKF-96365, 2-APB and 9-phenantrol, when expressed relative to the preceding contraction magnitude, showing the contribution of TRP channels to PE contractions. This paradoxical finding suggests that TRP channels play a relative larger role in mediating contraction in DOX-treated aortic segments, and therefore may not be responsible for the decreased VSMC contraction after DOX. Instead, DOX may target other NSCCs that result in attenuated

contraction. However, the lack of knowledge regarding the exact role of TRP channels in vascular function, the high diversity of the NSCC family and the interaction between NSCCs mutually [133] constitutes an important limitation in the current study. Further research to elucidate the mechanistic aspects of NSCCs in vascular biology and also how DOX targets these pathways would be interesting, yet lies beyond the scope of the present work.

Other agonists, such as endothelin-1, angiotensin II and serotonin were subsequently used to determine whether our observations were specific for PE-involved pathways. Endothelin-1, angiotensin II and serotonin were selected as representative agonists for NSCC-, sarcoplasmic reticulum- and VGCC-mediated contraction, respectively. More specifically, endothelin-1 mainly induces vasoconstriction through VGCC- and NSCC-mediated Ca^{2+}-influx, while angiotensin II mediates a phasic contraction through Ca^{2+}-release from intracellular Ca^{2+}-stores, such as the sarcoplasmic reticulum [137]. Serotonin promotes VSMC constriction through Ca^{2+}-release from the sarcoplasmic reticulum in a first transient phase and through primarily VGCC-mediated Ca^{2+}-influx in a second tonic phase [138]. DOX decreased VSMC contraction in response to endothelin-1, but not in the presence of angiotensin II, nor serotonin. These observations further corroborate that Ca^{2+}-release from intracellular Ca^{2+}-stores as well as Ca^{2+}-influx through VGCCs are not targeted by DOX, but that DOX may decrease VSMC contraction through interference with a specific, yet currently unknown, NSCC. Hence, DOX reduces VSMC contraction in a PE receptor-independent way.

Surprisingly, a single dose of DOX decreased *ex vivo* arterial stiffness at higher pressures, which is in contrast to our previous report where two weeks DOX treatment increased VSMC tone and arterial stiffness [120]. It is important to note that

endothelial and VSMC function together actively regulate vascular tone, thereby modulating arterial stiffness [42, 43]. As such, the occurrence of both impaired endothelium-dependent relaxation and diminished VSMC contraction may have a counteracting effect on arterial stiffness. Another possible explanation for the discrepancies regarding VSMC contraction in the previous [120] and current study, lies in the timing for evaluating arterial stiffness. It is conceivable that, in the first acute phase, DOX reduces both VSMC contraction and contributes to endothelial dysfunction, leading to a decrease in arterial stiffness. In a later phase, DOX-induced VSMC impairment reverses, most likely due to clearance of DOX from the vascular system over time, while endothelial dysfunction persists. This, in turn, will increase VSMC tone, thereby actively augmenting arterial stiffness.

In contrast to our previously reported work that DOX increased arterial stiffness after two weeks [120], we found no change in *in vivo* arterial stiffness and blood pressure 16 hours after DOX administration, possibly due to opposing effects of DOX on endothelial and VSMC function. Based on our previous and current data, these findings may have clinical consequences. More specifically, the unchanged and increased arterial stiffness after 16 hours and two weeks of DOX treatment, respectively, may highlight the importance of appropriate timing for evaluating arterial stiffness in DOX-treated patients.

Previous studies have reported decreased VSMC contraction after DOX treatment [63, 64]. In these reports, it is hypothesised that DOX-reduced contraction was mediated by diminished α1-adrenergic receptor expression, or to ROS-induced VSMC death. While others reported similar results [102, 116, 139-141], the data in the current study do not support these proposed mechanisms. In the case of reduced α1-adrenergic receptor expression, the entirety of the PE-contraction response would be

affected, including the IP_3-mediated contraction, which was not observed. Given the fact that DOX also reduced the endothelin-1-elicited VSMC contraction, further supports that DOX-decreased contraction occurs independently of α1-adrenergic receptors. Furthermore, depolarisation-induced contraction would be mitigated in the event of VSMC death [142, 143], yet contraction under 50 mM K^+-conditions was not affected, which excludes the occurrence of VSMC death. Hence, our data indicate that DOX decreases VSMC contraction without affecting α1-adrenergic receptor expression, or contributing to VSMC death.

The difference in the used dosage of DOX in the present study and the aforementioned literature [62-64] may provide an explanation for the divergent mechanisms. The recommended maximal cumulative DOX dose in patients is 450 mg/m^2, which corresponds to 12 mg/kg (assuming a body surface area of 1.9 m^2 and a body weight of 70-75 kg) [15, 96]. Additionally, the maximum tolerated dose (MTD) and median lethal dose (LD_{50}) of DOX in C57BL6/J mice are both 10 mg/kg [144]. Previous reports on reduced VSMC contraction following DOX treatment used a single high dose (> 10 mg/kg), which could induce VSMC death [63, 64, 121]. In the current work, however, a lower DOX dose (4 mg/kg) was used for optimal comparison with previous work, which may affect VSMC function differently.

As a secondary goal, we aimed to develop an *ex vivo* experimental platform for mechanistic studies and for drug screening. In this experimental setting, a DOX dose of 1 μM was used, which is within therapeutic range, since plasma concentrations of DOX have been reported to fluctuate between 0.3 and 1 μM in patients [102, 145]. Since the observed changes in vascular reactivity in response to DOX were similar *in vivo* and *ex vivo*, the platform holds potential for future drug screening.

In conclusion, the present study reports decreased VSMC contraction with coinciding endothelial dysfunction after DOX treatment (4 mg/kg). The decrease in contraction does not relate to alterations in intracellular Ca^{2+}-release, nor Ca^{2+}-influx through VGCCs, but points towards a modulating role for DOX in NSCC function. Experiments with TRP blocking agents failed to pinpoint the exact mechanism causing reduced VSMC contractions, suggesting that DOX may target other NSCCs instead. Importantly, the observation of unchanged *in vivo* arterial stiffness or blood pressure, possibly due to counteracting effects of DOX on EC and VSMC function, may highlight the importance of timing for evaluation of DOX-induced arterial stiffness in patients.

Supplementary Figures

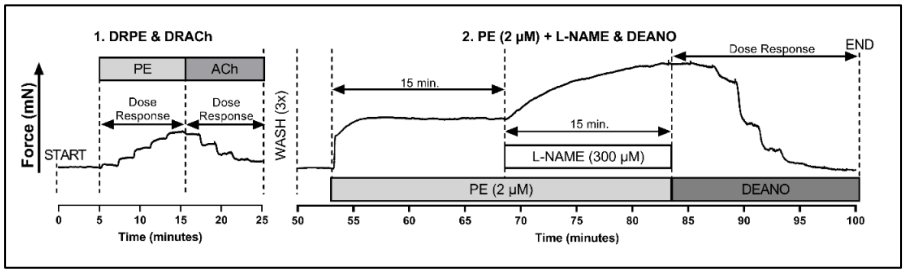

Supplementary Figure 4.1: Experimental protocol for vascular reactivity evaluation in aortic segments after in vivo DOX treatment.

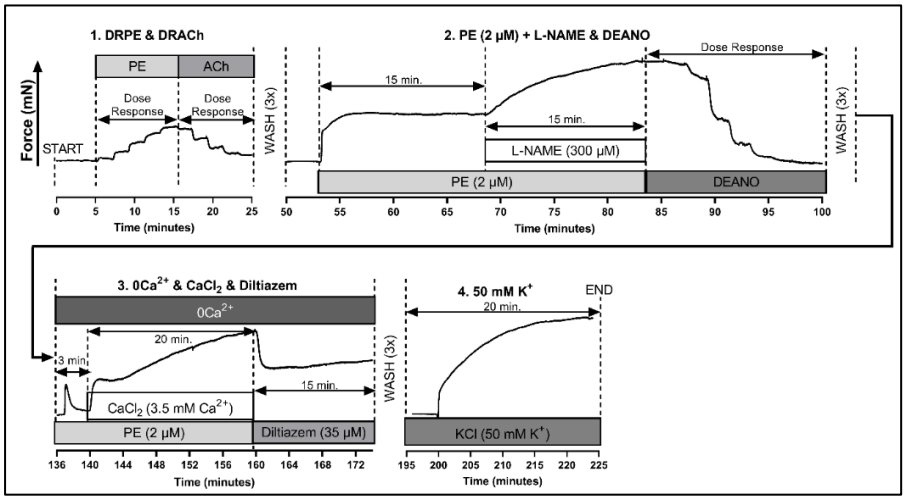

Supplementary Figure 4.2: Experimental protocol for vascular reactivity evaluation in aortic segments after ex vivo DOX treatment.

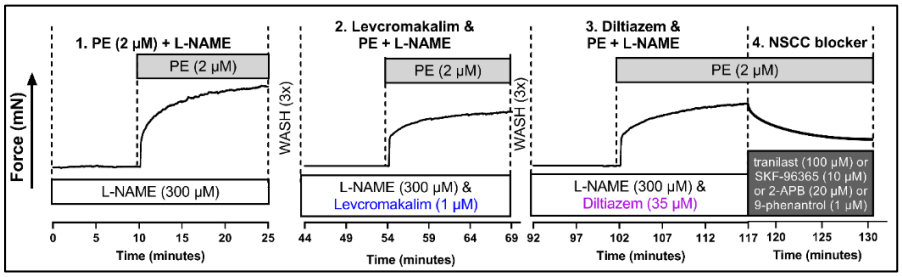

Supplementary Figure 4.3: Experimental protocol for investigation of DOX-induced reduction in VSMC contraction after VGCC inhibition.

CHAPTER V

Doxorubicin impairs endothelial function in a topoisomerase-IIβ-independent way: a preliminary *ex vivo* intervention study with dexrazoxane

In revision at *Plos One* as **Dexrazoxane Does Not Mitigate Doxorubicin-Induced Endothelial Dysfunction in an *ex vivo* Model of Vascular Toxicity**; Bosman M., Krüger D., Favere K., De Meyer G., Franssen C., Van Craenenbroeck E. and Guns P.-J.; Original Research Article

Abstract

Apart from cardiotoxicity, the chemotherapeutic doxorubicin (DOX) induces vascular toxicity, represented by arterial stiffness and endothelial dysfunction, which both have been proposed to further potentiate the risk for heart failure. Prevention of early vascular toxicity could therefore improve patient prognosis. Dexrazoxane (DEXRA), an iron chelator, is thus far the only approved drug for prevention of DOX-induced cardiotoxicity by inhibiting and depleting the DNA repair enzyme topoisomerase-IIβ (TOP-IIβ). However, it remains currently unclear whether DEXRA can mitigate DOX-induced vascular toxicity. Accordingly, the present study investigated the therapeutic potential of DEXRA against DOX-induced vascular toxicity. To this end, a previously-established *ex vivo* model was used where isolated murine (C57BL6/J) aortic segments received either saline (vehicle; 1:100), DOX (1 μM), DEXRA (10 μM) or both DOX and DEXRA for 16 hours. After 16 hours, vascular reactivity was evaluated. DOX impaired acetylcholine-stimulated endothelium-dependent vasodilation, irrespective of DEXRA. Similarly, DOX decreased vascular smooth muscle cell contraction regardless of DEXRA. To explain the inability of DEXRA to prevent DOX-induced vascular toxicity, we assessed TOP-IIβ expression. Unlike cardiomyocytes, murine aortic tissue did not express TOP-IIβ, indicating that neither DOX nor DEXRA targets this pathway. In conclusion, the present study demonstrates that DEXRA does not mitigate DOX-induced vascular toxicity, likely due to the lack of TOP-IIβ expression. From a clinical perspective, these data raise awareness that DEXRA, during early DOX treatment, may not be protective against vascular toxicity.

5.1) Introduction

Despite cardiotoxic side effects, the anthracycline doxorubicin (DOX) remains a first-line chemotherapeutic agent, especially in breast cancer and lymphoma. Clinical and preclinical work has demonstrated that DOX impairs endothelial function and increases arterial stiffness [146, 147], indicating that DOX also targets the vasculature. Interestingly, anthracycline-treated childhood cancer survivors show a higher incidence of systemic hypertension and coronary artery disease, which further potentiate the likelihood for cardiac events [26]. In this respect, it has been proposed that early vascular toxicity contributes to cardiac disease in DOX-treated patients [26]. Therapeutic targeting of early vascular toxicity could therefore represent a promising avenue to pursue.

Dexrazoxane (DEXRA), an iron chelator, is the only approved drug to prevent DOX-induced cardiotoxicity in patients by inhibiting and depleting topoisomerase-IIβ (TOP-IIβ), a DNA-repair enzyme targeted by DOX [23]. Moreover, the DEXRA-derived active metabolite ADR-925 acts as an antioxidant against DOX-induced oxidative damage, although the role of reactive oxygen species (ROS) formation in DOX-induced cardiotoxicity has recently been challenged [23]. Despite its cardioprotective effects, it remains unclear whether DEXRA can prevent vascular toxicity during DOX treatment. Accordingly, we evaluated the therapeutic potential of DEXRA against DOX-induced impairment of vascular function in a previously-established *ex vivo* model of acute vascular toxicity [147].

5.2) Materials & Methods

Animals and ethical approval

Male *C57BL/6J* mice (age: 10-12 weeks; body weight: 24-30 g; Charles River) were housed in the animal facility of the University of Antwerp in standard cages with 12–12 h light–dark cycles with access to regular chow and water *ad libitum*. All experiments were approved by the Animal Ethics Committee of the University of Antwerp (file 2019-34) and conformed with the ARRIVE guidelines and with the Belgian Royal Decree of 2013.

DOX treatment *in vitro* and *ex vivo*

In vitro: Murine cardiomyocytes (passage 3-4) were cultured in Dulbecco's modified Eagle medium (DMEM) medium (Thermo Fisher Scientific) supplemented with 1% penicillin/streptomycin and 10% foetal bovine serum (Thermo Fisher Scientific). Cardiomyocytes were treated with either phosphate-buffered saline solution (PBS) as vehicle (1:100), DOX (1 μM), DEXRA (10 μM) or a combination of DOX (1 μM) and DEXRA (10 μM) for 16 hours. For the latter, DEXRA was administered 15 minutes prior to DOX addition to allow the uptake of DEXRA first, as performed in patients [148]. After 16 hours, cell viability was evaluated with a Countess™ II FL instrument (Thermo Fisher Scientific).

Ex vivo: Mice were euthanised with sodium pentobarbital (200 mg/kg, intraperitoneal; Sanofi), followed by perforation of the diaphragm (when under deep anaesthesia) to isolate the thoracic aorta. Following isolation, the aorta was dissected into segments of 2 mm length and immediately transferred to DMEM medium (Thermo Fisher Scientific) supplemented with 1% penicillin/streptomycin (Thermo Fisher Scientific). Aortic segments were randomly divided and received either PBS as vehicle (1:100), DOX (1 μM), DEXRA (10 μM) or a combination of

DOX (1 μM) and DEXRA (10 μM) for 16 hours. For the latter, DEXRA was administered 15 minutes prior to DOX addition to allow the uptake of DEXRA first, as performed in patients [148]. DOX was diluted in PBS on the day of the experiment. After 16 hours, aortic segments were mounted between two hooks of an organ bath set-up (10 mL) filled with Krebs Ringer solution (37 °C, 95% O_2/5% CO_2, pH 7.4) for vascular reactivity evaluation.

Evaluation of vascular reactivity

Aortic segments were mounted at a preload of 20 mN, and the experimental protocol was started 20 min thereafter to allow optimal stabilisation. Vascular smooth muscle cell (VSMC) contraction was evaluated by adding a single dose of phenylephrine (PE; 2 μM), an α1-adrenergic receptor agonist, for 15 minutes. Next, endothelium-dependent vasodilation was investigated by addition of cumulative concentrations of acetylcholine (ACh; 3 nM–10 μM), a muscarinic receptor agonist. After washing steps to remove PE and ACh, PE-stimulated contraction was repeated, and, once stable, Nω-nitro-L-arginine methyl ester (L-NAME; 300 μM), an inhibitor of endothelial nitric oxide synthase was subsequently added. After 20 minutes, cumulative concentrations of the exogenous nitric oxide (NO)-donor diethylamine NONOate (DEANO; 0.3 nM–10 μM) were added to the organ bath to evaluate endothelium-independent vasodilation of VSMCs through the cGMP-mediated pathway.

Western blotting

Samples were lysed in Laemmli sample buffer (Bio-Rad) containing 5% β-mercaptoethanol (Sigma-Aldrich) and subsequently heat-denatured for 5 min at 100 °C. Next, samples were loaded on Bolt 4–12% Bis-Tris gels (Invitrogen) and after electrophoresis transferred to Immobilon-FL PVDF membranes (Merck). After blocking (1h, Odyssey Li–COR blocking buffer (Li-COR Biosciences)), membranes were

probed with primary antibodies, diluted in Odyssey Li−COR blocking buffer, overnight at 4 °C. The following primary antibodies were used: mouse anti-topoisomerase-IIβ (1:500; MAB6348, R&D systems (Bio-Techne)) and mouse anti-β-actin (1:5000; ab8226, Abcam). The next day, membranes were incubated with IRDye-labeled secondary goat anti-mouse IgG926−68070 (Li−COR Biosciences) for 1 h at room temperature. Membranes were visualised with an Odyssey SA infrared imaging system (Li−COR Biosciences).

Chemical compounds

DOX (Adriamycin®, 2 mg/mL) was purchased from Pfizer (Puurs, Belgium). PE, L-NAME, ACh and DEANO were obtained from Sigma-Aldrich (Overijse, Belgium). DEXRA was purchased from Tocris (Bio-Techne, Dublin, Ireland)

Statistical analysis

All results are expressed as the mean ± standard error of the mean (SEM). Statistical analyses were performed using GraphPad Software (Prism 9—Version 9.5.1; Graphpad, California, United States of America). A p-value < 0.05 was considered statistically significant.

5.3) Results

First, we validated DEXRA efficacy in DOX-treated cardiomyocytes (n=3). Cardiomyocyte viability was significantly lower in the DOX-treated cells (69.0 ± 3.6%) compared to the vehicle (95.7 ± 1.2%) and DEXRA (96.3 ± 0.9) group after 16 hours (One-way ANOVA with Tukey's multiple comparisons test). In comparison with the DOX-treated group, cardiomyocyte viability was significantly higher in cardiomyocytes receiving DOX combined with DEXRA (87.3 ± 3.1%; One-way ANOVA with Tukey's multiple comparisons test), implying that DEXRA is active.

Next, vascular reactivity was evaluated. ACh-stimulated endothelium-dependent vasodilation was impaired in the DOX-treated group (Figure 5.1A). Pre-treatment with DEXRA did not prevent DOX-induced endothelial dysfunction (Figure 5.1A). DEANO-stimulated endothelium-independent vasodilation was similar between all groups (Figure 5.1A). Finally, PE-induced contraction was lower in the DOX-treated group and for the aortic segments that received both DOX and DEXRA (Figure 5.1B).

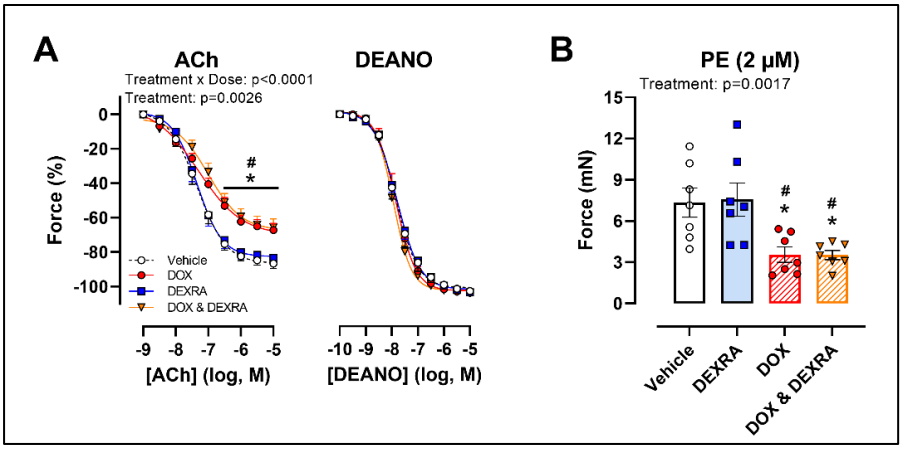

Figure 5.1: Evaluation of vascular reactivity in organ baths. *DOX impaired ACh-induced vasodilation (A) and PE-induced contraction (B), irrespective of DEXRA pre-treatment. For A: Repeated measures two-way ANOVA with Tukey's multiple comparisons test. For B: One-way ANOVA with Tukey's multiple comparisons test. n=7 in each group. *p<0.05 for vehicle vs. DOX group and for vehicle vs. DOX with DEXRA group; #p<0.05 for DEXRA vs. DOX group and for DEXRA vs. DOX with DEXRA group.*

Finally, we assessed whether TOP-IIβ is expressed in murine aortic tissue. TOP-IIβ was expressed in cardiac tissue whereas this was not observed in aortic segments (Figure 5.2).

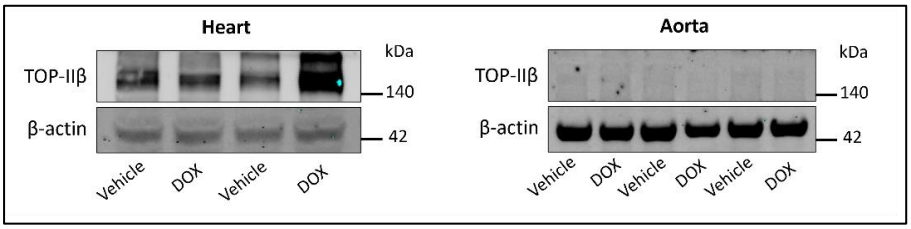

Figure 5.2: Assessment of TOP-IIβ expression in murine cardiac and aortic tissue with Western blotting. *Cardiac, but not aortic tissue, showed TOP-IIβ expression.*

5.4) Discussion

The present study is the first to evaluate the therapeutic potential of DEXRA in DOX-induced vascular toxicity. DOX impaired ACh-stimulated vasodilation and PE-induced contraction, which is identical to our previous observations [147], thus demonstrating the reproducibility of our *ex vivo* model. These results are also in line with our previous *in vivo* observations where DOX (4 mg/kg) impaired endothelium-dependent vasodilation in mice and decreased contraction, 16 hours after administration [147]. As such, the *ex vivo* observations are an accurate reflection of the *in vivo* situation. Importantly, DOX impeded vasodilation and -constriction regardless of DEXRA pre-incubation. Hence, our data indicate that DEXRA does not prevent vascular toxicity during acute DOX treatment.

Our data provide novel mechanistic insight into DOX-induced endothelial dysfunction. In contrast to cardiomyocytes, we did not observe TOP-IIβ expression in mouse aortic tissue. This is surprising as TOP-IIβ has been shown to be ubiquitously expressed in a wide variety of terminally differentiated cells [149]. In any event, the current work indicates that neither DOX nor DEXRA can target TOP-IIβ in the vasculature. DOX-induced endothelial dysfunction therefore most likely occurs through a pathway that does not involve TOP-IIβ.

DOX can be converted into a quinone structure in endothelial cells, thereby generating oxygen radicals that, when reacting with nitric oxide (NO), forms peroxynitrite [108]. As a result, NO levels decrease, which promote VSMC contraction and diminish vasodilation. However, our data do not support that DOX impairs endothelial function through ROS-mediated depletion of NO since DEANO-induced vasodilation curves were aligned in all treatment groups, implying that exogeneous NO is not captured and converted into peroxynitrite.

Previously, He et al. found that DOX decreases the expression of the NO-synthesising enzyme endothelial nitric oxide synthase (eNOS) and diminishes eNOS phosphorylation on its active sites [60]. Likewise, we previously showed lower eNOS expression after two weeks of DOX treatment (4 mg/kg/week) [120]. Conversely, here, we did not observe altered eNOS expression or phosphorylation as a result of DOX treatment (data not shown). Instead of changing expression in a very acute stage, it is possible that DOX inhibits eNOS function as DOX has been shown to bind to the reductase domain of eNOS [108], an important site for NO production. It seems that the impact of DOX on eNOS function is both dose- and time-sensitive. Regardless, our data suggest that, in a very acute phase, DOX impairs endothelial function by modulating eNOS function, and that DEXRA cannot prevent this.

Although our findings only apply to an *ex vivo* setting, the current platform holds translational value. The concentration of 1μM DOX is within clinical therapeutic range as plasma concentrations of DOX can fluctuate between 0.1 and 1μM in patients [150]. Furthermore, while the effect of DEXRA *ex vivo* may differ from the *in vivo* environment, it is reasonable to assume that DEXRA and its antioxidant metabolite ADR-925 were taken up into aortic segments since DEXRA is hydrolysed to ADR-925 in cell culture media, irrespective of present cells or their lysate, and both molecules diffuse readily over the cell membrane [151].

Collectively, our data show that DEXRA does not mitigate DOX-induced endothelial dysfunction. Moreover, DOX impairs endothelial function through a TOP-IIβ-independent pathway. From a clinical perspective, these data raise awareness that, during the early stages of DOX treatment, DEXRA may not be protective against vascular toxicity.

CHAPTER VI

Evaluation of functional and molecular diagnostic markers for doxorubicin-induced cardiovascular toxicity

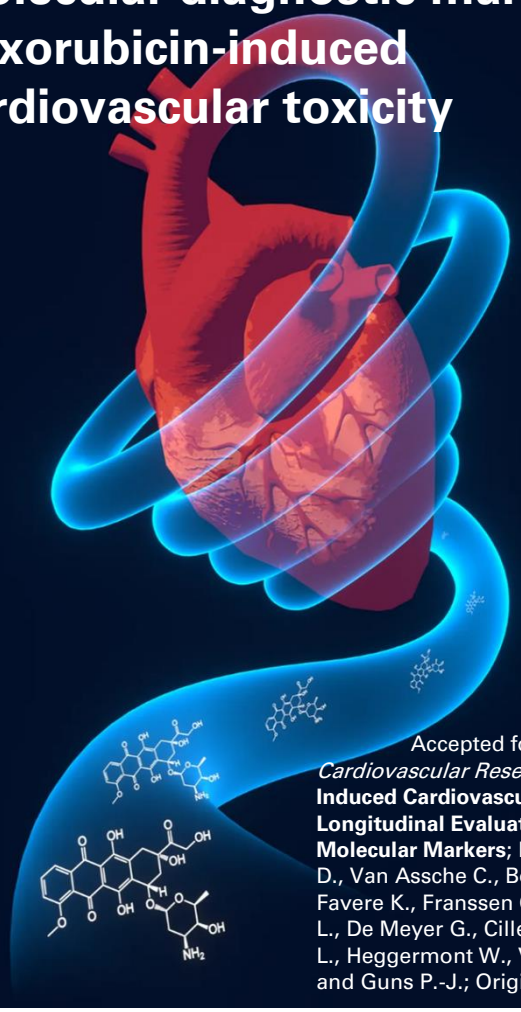

Accepted for publication in *Cardiovascular Research* as **Doxorubicin-Induced Cardiovascular Toxicity: a Longitudinal Evaluation of Functional and Molecular Markers**; Bosman M., Krüger D., Van Assche C., Boen H., Neutel C., Favere K., Franssen C., Martinet W., Roth L., De Meyer G., Cillero-Pastor B., Delrue L., Heggermont W., Van Craenenbroeck E. and Guns P.-J.; Original Research Article

Abstract

Aims: Apart from cardiotoxicity, the chemotherapeutic doxorubicin (DOX) induces vascular toxicity, represented by arterial stiffness and endothelial dysfunction. Both parameters are of interest for cardiovascular risk stratification as they are independent predictors of future cardiovascular events in the general population. However, the time course of DOX-induced cardiovascular toxicity remains unclear. Moreover, current biomarkers for cardiovascular toxicity prove insufficient. Here, we longitudinally evaluated functional and molecular markers of DOX-induced cardiovascular toxicity in a murine model. Molecular markers were further validated in patient plasma.

Methods and Results: DOX (4 mg/kg) or saline (vehicle) was administered intraperitoneally to young, male mice weekly for six weeks. *In vivo* cardiovascular function and *ex vivo* arterial stiffness and vascular reactivity were evaluated at baseline, during DOX therapy (week 2 and 4) and after therapy cessation (week 6, 9 and 15). Left ventricular ejection fraction (LVEF) declined from week 4 in the DOX group. DOX increased arterial stiffness *in vivo* and *ex vivo* at week 2, which reverted thereafter. Importantly, DOX-induced arterial stiffness preceded reduced LVEF. Further, DOX impaired endothelium-dependent vasodilation at week 2 and 6, which recovered at week 9 and 15. Conversely, contraction with phenylephrine was consistently higher in the DOX-treated group. Furthermore, proteomics analysis on aortic tissue identified increased thrombospondin-1 (THBS1) and alpha-1-antichymotrypsin (SERPINA3) at week 2 and 6. Upregulated THBS1 and SERPINA3 persisted during follow-up. Finally, THBS1 and SERPINA3 were quantified in plasma of patients. Cancer survivors with anthracycline-induced cardiotoxicity (AICT; LVEF<50%) showed elevated THBS1 and SERPINA3 levels compared to age-matched control patients (LVEF≥60%).

Conclusions: DOX increased arterial stiffness and impaired endothelial function, which both preceded reduced LVEF. Vascular dysfunction restored after DOX therapy cessation whereas cardiac dysfunction persisted. Further, we identified SERPINA3 and THBS1 as promising biomarkers of DOX-induced cardiovascular toxicity, which were confirmed in AICT patients.

Translational perspective

DOX induced arterial stiffness and endothelial dysfunction, which preceded impairment of left ventricular systolic function. Hence, arterial stiffness and endothelial dysfunction represent potential early, functional markers of future cardiovascular dysfunction in patients receiving DOX. Of note, DOX-induced arterial stiffness and endothelial dysfunction were transient, highlighting the importance of timing for evaluating these vascular parameters in patients. Furthermore, AICT patients showed elevated SERPINA3 and THBS1 in plasma, raising awareness for a role of these proteins in cardiovascular toxicity with possible diagnostic value in DOX-treated patients.

6.1) Introduction

Doxorubicin (DOX), an anthracycline, is a potent chemotherapeutic agent in the treatment of breast cancer, leukaemia and lymphoma [152]. Today, it has been estimated that more than half of lymphoma and childhood cancers and one third of breast cancers are treated with a DOX-based regimen [14]. However, DOX can cause cardiotoxicity and eventually lead to heart failure (HF) [111, 113], which has been extensively investigated in the past (reviewed elsewhere [89]). Interestingly, concomitant presence of modifiable risk factors, such as systemic hypertension, further potentiate the likelihood for cardiovascular events in DOX-treated cancer survivors [26]. Therefore, DOX-induced vascular toxicity could be an early indicator of future cardiovascular events.

Among representations of vascular toxicity, enhanced arterial stiffness and endothelial dysfunction are of particular interest for cardiovascular risk assessment as they have previously been shown to independently predict future cardiovascular events in the general population [47-52]. Despite clinical trials reporting increased arterial stiffness and impaired cardiac function after 3 to 6 months of DOX therapy initiation [27-30, 146], the temporal relationship between these events has not been characterised. Moreover, it remains unclear whether arterial stiffness is reversible after DOX therapy cessation. Finally, while some childhood cancer survivors exhibit endothelial dysfunction months to years after anthracycline therapy completion [31, 32], development of endothelial dysfunction has not been longitudinally investigated so far.

Furthermore, current biomarkers for identification of early myocardial damage in DOX-treated patients prove insufficient. While circulating troponin and (N-terminal pro-)B-type natriuretic peptide show promise to identify patients at cardiac risk, these proteins do not predict adverse cardiac outcome in every subject

[67, 68]. A broadening of the biomarker panel is therefore recommended by the current European Society of Cardiology (ESC) guidelines on cardio-oncology [13].

Here, in a murine model, we evaluated cardiovascular function both during and after DOX therapy to characterise the time course of DOX-induced cardiovascular toxicity. In addition, a proteomics approach was implemented to identify new potential biomarkers, which were further clinically validated.

6.2) Materials & Methods

Animals and ethical approval

Male C57BL/6J mice (Charles River, France) with an age between 10 and 12 weeks and a body weight between 26 and 30 g were used in all experiments. All mice were housed in the animal facility of the University of Antwerp in standard cages with 12–12 hours light-dark cycles with access to regular chow and water *ad libitum*. The Ethical Committee of the University of Antwerp approved all experiments (file 2019-34 and 2020-74), which were conform to Directive 2010/63/EU, the ARRIVE guidelines and to the Guide for the Care and Use of Laboratory Animals published by the US National Institutes of Health (NIH Publication no.85–23, revised 1996).

DOX treatment and experimental workflow

Mice were randomly divided into three cohorts of 16 mice each, namely Cohort 1, Cohort 2 and Cohort 3. In each cohort, half of the mice were intraperitoneally injected with either DOX (4 mg/kg; Adriamycin®, Pfizer, Puurs, Belgium) or vehicle (10 mL/kg of a 0.9% NaCl solution; B. Braun, Belgium) once per week for a total of six weeks. The first and final injection were administered at baseline (week 0) and at week 5, respectively. All cohorts received the same treatment regimen, but differ in the duration of follow-up. There was one week of follow-up for Cohort 1 (up to week 6), four weeks for Cohort 2 (up to week 9) and ten weeks for Cohort 3 (up to week 15). For all cohorts, *in vivo* cardiovascular function was assessed at baseline, week 2 and week 6 with high-frequency ultrasound imaging. *In vivo* cardiovascular function was additionally evaluated at week 4 for Cohort 1, at week 9 for Cohort 2 and at week 15 for Cohort 3. For *ex vivo* assessment of arterial stiffness and vascular reactivity and to perform molecular experiments, Cohort 1, 2 and 3 were sacrificed at week 6, 9 and 15, respectively. To this end, mice were euthanised by

intraperitoneal injection of a single dose of sodium pentobarbital (200 mg/kg; Sanofi, Belgium), followed by perforation of the diaphragm (when under deep anaesthesia) in order to preserve vascular physiology and structure.

High-frequency ultrasound imaging

Ultrasound imaging was performed in anaesthetised mice under 1.5–2.5% (v/v) isoflurane (Forene; Abbvie, Wavre, Belgium) using a high-frequency ultrasound system (Vevo2100, VisualSonics, Toronto, Canada). Images were acquired with a 24 MHz transducer when heart rate and body temperature met the inclusion criteria, i.e., 500 ± 50 beats/min and 37 ± 1 °C, respectively. M-mode images were obtained for measurement of left ventricular anterior wall (LVAW) thickness, left ventricular posterior wall (LVPW) thickness, left ventricular internal diameter (LVID) and calculation of left ventricular ejection fraction (LVEF) and fractional shortening (FS) with Vevo LAB Software (Version 3.2.0, VisualSonics, Toronto, Canada). In the same session, abdominal aorta PWV (aaPWV), a measure for *in vivo* arterial stiffness, was determined according to the method developed by Di Lascio et al. [84]. Briefly, pulse wave Doppler tracing was used to measure aortic flow velocity (V). Immediately thereafter, aortic diameter (D) was measured on 700 frames-per-second B-mode images of the abdominal aorta in ECG-gated kilohertz visualisation (EKV) imaging mode. The ln(D)-V loop method was then applied to calculate aaPWV, using MATLAB v2014 software (MathWorks, Eindhoven, the Netherlands).

Blood pressure evaluation

Systolic and diastolic blood pressure (BP) were determined non-invasively in restrained, awake mice using a tail-cuff system with a programmed electrosphygmomanometer (Coda, Kent Scientific Corporation, Torrington, United States of America). Mice were trained for two days prior to the actual

measurements to reduce stress and variability during measurements. To this end, the cuff system was placed on the mouse tail as performed during the actual measurements. The duration of the training and measurement sessions was 30 minutes. Measurements were only performed in Cohort 3 at baseline and at week 2, 6, 9 and 15.

Ex vivo evaluation of aortic stiffness and vascular reactivity

Mice were intraperitoneally injected with sodium pentobarbital (single dose of 200 mg/kg; Sanofi, Belgium), followed by perforation of the diaphragm (under deep anaesthesia). The thoracic aorta was carefully dissected and cut into segments of 2 mm length, which were subsequently mounted between two hooks of an organ bath set-up (10 mL) filled with Krebs Ringer solution (37 °C, 95 % O_2/5% CO_2, pH 7.4) containing (in mmol/L): NaCl 118, KCl 4.7, $CaCl_2$ 2.5, KH_2PO_4 1.2, $MgSO_4$ 1.2, $NaHCO_3$ 25, CaEDTA 0.025, and glucose 11.1.

Ex vivo assessment of aortic stiffness was performed with the in-house developed organ bath set-up, called "Rodent Oscillatory Tension Set-up to measure Arterial Compliance" (ROTSAC) as previously described [87, 120, 153]. In brief, segments were continuously stretched between alternating preloads corresponding to "systolic" and "diastolic" transmural pressures and at a physiological frequency of 10 Hz to mimic the physiological heart rate in mice (600 beats/ min). Calibration of the set-up allows calculation of the Peterson's modulus (Ep), a measure of *ex vivo* arterial stiffness, based on LaPlace's equation. Ep was calculated as follows: $Ep = D_0 * \Delta P/\Delta D$, with ΔP = difference in pressure (kept constant at 40 mmHg), D_0 = "diastolic" diameter and ΔD = the change in diameter between "diastolic" and "systolic" pressure. The ROTSAC protocol included the evaluation of aortic stiffness (Ep) at 80 – 120 mmHg, under Krebs-Ringer, diethylamine NONOate (DEANO; 2 µM) and

phenylephrine (PE; 2 μM) conditions. DEANO is an exogenous nitric oxide (NO) donor, which removes vascular tone and allows the investigation of the contribution of primarily passive/structural elements to aortic stiffness [42]. PE is an α_1-adrenergic receptor agonist and allows the evaluation of vascular tone in aortic stiffness.

Ex vivo vascular reactivity was studied by mounting aortic segments at a preload of 20 mN. Since we have previously shown that basal NO declines over time [94], the experimental protocol was started 70 min after puncture of the diaphragm to minimise time-dependent biases. Vascular smooth muscle cell (VSMC) contraction was evaluated by adding cumulative concentrations of PE (3 nM – 10 μM). PE-induced contraction is repressed by basal NO [42, 94]. By performing PE-induced contraction after pre-incubation with the endothelial NO synthase (eNOS) inhibitor Nω-nitro-L-arginine methyl ester (L-NAME; 300 μM), and comparing this to PE-induced contraction without L-NAME, the capability of endothelial cells (ECs) to produce basal NO can be investigated [42, 94]. Low basal NO levels lead to higher PE-induced contraction, and similar contraction magnitude in the presence of L-NAME [42, 94]. Endothelium-dependent relaxation was investigated by addition of cumulative concentrations of acetylcholine (ACh) (3 nM – 10 μM), a muscarinic receptor agonist. Finally, Endothelium-independent relaxation was evaluated by using different cumulative concentrations of DEANO (0.3 nM – 10 μM).

Western blotting

Aortic samples were lysed in Laemmli sample buffer (Bio-Rad, Temse, Belgium) containing 5% β-mercaptoethanol (Sigma-Aldrich, Overijse, Belgium) and subsequently heat-denatured for 5 min at 100 °C. Next, samples were loaded on Bolt 4–12 % Bis-Tris gels (Invitrogen, Merelbeke, Belgium) and

after electrophoresis transferred to Immobilon-FL PVDF membranes (Merck, Hoeilaart, Belgium). Of note, no assay to determine the protein concentration could be performed prior to sample loading due to the limited amount of aortic sample (after vascular reactivity and arterial stiffness evaluation). After blocking (1h, Odyssey Li–COR blocking buffer (Li-COR Biosciences, Bad Homburg, Germany)), membranes were probed with primary antibodies, diluted in Odyssey Li–COR blocking buffer, overnight at 4 °C. The following primary antibodies were used: rabbit anti-thrombospondin 1 (1:500; ab267388, Abcam, Cambridge, UK), goat anti-alpha-1-antichymotrypsin (1:1000; catalog number AF4709, Bio-Techne, Dublin, Ireland) and mouse anti-β-actin (1:5000; ab8226, Abcam, Cambridge, UK). The next day, membranes were incubated with IRDye-labeled secondary antibodies (goat anti-rabbit IgG926–32211, donkey anti-goat IgG926-32214 and goat anti-mouse IgG926–68070, all purchased from Li–COR Biosciences, Bad Homburg, Germany) for 1 h at room temperature. Membranes were visualised with an Odyssey SA infrared imaging system (Li–COR Biosciences Bad Homburg, Germany). Western blot data were quantified using ImageJ software. Signal intensity of the proteins of interest were normalised to the β-actin signal intensity.

Histology

Aortic segments were fixed in 4% formalin for 24 h, dehydrated overnight in 60% isopropanol and then embedded in paraffin. Transversal sections (5 μm) were stained with Sirius red or Orcein to determine total collagen and elastin content. Images were acquired with Universal Graph 6.1 software using an Olympus BX40 microscope and quantified with ImageJ software. Total collagen and elastin content were quantified by calculating the signal-to-wall area ratio (expressed as percentage).

Proteomics

Aortic samples (2 segments of 2 mm each) were collected in 5 M urea, 50 mM ammonium bicarbonate (ABC) in 1.5 ml Eppendorf tubes. Cell lysis was performed using a bead beater, followed by three freeze-thaw cycles, using -80°C freezer for freezing and sonicating in an ultrasonic bath for thawing. Undissolved particles were removed by centrifugation (30 minutes; 15.000 g; 4°C) and proteins in solution were transferred to new tubes. Protein samples were reduced with dithiothreitol (DTT; 20 mM) for 45 minutes and alkylated with iodoacetamide (IAM; 40 mM) for 45 minutes in the dark. The alkylation was terminated by adding an additional 20 mM DTT to consume any excess IAM. Next, protein digestion was performed with a mixture of LysC and Trypsin, which was added at a ratio of 1:25 (enzyme to protein). After two hours of digestion at 37°C in a thermoshaker at 750 rpm, the lysate was diluted with ABC (50 mM) to 1M Urea and further digested overnight in the thermoshaker. The digestion was terminated by addition of formic acid (FA) to a total of 1%. Peptide separation was subsequently performed on a Thermo Scientific (Dionex) Ultimate 3000 Rapid Separation ultra-high performance liquid chromatography (UHPLC) system equipped with a PepSep C18 analytical column (15 cm, ID 75 µm, 1,9 µm Reprosil, 120Å). Peptide samples were first desalted on an online installed C18 trapping column. After desalting peptides were separated on the analytical column with a 90 minute linear gradient from 5% to 35% Acetonitrile (©) with 0.1% FA at 300 nL/min flow rate. The UHPLC system was coupled to a Q Exactive HF mass spectrometer (Thermo Scientific) with the following settings: Full MS scan between 250 – 1,250 m/z at resolution of 120,000 followed by MS/MS scans of the top 15 most intense ions at a resolution of 15,000.

For protein identification and quantitation, the DDA spectra were analyzed with Proteome Discoverer (PD) version 2.2. Within the PD software, the search engine Sequest was used with the SwissProt protein database *Mus musculus* (C57BL/6J) (SwissProt TaxID=10090). The database search was performed with the following settings. Enzyme was trypsin, a maximum of 2 missed cleavages, minimum peptide length of 6, precursor mass tolerance of 10 ppm, fragment mass tolerance of 0.02 Da, dynamic modifications of methionine oxidation and protein N-terminus acetylation, static modification of cysteine carbamidomethylation. Protein quantitation was performed by using default LFQ (Label Free Quantitation) settings in PD 2.2. In short, for peptide abundancies, the peptide precursor intensities were used and normalization was performed on total peptide amount. Protein ratios were calculated as the median of all possible pairwise peptide ratios (compared to vehicle) between biological replicates, and background-based ANOVA hypothesis testing was used to ascertain which proteins were significantly differentially expressed. In principle, the background-based method assesses the "distance" of each protein ratio from the corresponding background protein ratios. In brief, the algorithm first establishes a distribution of all proteins with similar abundance and abundance ratios, i.e. "background", and calculates a median abundance ratio and confidence interval for this background population. Of note, the background population is determined for each protein-of-interest individually depending on its absolute abundance with high-abundant proteins-of-interest always being compared to high-abundant background proteins and low-abundant proteins-of-interest to low-abundant background proteins. In a next step, the algorithm assumes that the protein-of-interest has a similar confidence interval, and considers this protein as differentially expressed when confidence intervals do not overlap. Benjamini-Hochberg correction was performed for multiple testing and to calculate

adjusted (adj.) p-values. For a more detailed overview on the background-based method, we refer the reader to a study performed by Navarro et al. on which the PD algorithm was based [154].

Quantification of SERPINA3 and THBS1 in plasma of patients with anthracycline-induced cardiotoxicity

Two cohorts of patients were enrolled, namely cancer survivors with anthracycline-induced cardiotoxicity (AICT; n=14) and control patients (n=27). For the AICT population, cardiotoxicity was defined as development of LVEF below 50% during or following anthracycline treatment. Blood was collected 5 years (median) after anthracycline therapy completion. At the time of blood sampling, AICT patients exhibited a LVEF below 50%. For comparison, age-matched control patients, scheduled for diagnostic heart catheterisation, were included as well. Control patients had normal cardiac function (LVEF ≥ 60%) and no prior history of cancer/cancer treatment. All patients received heparin. This study was approved by the Ethical Committee of the OLV Aalst Hospital and all patients signed an informed consent.

Plasma SERPINA3 and THBS1 levels were quantified using commercially available ELISA kits (Human Alpha 1-Antichymotrypsin ELISA, Immunology Consultants Laboratory, Inc., USA and Human Thrombospondin-1 Quantikine ELISA, Biotechne Ltd.®, R&D Systems®, Abingdon, UK), according to the manufacturer's instructions.

Chemical compounds

PE, L-NAME, ACh and DEANO were obtained from Sigma-Aldrich (Overijse, Belgium).

Statistical analysis

All results were expressed as the mean ± standard error of the mean (SEM), unless stated otherwise. Statistical analyses were performed using GraphPad Software (Prism 9—Version 9.4.0; Graphpad, California, USA). A *p*-value < 0.05 was considered statistically significant. For proteomics, identified proteins were considered differentially expressed when the adj. p-value was below 0.05.

6.3) Results

Survival of DOX-treated mice

No mortality was observed in vehicle-treated mice whereas seven DOX-treated mice died across the cohorts. More specifically, in Cohort 1, one DOX-treated mouse died shortly after the final *in vivo* measurement at week 6. One mouse in the DOX-treated group of Cohort 2 died at week 8. From week 10 to 15, three DOX-treated mice died in Cohort 3. In addition, one mouse in Cohort 2 (at week 5) and one mouse in Cohort 3 (after the *in vivo* measurement at week 15) required euthanasia due to poor health (weight loss >20%, hunched back and lack of grooming). Mice survival for each cohort is summarised in Supplementary Figure 6.1.

DOX transiently increases *in vivo* arterial stiffness

The study design is schematically illustrated in Figure 6.1A.

In all cohorts, DOX consistently increased aaPWV (by 1.3 fold on average) after 2 weeks of treatment, which was no longer observed at week 6, 9 and 15 of follow-up (Figure 6.1B). Of note, DOX-induced arterial stiffness reverted to baseline before the end of the treatment period (at week 4; Figure 6.1B; Cohort 1). Furthermore, LVEF decreased by 10% on average in the DOX group at week 6 in all cohorts, which tended to persist at week 9 and 15 (Figure 6.1C). Pearson correlation between aaPWV at week 2 and LVEF at week 6 for all cohorts showed an inverse correlation (Figure 6.1D). Additional parameters of cardiac function are summarised in Table 6.1, which show lower FS in the DOX-treated group at week 6, 9 and 15. Finally, systolic and diastolic BP, which were only assessed in Cohort 3, were not different during and after DOX treatment (Figure 6.1E). Pulse pressure, the

difference between systolic and diastolic BP, remained unaffected as well (data not shown).

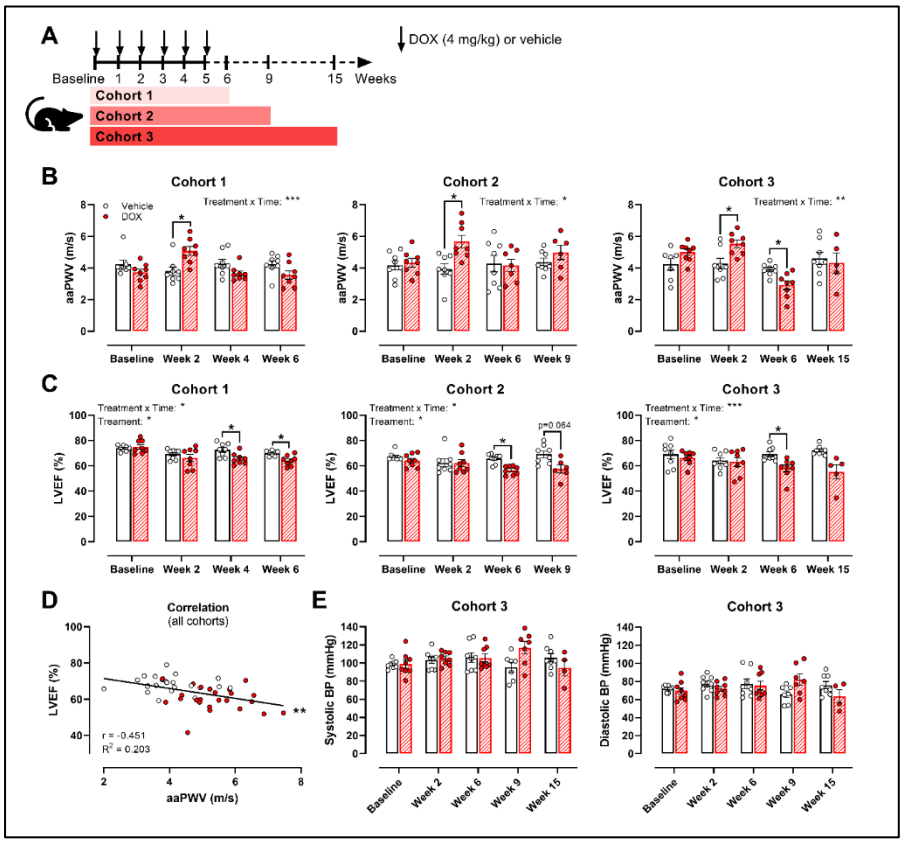

Figure 6.1: Evaluation of in vivo cardiovascular function during and after DOX treatment in each cohort. *Schematic overview of the study design with full and dotted black lines representing treatment and follow-up period, respectively (A). In each cohort, DOX increased aaPWV after 2 weeks of treatment, followed by a return to baseline during follow-up (B). DOX consistently and persistently decreased LVEF in all cohorts (C). LVEF at week 6 showed an inverse correlation with aaPWV at week 2 (D). Systolic and diastolic BP did not change during and after DOX treatment (E). For panels B, C & E: Repeated measures two-way ANOVA with Šídák's multiple comparisons test. For each cohort at baseline: n=8 in vehicle- and DOX-treated group. *, **, ***, p < 0.05, 0.01, 0.001.*

Table 6.1: Cardiac function and body weight at baseline and time point of sacrifice for each cohort.

	Cohort 1		Cohort 2		Cohort 3	
	Baseline Vehicle (n=8) vs. DOX (n=8)	Week 6 Vehicle (n=8) vs. DOX (n=7)	Baseline Vehicle (n=8) vs. DOX (n=8)	Week 9 Vehicle (n=8) vs. DOX (n=6)	Baseline Vehicle (n=8) vs. DOX (n=8)	Week 15 Vehicle (n=8) vs. DOX (n=5)
FS (%)	41.5 ± 0.7 vs. 42.7 ± 1.6	38.9 ± 0.5 vs. 33.9 ± 0.8 **	36.9 ± 1.0 vs. 34.5 ± 1.4	38.3 ± 2.2 vs. 29.9 ± 2.1 **	37.9 ± 2.8 vs. 35.9 ± 1.4	40.7 ± 1.1 vs. 28.6 ± 3.3 **
LVAW (mm; diastole)	0.73 ± 0.04 vs. 0.73 ± 0.02	0.77 ± 0.03 vs. 0.71 ± 0.02	0.80 ± 0.04 vs. 0.80 ± 0.04	0.85 ± 0.05 vs. 0.70 ± 0.05	1.03 ± 0.06 vs. 0.93 ± 0.10	0.85 ± 0.04 vs. 0.71 ± 0.03
LVAW (mm; systole)	1.09 ± 0.04 vs. 1.13 ± 0.04	1.18 ± 0.02 vs. 1.04 ± 0.03 *	1.2 ± 0.05 vs. 1.1 ± 0.06	1.25 ± 0.06 vs. 0.97 ± 0.07 **	1.59 ± 0.07 vs. 1.49 ± 0.09	1.24 ± 0.06 vs. 0.99 ± 0.04 #
LVPW (mm; diastole)	0.83 ± 0.03 vs. 0.85 ± 0.03	0.88 ± 0.06 vs. 0.83 ± 0.04	0.71 ± 0.02 vs. 1.01 ± 0.25	0.75 ± 0.04 vs. 0.79 ± 0.03	1.19 ± 0.08 vs. 1.07 ± 0.06	0.95 ± 0.02 vs. 1.00 ± 0.13
LVPW (mm; systole)	1.42 ± 0.05 vs. 1.43 ± 0.07	1.42 ± 0.05 vs. 1.25 ± 0.03 *	1.25 ± 0.07 vs. 1.24 ± 0.02	1.24 ± 0.05 vs. 1.13 ± 0.05	1.53 ± 0.11 vs. 1.43 ± 0.08	1.58 ± 0.05 vs. 1.27 ± 0.17
LVID (mm; diastole)	3.04 ± 0.17 vs. 3.16 ± 0.10	3.68 ± 0.08 vs. 3.38 ± 0.04	3.68 ± 0.08 vs. 3.70 ± 0.07	3.77 ± 0.10 vs. 3.70 ± 0.12	2.95 ± 0.13 vs. 3.34 ± 0.17	3.64 ± 0.09 vs. 3.87 ± 0.32
LVID (mm; systole)	1.78 ± 0.10 vs. 1.81 ± 0.09	2.25 ± 0.06 vs. 2.23 ± 0.04	2.32 ± 0.05 vs. 2.42 ± 0.08	2.33 ± 0.12 vs. 2.59 ± 0.11	1.82 ± 0.10 vs. 2.14 ± 0.11	2.16 ± 0.09 vs. 2.80 ± 0.37 *
Heart mass (mg)	N.A.	154.8 ± 5.2 vs. 128.1 ± 3.7 **	N.A.	160.2 ± 8.6 vs. 154.0 ± 8.1	N.A.	136.3 ± 11.6 vs. 152.0 ± 11.6
Body Weight (mg)	28.6 ± 0.6 vs. 28.3 ± 0.5	30.4 ± 0.6 vs. 26.5 ± 0.8 ***	25.1 ± 0.7 vs. 26.0 ± 0.6	30.7 ± 1.0 vs. 26.2 ± 1.1 **	25.5 ± 0.8 vs. 25.0 ± 0.6	30.5 ± 0.9 vs. 26.1 ± 1.2 **

For each cohort: Repeated measures Two-Way ANOVA with Šídák's multiple comparisons test. Asterisk indicates statistical significant outcome from multiple comparisons test *, **, *** $p < 0.05, 0.01, 0.001$; # $0.05 < p < 0.06$.

Next, *ex vivo* experiments were performed with the in-house developed ROTSAC set-up, which allows for evaluation of *ex vivo* arterial stiffness in the absence of possible haemodynamic confounders. Of note, the "week 2" data has previously been published, but is shown here to allow for comparison with other time points [120]. Ep was measured at 80-120 mmHg for all conditions. Under unstimulated Krebs conditions, Ep was not altered (Figure 6.2A). On the other hand, DOX increased Ep in the presence of PE at week 2, which was no longer observed at week 6, 9 and 15 (Figure 6.2B). This is in line with the *in vivo* measurements. Finally, Ep values were similar between vehicle- and DOX-treated groups under DEANO (Figure 6.2C).

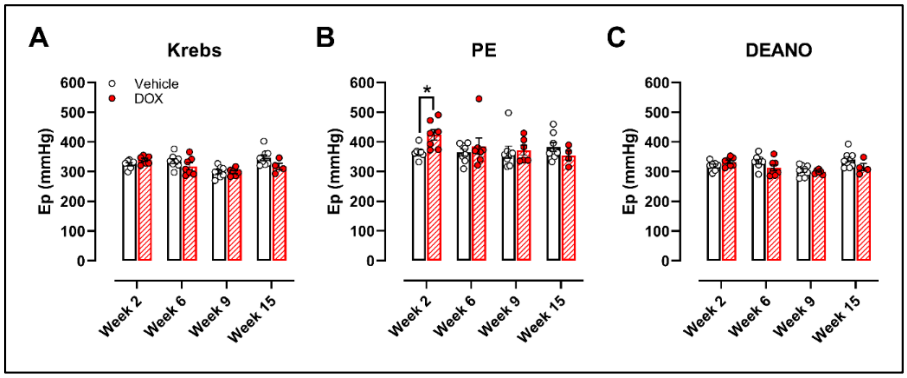

Figure 6.2: Assessment of ex vivo arterial stiffness in aortic segments isolated from vehicle- and DOX-treated mice in ex vivo ROTSAC set-up. *Ep did not differ in Krebs (A). Ep was higher in the DOX-treated group upon PE-induced contraction at week 2 and returned to baseline during follow-up (B). Under DEANO conditions, Ep was not altered (C). For each panel: Repeated measures two-way ANOVA with Šídák's multiple comparisons test. For vehicle: n=8 at each time point; for DOX-treated group: n=7 at week 2 and 6, n=6 at week 9 and n=4 at week 15.*

DOX impairs endothelium-dependent vasodilation which eventually recovers

Vascular reactivity was subsequently examined in depth. Endothelium-dependent vasodilation with ACh was decreased in the DOX-treated group at week 6, which was no longer observed at week 9 and 15 (Figure 6.3A). Endothelium-independent relaxation with DEANO was not altered at any time point (Figure 6.3B).

PE-induced contraction was higher at week 6 and 9 (Figure 6.4A). When contraction in panel A was normalised to maximum contraction, aortic segments from DOX-treated mice exhibited increased sensitivity of contraction at week 6, 9 and 15 (Figure 6.4B). Next, PE-induced contraction after prior incubation of aortic segments with the eNOS inhibitor L-NAME was only higher in DOX-treated mice at week 9 (Figure 6.4C). Normalised contraction from panel C was identical at week 6, 9 and 15 (Figure 6.4D).

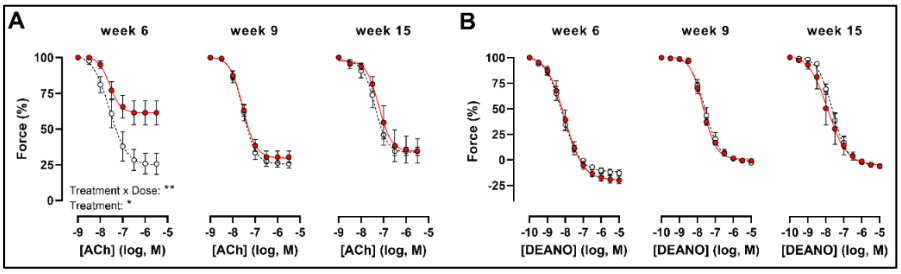

Figure 6.3: Endothelium-dependent (ACh; A) and endothelium-independent (DEANO; B) vasodilation in aortic segments from vehicle- and DOX-treated mice in organ baths. *DOX impaired ACh-induced endothelium-dependent vasodilation at week 6, which recovered thereafter (A). DOX did not affect DEANO-induced endothelium-independent vasodilation at any time point (B). For vehicle: n=8 for each time point; for DOX-treated group: n=7 at week 6, n=6 at week 9 and n=4 at week 15. For each time point in each panel: Repeated measures two-way ANOVA with Šídák's multiple comparisons test. *, ** p < 0.05, 0.01*

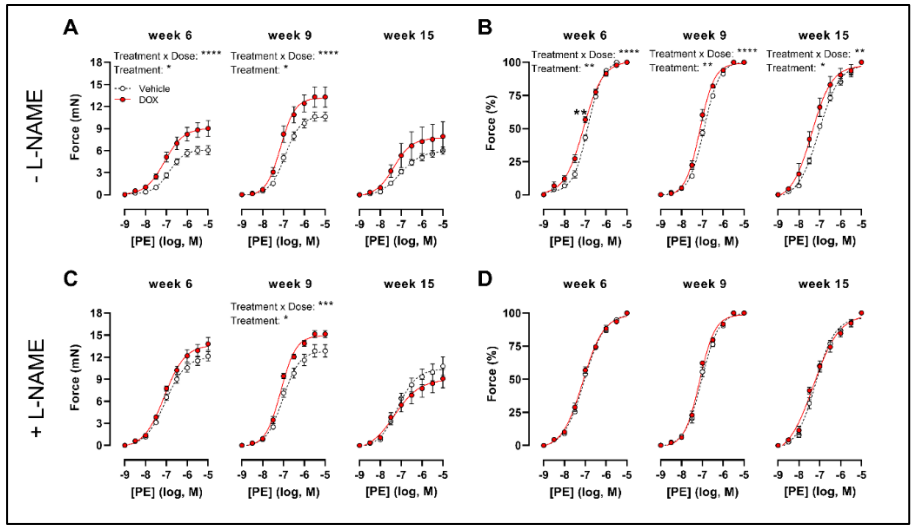

Figure 6.4: PE-induced VSMC contraction in aortic segments from vehicle- and DOX-treated mice in organ baths. *DOX increased PE-induced contraction at week 6 and 9 (A). Normalisation of panel A to maximum contraction revealed higher contraction in the DOX-treated group at all time points (B). PE-induced contraction after pre-incubation with L-NAME was higher in DOX-treated mice at week 9 (C). Normalisation of panel C to maximum contraction revealed similar contraction at all time points (D). For vehicle: n=8 for each time point; for DOX-treated group: n=7 at week 6, n=6 at week 9 and n=4 at week 15. For each time point in each panel: Repeated measures two-way ANOVA with Šídák's multiple comparisons test. *, **, ***, **** p < 0.05, 0.01, 0.001*

DOX does not alter collagen and elastin content nor induces outward structural remodelling

Next, we investigated the occurrence of structural changes in the aortic wall to elucidate why DOX-induced arterial stiffness was no longer present at week 6 despite persistent endothelial dysfunction. Total collagen and elastin content, histologically stained with Sirius red and Orcein respectively, were similar between the vehicle- and DOX-treated group (Supplementary Figure 6.2). Furthermore, aortic diameters, assessed with the ROTSAC set-up under DEANO, did not differ. More specifically, diameters were as follows for the vehicle vs. DOX group: 0.94 ±

0.01 vs. 0.96 ± 0.02 mm at week 2, 1.01 ± 0.04 vs. 0.97 ± 0.02 mm at week 6, 1.07 ± 0.04 vs. 1.06 ± 0.03 mm at week 9 and 1.01 ± 0.01 vs. 1.01 ± 0.06 mm at week 15.

DOX increases THBS1 and SERPINA3 levels during treatment

Proteomics analysis of aortic samples identified a total of 966 proteins (755 with high and 211 with medium confidence), of which 37 were differentially expressed (28 upregulated and 9 downregulated) at week 2 (Table 6.2). At week 6, 25 proteins were differentially expressed (15 upregulated and 10 downregulated) (Table 6.3). The results are visually summarised in Figure 6.5A.

Thrombospondin-1 (THBS1) and α-1-antichymotrypsin orthologue "n" (SERPINA3N; hereafter called "SERPINA3") showed the highest expression levels at week 2 and 6, respectively. We further validated the differential expression of these proteins using Western blotting and investigated whether the upregulation persisted at week 9. For DOX-treated mice, Western blotting revealed increased SERPINA3 at week 2 and 6 (Figure 6.5B). The elevated SERPINA3 levels after 6 weeks of DOX therapy corroborate the proteomics findings. SERPINA3 levels remained higher at week 9 (Figure 6.5B). Furthermore, in the DOX group, increased expression of THBS1 at week 2 and 6 was observed, which is in line with the proteomics results (Figure 6.5B). THBS1 tended to remain high at week 9 ($p=0.052$; Figure 6.5B). For each time point, Western blot images for SERPINA3 and THBS1 are shown in Figure 6.5C. Uncropped blots are shown in the supplementary PDF file.

Table 6.2: Differentially upregulated proteins

	Protein (full name)	Protein (abbreviation)	Abundance ratio (log2)	Adj. P-value
week6 →	Serine protease inhibitor A3N	Serpina3n	1,76	2,96957E-11
	Metallothionein-2	Mt2	1,7	1,51613E-10
	Mannose-binding protein C	Mbl2	1,55	8,50995E-09
	Metallothionein-1	Mt1	1,53	1,43311E-08
	Thrombospondin-1	Thbs1	1,14	0,000102909
	Ferritin light chain 1	Ftl1	1,04	0,000568699
	Collagen alpha-1(XIV) chain	Col14a1	0,91	0,005226539
	Galectin-3-binding protein	Lgals3bp	0,9	0,005619499
	Inter-alpha-trypsin inhibitor heavy chain H1	Itih1	0,81	0,019710441
	Histone H1.0	H1-0	0,81	0,019710441
	Ferritin heavy chain	Fth1	0,78	0,022520654
	Histone H1.2	H1-2	0,76	0,026718423
	Guanine deaminase	Gda	0,71	0,041704211
	Histone H1.4	H1-4	0,71	0,041704211
	Cell surface glycoprotein MUC18	Mcam	0,7	0,048374384
← week2	Thrombospondin-1	Thbs1	1,54	4,84583E-16
	Hemoglobin subunit alpha	Hba	1,24	2,39645E-12
	Hemoglobin subunit beta-1	Hbb-b1	1,19	2,31024E-11
	Mannose-binding protein C	Mbl2	1,14	1,51158E-10

	Carbonic anhydrase 1	Ca1	0,98	5,38887E-08
	Keratin, type I cytoskeletal 15	Krt15	0,8	1,33875E-05
	Spectrin alpha chain, erythrocytic 1	Spta1	0,76	4,56397E-05
	Galectin-3-binding protein	Lgals3bp	0,74	6,7754E-05
	Carbonic anhydrase 2	Ca2	0,71	0,000173933
	Collagen alpha-1(XIV) chain	Col14a1	0,61	0,001516979
	60S ribosomal protein L6	Rpl6	0,6	0,002142236
	von Willebrand factor A domain-containing protein 1	Vwa1	0,58	0,002983958
	60S ribosomal protein L37a	Rpl37a	0,55	0,005777724
	Macrophage-capping protein	Capg	0,53	0,008237738
	Fibrinogen beta chain	Fgb	0,51	0,012023847
	Prolyl 4-hydroxylase subunit alpha-1	P4ha1	0,51	0,013619886
	Peroxiredoxin-5, mitochondrial	Prdx5	0,5	0,014595525
	Actin-related protein 2/3 complex subunit 5-like protein	Arpc5l	0,5	0,014536958
	ATP synthase subunit e, mitochondrial	Atp5me	0,5	0,014499346
	Cytochrome b-c1 complex subunit 7	Uqcrb	0,49	0,018459254
	Splicing factor 1	Sf1	0,48	0,019403422
	Ubiquitin-conjugating enzyme E2 variant 1	Ube2v1	0,47	0,023421801
	GTP:AMP phosphotransferase AK3, mitochondrial	Ak3	0,47	0,023421801
	Fibrinogen gamma chain	Fgg	0,47	0,023409247
	Rho GDP-dissociation inhibitor 2	Arhgdib	0,45	0,035229889
	Acylamino-acid-releasing enzyme	Apeh	0,45	0,035229889

	Histone H2B type 1-M	H2bc14	0,44	0,039779678
	Probable ATP-dependent RNA helicase DDX49	Ddx49	0,44	0,039800113

Table 6.3: Differentially downregulated proteins

	Protein (full name)	Protein (abbreviation)	Abundance ratio (log2)	Adj. P-value
week 6 →	Alpha-1-antitrypsin 1-5	Serpina1e	-2,7	7,76E-16
	Non-histone chromosomal protein HMG-17	Hmgn2	-2,02	2,72819E-13
	60S ribosomal protein L26	Rpl26	-0,98	0,00800989
	Immunoglobulin heavy constant mu	Ighm	-0,98	0,008195314
	Hepcidin	Hamp	-0,91	0,019710441
	ATP synthase subunit e, mitochondrial	Atp5me	-0,89	0,022520654
	Apolipoprotein A-II	Apoa2	-0,88	0,02259218
	Keratin, type I cytoskeletal 15	Krt15	-0,87	0,023702591
	Mitogen-activated protein kinase 9	Mapk9	-0,82	0,038824116
	Splicing factor 1	Sf1	-0,8	0,046903164
← Week 2	UV excision repair protein RAD23 homolog A	Rad23a	-0,9	5,29428E-05
	Ig gamma-1 chain C region, membrane-bound form	Ighg1	-0,89	6,00727E-05
	Band 3 anion transport protein	Slc4a1	-0,82	0,000360669
	Alpha-1-antitrypsin 1-5	Serpina1e	-0,75	0,001648708
	ATP-citrate synthase	Acly	-0,68	0,008056176
	Cytochrome c oxidase copper chaperone	Cox17	-0,63	0,017198238
	Sodium/potassium-transporting ATPase subunit alpha-1	Atp1a1	-0,63	0,017198238
	Hepcidin	Hamp	-0,61	0,023421801
	Clathrin heavy chain 1	Cltc	-0,57	0,047228202

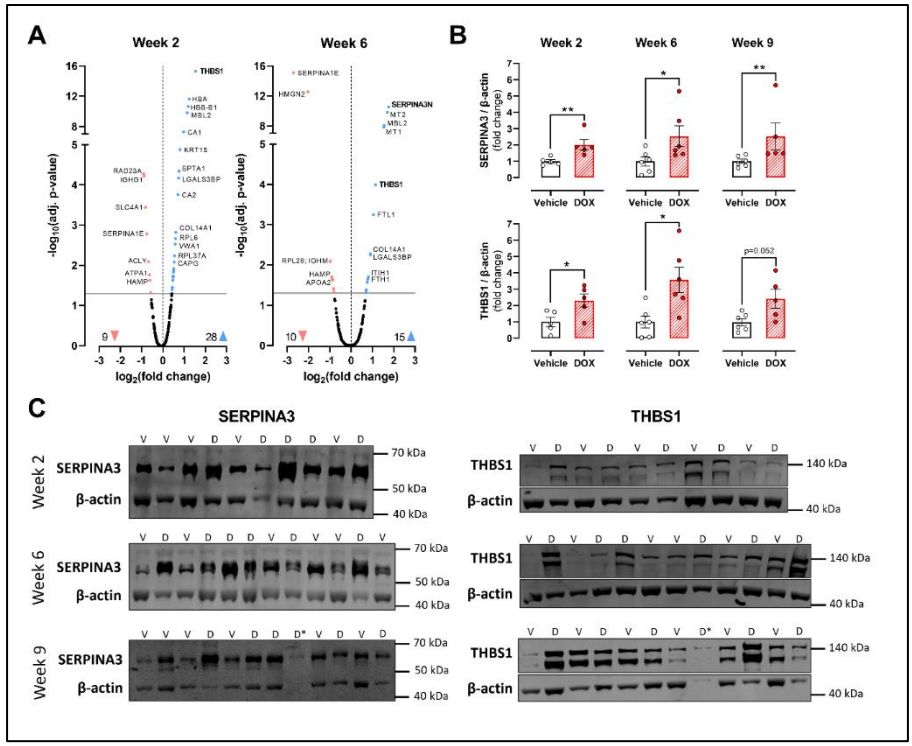

Figure 6.5: Proteomics analysis of aortic samples from DOX-treated mice at week 2 and 6 and validation of most promising biomarkers with Western blotting. *Plots of differentially expressed proteins at week 2 and 6 (A). For A: horizontal grey line indicates significance threshold ($p < 0.05$); upregulated and downregulated proteins are indicated in blue and red, respectively; differentially expressed proteins are abbreviated (full names are listed in abbreviations list). Western blotting shows and corroborates higher levels of SERPINA3 in DOX-treated mice at week 2 and 6, which persist at week 9 (B). Western blotting also confirms higher levels of THBS1 in the DOX-treated group at week 2 and 6, and shows a trend ($p=0.052$) towards increased THBS1 levels at week 9 (B). Representative Western blot images for SERPINA3 and THBS1 at week 2, 6 and 9 (C). For C: "V" and "D" indicate lanes with vehicle and DOX aortic samples, respectively. D* on the blot at week 9 contains a DOX sample for which no protein was detected and was excluded from analysis as such. For A: n=8 in vehicle and DOX group for both week 2 and 6. For B: vehicle group: n=5, n=6 and n=6 at week 2, 6 and 9, respectively; DOX group: n=5, n=6, n=5 at week 2, 6 and 9, respectively. For B: Mann-Whitney test for each time point. *, ** $p < 0.05, 0.01$.*

SERPINA3 and THBS1 increase in plasma of patients with anthracycline-induced cardiotoxicity

The upregulation of SERPINA3 and THBS1 places these proteins as potential biomarkers for DOX-induced cardiovascular toxicity. As such, SERPINA3 and THBS1 levels were quantified in plasma samples from AICT and control patients.

An overview of the patient cohorts is illustrated in Figure 6.6A. Patient characteristics are summarised in Table 6.4 and were as follows: AICT patients (n=14) were aged 59 years (median; range: 41-75 years) and 12 patients (86%) were female. AICT patients were treated for breast cancer (n=11), T-cell lymphoma (n=1), non-Hodgkin lymphoma (n=1) or Hodgkin lymphoma (n=1). For AICT patients, median LVEF was 36% (range: 14-41%) at the time of blood collection. Noteworthy, 12 patients (86%) showed severe cardiotoxicity (LVEF < 40%) as defined by the current ESC guidelines on cardio-oncology [13], and 2 patients (14%) exhibited a LVEF of 40-41%. Furthermore, hypertension and hypercholesterolemia was observed in 1 AICT patient (7%) and 7 AICT patients (50%), respectively. None of the AICT patients had diabetes. For the control group (n=27), patients were aged 57 years (median; range: 48-78 years) and 15 (56%) were female, 11 patients (41%) exhibited hypertension, 11 (41%) showed hypercholesterolemia and 3 (11%) had diabetes. In control patients, median LVEF was 73% (range: 60-88%) at the time of blood collection.

SERPINA3 and THBS1 were both detected in plasma, indicating that these proteins are secreted, and were significantly higher in the AICT group compared to control patients (Figure 6.6B). No differences were observed in SERPINA3 and THBS1 levels between male and female control patients (data not shown). Pearson correlation showed an inverse correlation

between SERPINA3 and LVEF and between THBS1 and LVEF (Figure 6.6C).

Table 6.4: Patient cohort characteristics

	AICT patients	Control patients
Population (n)	14	27
Age (years; median)	59	57
Proportion of females (%)	86	56
Cancer type		
Breast cancer (n)	11	None
T-cell lymphoma (n)	1	None
Non-Hodgkin lymhoma (n)	1	None
Hodgkin lymhoma (n)	1	None
LVEF (%; median)	36	73
Patients with hypertension (n)	1	11
Patients with hypercholesterolemia (n)	7	11
Patients with diabetes (n)	None	3

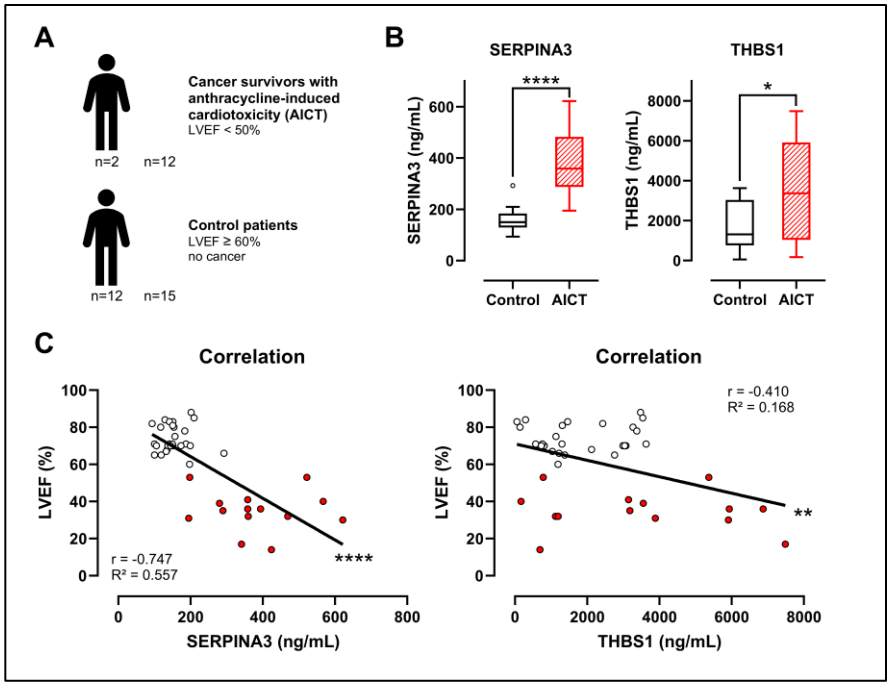

Figure 6.6: Quantification of SERPINA3 and THBS1 levels in plasma of control and AICT patients using ELISA. *Schematic overview of the patient cohorts (A). AICT patients exhibited higher SERPINA3 and THBS1 levels compared to the control group (B). Both SERPINA3 and THBS1 showed an inverse Pearson correlation with LVEF (C). For B: Data is presented as Tukey box plots with median (horizontal line) and the 25th and 75th percentile whiskers. For C: white and red dots represent control and AICT patients, respectively. n numbers are shown in panel A. For B: Mann-Whitney test. *, **** p < 0.05, 0.0001.*

6.4) Discussion

The present study is, to the best of our knowledge, the first to characterise the time course of DOX-induced cardiovascular toxicity, complemented by a biomarker-oriented proteomics approach.

DOX enhanced arterial stiffness by 1.3 fold and decreased LVEF and FS by 10%. This is in line with clinical trials that have reported a 1.2 fold increase in arterial stiffness and a 10% decline in LVEF in cancer patients receiving DOX every 14 to 21 days (cumulative dose range: 50-400 mg/m^2) [27-30, 146]. Hence, the experimental model has translational value. Of note, a decrease of 10% in LVEF is defined as moderate cardiotoxicity in current ESC guidelines [13]. Early identification of moderate cardiotoxicity is important to allow timely intervention before it turns symptomatic and/or irreversible [13]. In light of this growing awareness, our DOX dosing and treatment regimen were designed accordingly and were based on a study by Zhang et al. that reported a 10% decrease in LVEF during DOX treatment [22].

Interestingly, DOX-induced arterial stiffness preceded moderate cardiotoxicity. Additionally, there was an inverse correlation between DOX-induced arterial stiffness after 2 weeks and LVEF decline at week 6. Although these data do not evince a direct contributory role for DOX-induced arterial stiffness to cardiac dysfunction, our data place arterial stiffness as a potential diagnostic marker of future cardiac events in DOX-treated patients.

Decreased left ventricular systolic function persisted after DOX therapy cessation whereas enhanced arterial stiffness recovered rapidly during the treatment period. To corroborate the latter finding, the *ex vivo* ROTSAC set-up was used to assess arterial stiffness in the absence of possible *in vivo* haemodynamic confounders since cardiac function can influence vascular

stiffness [155]. The ROTSAC set-up confirmed the *in vivo* measurements, as evidenced by increased *ex vivo* arterial stiffness at week 2 (under PE conditions), followed by recovery during follow-up. Taken together, these findings indicate that DOX-induced arterial stiffness is transient and reverts independently from *in vivo* haemodynamics.

Our preclinical findings showing recovery of DOX-induced arterial stiffness are in line with the observations of Novo et al. in patients [30]. In their clinical trial, the authors reported enhanced arterial stiffness in breast cancer patients upon DOX therapy completion, followed by recovery at 3 and 9 months after treatment end, while LVEF was lower at all time points [30]. Furthermore, temporary DOX-induced arterial stiffness has been indirectly observed in DOX-treated non-human primates as well [156]. More specifically, Engwall et al. treated these primates with DOX over a period of 19 weeks (cumulative DOX dose of 11-17 mg/kg), and reported that pulse pressure increased after two weeks and subsequently decreased in the DOX group [156]. Since pulse pressure has been proportionally associated with arterial stiffness [70], its biphasic response in the study by Engwall et al. is indicative of transient arterial stiffness.

In the current work, we did not discern changes in either BP or pulse pressure during DOX treatment. This differs from epidemiological studies reporting a higher incidence of systemic hypertension in 5-year anthracycline-treated childhood cancer survivors [26]. It should be mentioned that the experimental design in the current work shows a shorter time frame compared to the 5-year follow-up period in these cancer survivors. Furthermore, our unchanged blood pressure data also differ from Engwall et al. reporting a decrease in BP in DOX-treated non-human primates [156]. This is most likely attributable to different BP assessment methodology. While Engwall et al. evaluated central BP by using telemetry in primates at rest [156], we

assessed peripheral BP with a tail-cuff system in restrained mice. Collectively, these studies indicate that the impact of DOX on BP remains poorly understood.

Although our results show recovery of DOX-induced arterial stiffness, this does not necessarily mean reversal of vascular toxicity. Arterial stiffness is modulated by passive biomechanical properties, such as the collagen-to-elastin ratio [76], by active processes, such as the regulation of vascular tone by VSMCs and ECs [42, 43], and by the mutual interplay between these passive and active elements [76]. As such, multiple vascular events could collectively exert opposing actions on arterial stiffness. For example, in the acute phase (16 hours treatment with 4 mg DOX/kg *in vivo*), we previously observed impaired endothelial function and reduced VSMC contraction, exerting mutual opposing effects, which eventually resulted in unaltered arterial stiffness [147]. This highlights the importance of evaluating both active and passive mechanisms to obtain a complete profile of vascular toxicity.

In depth vascular reactivity evaluation revealed important findings. Previously, we demonstrated that the increase in *in vivo* and *ex vivo* arterial stiffness during the first 2 weeks of DOX treatment resulted from endothelial dysfunction, as evidenced by impaired ACh-stimulated vasodilation and a decreased basal NO index [120]. In the present work, ACh-induced vasodilation in the DOX-treated group remained impaired at week 6, but restored at week 9 and 15. As such, the reversibility of DOX-induced arterial stiffness does not seem attributable to endothelial dysfunction recovery. Surprisingly, PE-induced contraction remained higher during follow-up in the absence, but not in the presence, of L-NAME. We previously reported that such observation is indicative of low basal NO levels [42, 94]. Likewise, decreased basal NO levels and similar ACh-induced vasodilation have been reported in atherosclerotic mouse models with endothelial dysfunction

[157, 158]. Therefore, DOX-induced endothelial dysfunction may only partially restore after therapy cessation, but these data should be interpreted with caution as basal NO levels were not directly measured nor quantified. In any event, our data indicate that, as long as DOX treatment continues, ACh-stimulated vasodilation and basal NO levels remain impaired.

We previously demonstrated that DOX (4 mg/kg) provoked endothelial dysfunction as early as 16 hours after administration, without affecting arterial stiffness or cardiac function [147]. In the present study, DOX increased arterial stiffness after 2 weeks and decreased LVEF from week 4. Taken together, DOX provokes endothelial dysfunction soon after administration, which precedes both arterial stiffness and moderate cardiotoxicity. In this respect, endothelial dysfunction may be an early indicator of future cardiovascular events in cancer patients during DOX therapy.

In an attempt to explain arterial stiffness recovery despite continued endothelial dysfunction (at week 6), we investigated whether structural remodelling was the discriminating factor. Sirius red and orcein stains showed similar amounts of collagen and elastin, and *ex vivo* arterial stiffness under DEANO did not differ. In addition, no outward remodelling occurred, as suggested by similar aortic diameters. However, proteomics on aortic samples revealed differential expression of particularly glycoproteins, such as THBS1, SERPINA3, SERPINA1, MBL2 and LGALS3BP. While these glycoproteins mediate cell-cell and cell-extracellular matrix interactions (GeneCards®; accessed on April 12th 2023), their exact role in vascular physiology and arterial stiffness remains incompletely understood. Further investigating this lies beyond the scope of the current work. Of note, SERPINA3 and THBS1 represented the highest upregulated proteins in response to DOX. Western blotting further confirmed the upregulated expression, and showed that both SERPINA3 and

THBS1 levels remained higher after DOX therapy cessation. As such, SERPINA3 and THBS1 were selected as promising biomarker candidates for clinical validation.

Plasma SERPINA3 and THBS1 levels were higher in middle-aged AICT cancer survivors compared to control patients. Moreover, in these patients, there was an inverse correlation between SERPINA3 and LVEF and between THBS1 and LVEF.

SERPINA3 is a serine protease inhibitor, involved in acute-phase inflammatory responses [159], and has been implicated in Alzheimer's disease and various types of cancer, such as breast and colorectal cancer [159-161]. In recent years, SERPINA3 has been proposed as a prognostic marker for cardiovascular disease [162-166]. More specifically, Zhao et al. suggested that SERPINA3 predicts adverse cardiac events in patients with myocardial infarction [166]. Similarly, Delrue et al. reported circulating SERPINA3 to be associated with worse outcome in patients with *de novo* or worsened HF [163]. Finally, SERPINA3 has also been shown to be increased in plasma of patients with coronary heart disease [165]. Despite its association with adverse cardiovascular outcome, it remains unclear whether SERPINA3 actively contributes to cardiovascular disease development or whether it is released as a general response to toxic events. Also the role of SERPINA3 in normal cardiovascular physiology is poorly understood [159]. In any event, the present study is the first to demonstrate that DOX treatment is associated with increased SERPINA3 in the vasculature and to find upregulated SERPINA3 in plasma of AICT patients. Our data therefore raise awareness for a role of SERPINA3 in cardiovascular toxicity and place SERPINA3 as a potential diagnostic biomarker for anthracycline-induced cardiovascular toxicity.

THBS1 is a secretory ECM protein and primarily mediates cell-to-cell and cell-to-matrix interactions. It has been shown that THBS1 can prevent vascular endothelial growth factor-mediated eNOS and guanylate cyclase activation, which could be an explanation why impaired basal NO production possibly persists after DOX therapy cessation, and thus may explain the higher PE contractions [167]. Apart from inhibiting eNOS, THBS1 has been proposed to fulfil a protective role in the cardiovascular system as THBS1 deficiency in rodent models deleteriously impacts cardiovascular physiology [168]. For example, THBS1 deficiency has been observed to provoke early onset of cardiac hypertrophy following pressure overload [169], prolong and enhance inflammatory responses after myocardial infarction [170], and accelerate atherosclerotic plaque maturation [171]. In rodent models of HF, THBS1 has also been shown to be upregulated, presumably in an adaptive attempt to maintain cardiac function by promoting cardiac remodelling [172, 173]. As such, increased THBS1 levels have been proposed as indicators of future HF [173]. To our knowledge, the current work is the first to show increased plasma THBS1 levels in AICT patients. Whether THBS1 is upregulated in response to HF remains unclear, but highlights this protein as a possible indicator of future cardiac events in patients receiving DOX.

Apart from SERPINA3 and THBS1, the other identified glycoproteins (i.e. SERPINA1, MBL2 and LGALS3BP) have been implicated in cardiovascular disease as well. For example, it has been demonstrated that patients with SERPINA1 deficiency exhibit a higher incidence of systemic hypertension, chronic heart failure and cardiac arrythmia [174]. Moreover, elevated MBL2 levels in serum have been associated with development of coronary artery disease [175]. Finally, LGALS3BP overexpression and secretion have been proposed to play an important part in heart failure and atherosclerosis [176]. Similar to SERPINA3 and

THBS1, the exact role of SERPINA1, MBL2 and LGALS3BP in cardiovascular (patho)physiology remains incompletely understood.

In summary, left ventricular systolic function was persistently reduced in DOX-treated mice whereas arterial stiffness and endothelial dysfunction were transient. Interestingly, arterial stiffness preceded impairment of systolic function and showed an inverse correlation with LVEF decline. Moreover, endothelial dysfunction manifested prior to arterial stiffness and reduced LVEF, and persisted during the DOX treatment period. Hence, we propose that arterial stiffness and endothelial dysfunction hold potential as diagnostic, but time-sensitive, functional markers of future cardiovascular events in patients receiving DOX. Furthermore, we identified SERPINA3 and THBS1 upregulation in murine aortic tissue during DOX treatment. In AICT patients, plasma SERPINA3 and THBS1 levels were elevated as well, highlighting these proteins as potential contributors or response proteins to cardiotoxicity. As such, SERPINA3 and THBS1 hold possible diagnostic value for cardiovascular risk assessment in adult DOX-treated patients.

Limitations

The present study has several limitations. First, our findings apply to young, male mice, which may differ from female and old mice. Young, male mice were chosen as they are more sensitive to DOX-induced cardiotoxicity [177-179], and to avoid the influence of cyclic changes in female hormones as confounding factors. Similarly, female sex offers protection against DOX-related cardiotoxicity in patients [177]. Second, the DOX administration route in the current work differs from the clinical setting where DOX is mainly administered intravenously. Third, although we position arterial stiffness and endothelial dysfunction as potential markers for cardiotoxicity in DOX-treated

patients, further clinical validation is required with well-defined time points. Finally, our data only show an increase in SERPINA3 and THBS1 levels in adult AICT patients, and more research is required to investigate whether SERPINA3 and THBS1 can actually predict cardiovascular events in DOX-treated patients of all ages.

Supplementary Figures

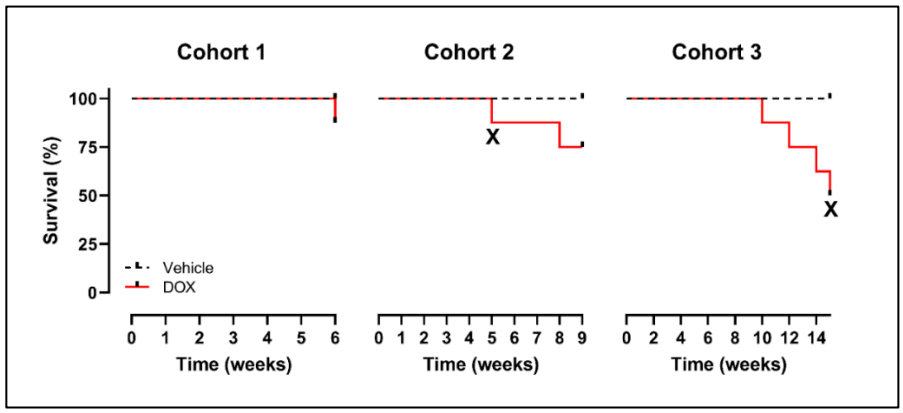

Supplementary Figure 6.1: Mice survival in each cohort. *Survival curves of Cohort 1, 2 and 3 (A). Note: "X" indicates a time point where a DOX-treated mouse was prematurely sacrificed as a consequence of poor health (weight loss > 20%, hunched back and lack of grooming).*

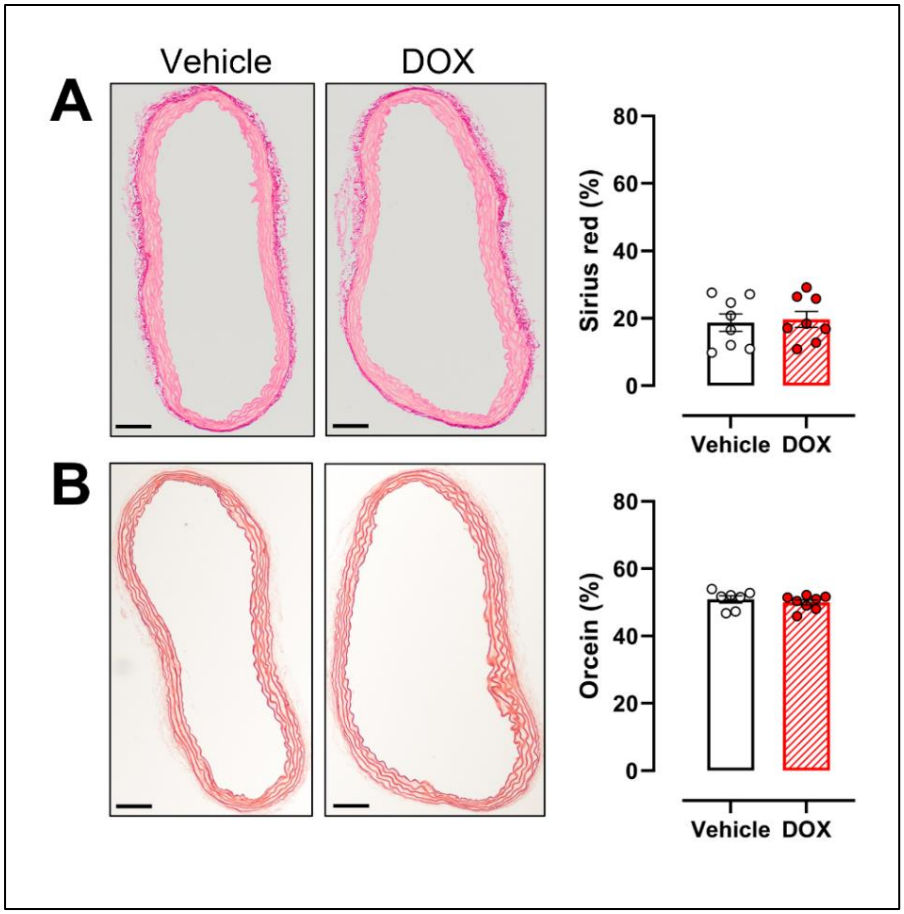

Supplementary Figure 6.2: Determination of total collagen and elastin content at week 6. *Sirius red and orcein positivity for total collagen (A) and elastin (B), respectively. For both panels: Unpaired samples t-test ($p > 0.05$). n=8 in each group. Scale Bar: 100 µm.*

CHAPTER VII

Doxorubicin does not exacerbate atherosclerotic plaque formation in apolipoprotein E-deficient mice

Abstract

AIMS: The chemotherapeutic agent and anthracycline doxorubicin (DOX) induces cardiotoxicity. Interestingly, epidemiological data in anthracycline-treated cancer survivors reveal a higher incidence of atherosclerosis, which has been associated with increased risk for heart failure in these patients. Previously, we and others showed that DOX induces arterial stiffness and endothelial dysfunction, both key antecedents to atherosclerosis development. In this respect, DOX may accelerate atherosclerotic plaque formation, yet this has not been investigated so far. Accordingly, the present study investigated whether DOX exacerbates atherosclerosis development.

METHODS: Apolipoprotein E-deficient ($ApoE^{-/-}$) mice (age 6-7 weeks; male and female) were fed a high-fat (HF) diet for 17 weeks. Starting at week 3, DOX (4 mg/kg) was administered intraperitoneally to half of the mice in each group once a week for 3 weeks. After 17 weeks, mice were humanely killed to assess the amount and the content of plaque in the thoracic aorta, proximal aorta and brachiocephalic artery.

RESULTS: Overall, total plaque amount and plaque content did not differ in the thoracic aorta and brachiocephalic artery of DOX-treated mice while sex differences in plaque size were observed. Paradoxically, DOX treatment resulted in smaller plaques in female mice, but not male mice.

CONCLUSIONS: In contrast to epidemiological reports, DOX does not seem to accelerate atherosclerotic plaque formation, although this study needs to be confirmed in a treatment study with shorter follow-up.

7.1) Introduction

Doxorubicin (DOX), a member of the anthracycline family, is routinely used in chemotherapy of solid and haematological tumours, but also induces cardiotoxicity, which can eventually lead to heart failure [180, 181]. Interestingly, epidemiological data reveal a higher incidence of coronary artery disease in anthracycline-treated childhood cancer survivors compared to control siblings, which further potentiates the risk for heart failure in these patients [26].

Atherosclerosis is a chronic inflammatory disease, which is characterised by lipid-containing plaque formation in the vascular wall of medium- and large-sized blood vessels [182, 183]. Mechanistically, endothelial dysfunction, a pro-vasoconstriction and pro-inflammatory state of the endothelium typically resulting from decreased nitric oxide (NO) production, represents the predominant initiator of plaque formation [59, 184-186]. Moreover, endothelial dysfunction enhances vascular tone, thereby augmenting arterial stiffness [42, 43], which has also been proposed to promote atherosclerotic plaque formation [187, 188].

Previously, we and others have demonstrated that DOX increases arterial stiffness and provokes endothelial dysfunction [60, 120, 146, 147]. As such, we hypothesised that DOX accelerates atherosclerosis development by inducing arterial stiffness and endothelial dysfunction. However, a direct link between DOX treatment and atherosclerosis development has not been established at present. Accordingly, here, we assessed whether DOX exacerbated atherosclerotic plaque formation in young apolipoprotein E-knockout ($ApoE^{-/-}$) mice that were fed a high-fat (HF) diet.

7.2) Materials & Methods

Animals and ethical approval

Standard male and female ApoE$^{-/-}$ mice (Charles River, France) with an age between 6 and 7 weeks and a body weight between 17 and 20 g were used in all experiments. All mice were housed in the animal facility of the University of Antwerp in standard cages with 12–12 hours light-dark cycles with access to regular chow and water *ad libitum*. The Ethical Committee of the University of Antwerp approved all experiments (file 2021-19), which were conform to Directive 2010/63/EU, the ARRIVE guidelines and to the Guide for the Care and Use of Laboratory Animals published by the US National Institutes of Health (NIH Publication no.85–23, revised 1996).

DOX treatment and experimental workflow

At the age of 6 weeks, all mice were placed on a HF diet, containing in g/kg: 195.0 casein, 3.0 DL-methionine, 341.46 sucrose, 150.0 corn starch, 210.0 anhydrous milkfat, 1.5 cholesterol, 50.0 cellulose, 35.0 mineral mix, 4.0 calcium carbonate, 10.0 vitamin mix, 0.04 ethoxyquin (TD.88137; Inotiv (Envigo), Italy), for a total period of 17 weeks. After 2 weeks of HF diet (at the age of 8 weeks), male and female ApoE$^{-/-}$ mice were randomly divided into two groups where one group received DOX (4 mg/kg; Adriamycin®, Pfizer, Belgium; intraperitoneal) once per week for three consecutive weeks and the other group received vehicle (10 mL/kg of a 0.9% NaCl solution; B. Braun, Belgium). HF diet was not interrupted during the treatment period and continued after treatment end. Using ultrasound imaging, cardiovascular function was evaluated just before the first DOX injection at 8 weeks of age (baseline), at the age of 10 weeks (treatment end) and during follow-up at the age of 14 and 23 weeks. At the age of 23 weeks (after 17 weeks of HF diet), all mice were sacrificed by intraperitoneal injection of sodium

pentobarbital (single dose of 200 mg/kg; Sanofi, Belgium), followed by perforation of the diaphragm (when under deep anaesthesia). The thoracic aorta, brachiocephalic artery and the proximal ascending aorta were isolated and fat tissue was carefully removed for quantification of plaque amount and molecular analysis of plaque content. An overview of the experimental design is illustrated schematically in Supplementary Figure 7.1.

High-frequency ultrasound imaging

Ultrasound imaging was performed in anaesthetised mice under 1.5–2.5% (v/v) isoflurane (Forene; Abbvie, Wavre, Belgium) using a high-frequency ultrasound system (Vevo2100, VisualSonics, Toronto, Canada). Images were acquired with a 24 MHz transducer when heart rate and body temperature met the inclusion criteria, i.e., 500 ± 50 beats/min and 37 ± 1 °C, respectively. M-mode images were obtained for measurement of left ventricular anterior wall (LVAW) thickness, left ventricular posterior wall (LVPW) thickness, left ventricular internal diameter (LVID) and calculation of left ventricular ejection fraction (LVEF) with Vevo LAB Software (Version 3.2.0, VisualSonics, Toronto, Canada). In the same session, abdominal aorta PWV (aaPWV), a measure for *in vivo* arterial stiffness, was determined according to the method developed by Di Lascio et al. [84]. Briefly, pulse wave Doppler tracing was used to measure aortic flow velocity (V). Immediately thereafter, aortic diameter (D) was measured on 700 frames-per-second B-mode images of the abdominal aorta in ECG-gated kilohertz visualisation (EKV) imaging mode. The ln(D)-V loop method was then applied to calculate aaPWV, using MATLAB v2014 software (MathWorks, Eindhoven, the Netherlands).

Plasma cholesterol level quantification

Total plasma cholesterol levels were quantified by using a commercially available kit according to the manufacturer's instructions (Randox, Crumlin, UK).

Quantification of plaque amount and molecular analysis of plaque content

The thoracic aorta was stained *en face* with Oil Red O to determine plaque burden. The brachiocephalic artery and proximal ascending aorta were fixed in 4% formaldehyde (pH7.4) for 24 hours, dehydrated overnight in 60% isopropanol and subsequently embedded in paraffin. Serial cross-sections (5µm) of the proximal parts of the brachiocephalic artery and proximal ascending aorta were prepared in random for histological analyses. Atherosclerotic plaque size and necrotic core area (defined as acellular areas with a threshold of 3000 μm^2) were analysed on haematoxylin-eosin (H&E) stained sections. For molecular analysis of plaque content, macrophage and VSMC levels were determined using immunohistochemistry with the following antibodies, respectively: anti-MAC3 (BD Pharmingen, 550292, San Diego, CA, USA) and anti-α-smooth muscle actin (αSMA, 12547, Sigma-Aldrich, St. Louis, MO, USA). Images were acquired with an Olympus BX43 microscope, which was calibrated for each magnification. Plaque size was measured based on pixels per µm, which was determined during the calibration of the microscope. Per mouse, one section was analysed. Plaques were manually delineated in Image J software (National Institutes of Health) to establish the region of interest (ROI). Immunohistochemical analyses within the ROIs were performed using colour thresholding.

Statistical analysis

All results were expressed as the mean ± standard error of the mean (SEM). Statistical analyses were performed using GraphPad Software (Prism 9—Version 9.4.0; Graphpad, USA). A p-value < 0.05 was considered statistically significant.

7.3) Results

DOX-induced arterial stiffness continues after therapy cessation in male, but not female, mice

First, cardiovascular function was evaluated to validate our model. In both male and female mice, DOX increased aaPWV after two weeks of treatment (Figure 7.1A & 7.1B). Interestingly, DOX-induced arterial stiffness continued after therapy cessation in male mice whereas this recovered in female mice (Figure 7.1A & 7.1B). LVEF decreased in the DOX-treated female, but not in the male, mice (Figure 7.1C & 7.1D).

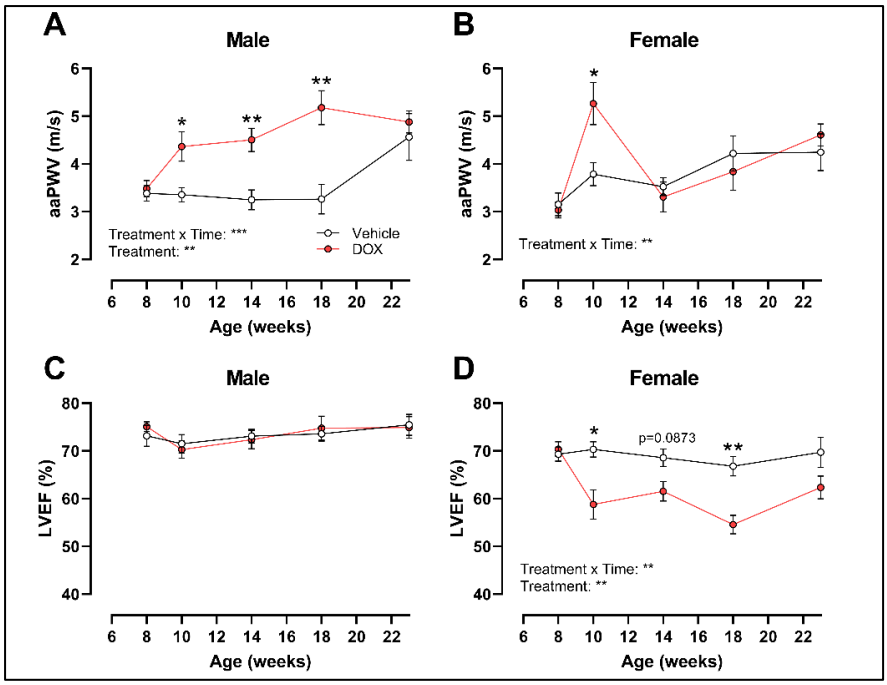

Figure 7.1: Longitudinal evaluation of cardiovascular function with ultrasound imaging in vehicle- and DOX-treated male and female ApoE$^{-/-}$ mice on HF diet. *aaPWV increased after two weeks of DOX treatment regardless of sex, which recovered in female, but not male, mice (A & B). DOX reduced LVEF in female, but not male, mice (C & D). For all panels: Repeated measures two-way ANOVA with Šídák's multiple comparisons; n=11-12 in each group. *, **, ***, p < 0.05, 0.01, 0.001.*

Cholesterol levels

Next, plasma cholesterol levels were quantified to confirm HF diet efficacy. The total cholesterol concentrations were similar in all groups, and were as follows: 633.8 ± 38.9 mg/dL in vehicle-treated male group; 702.1 ± 26.5 mg/dL in DOX-treated male group; 495.6 ± 25.3 mg/dL in vehicle-treated female group and 506.7 ± 23.8 mg/dL in DOX-treated female group. As such, all mice exhibited comparable food intake.

DOX does not exacerbate atherosclerotic plaque formation

Plaque amount in the thoracic aorta, brachiocephalic artery and proximal ascending aorta was subsequently investigated. In the thoracic aorta, there were no differences in plaque amount between the vehicle and DOX-treated groups for both male and female sex (Figure 7.2A). Likewise, DOX did not alter plaque amount in the brachiocephalic artery of both male and female mice (Figure 7.2B). Surprisingly, plaque area in the proximal ascending aorta of female DOX-treated mice was lower (Figure 7.2C). This was not observed in the male group (Figure 7.2C).

Plaque composition in the brachiocephalic artery and proximal ascending aorta were subsequently evaluated in depth where necrotic core, macrophage and VSMC content was determined. Overall, DOX did not induce consistent changes in plaque composition in the male and female groups. These results are summarised in Table 7.1. Representative images are shown in Figure 7.3.

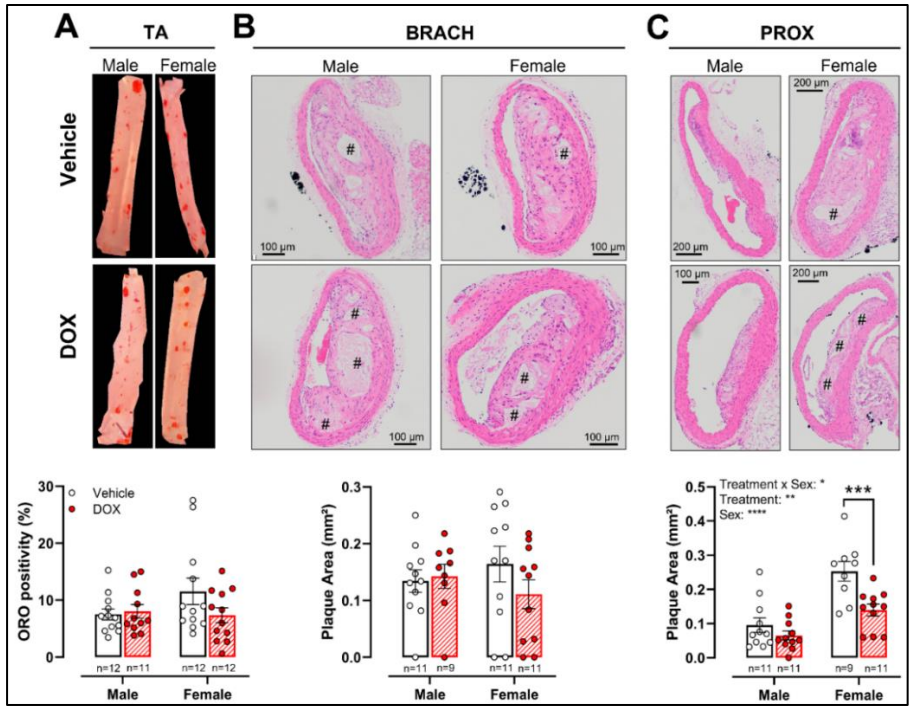

Figure 7.2: Plaque amount in thoracic aorta (TA), brachiocephalic artery (BRACH) and proximal aorta (PROX) in vehicle- and DOX-treated male and female ApoE$^{-/-}$ mice on HF diet. *ORO positivity did not differ between vehicle- and DOX-treated groups for both male and female sex (A). DOX did not change plaque area in male and female brachiocephalic artery plaques (B). Plaque area in the proximal aorta of female DOX-treated, but not male, mice was lower compared to the vehicle group (C). For A-C: Two-way ANOVA with Šidàk's multiple comparisons test. n numbers are displayed on graphs. For A: ORO staining. For B&C: H&E staining. n numbers are displayed on graphs. "#" indicates necrotic core. *, **, ***, **** p < 0.05, 0.01, 0.001, 0.0001*

Table 7.1: Plaque composition in brachiocephalic artery (BRACH) and proximal aorta (PROX) of vehicle- and DOX-treated male and female ApoE$^{-/-}$ mice.

BRACH	**Male**		**Female**	
	Vehicle (n=10)	DOX (n=8)	Vehicle (n=8-9)	DOX (n=8-11)
Necrotic core (%)	5.91 ± 1.83	14.84 ± 3.48 *	6.41 ± 0.98	7.58 ± 2.15
Mac3 (%)	1.15 ± 0.38	1.12 ± 0.23	1.59 ± 0.55	2.29 ± 0.50
α-SMA (%)	1.59 ± 0.43	1.50 ± 0.56	1.05 ± 0.22	1.02 ± 0.16
PROX	**Male**		**Female**	
	Vehicle (n=10-11)	DOX (n=10-11)	Vehicle (n=8-9)	DOX (n=11)
Necrotic core (%)	0.35 ± 0.35	0.62 ± 0.62	6.67 ± 2.35	5.90 ± 1.77
Mac3 (%)	17.01 ± 2.46	16.54 ± 3.79	7.53 ± 1.28	6.46 ± 1.36
α-SMA (%)	5.37 ± 0.69	8.75 ± 1.16 *	3.75 ± 0.76	3.12 ± 1.04

*, **, $p < 0.05$, 0.01 compared to sex-matched vehicle-treated group

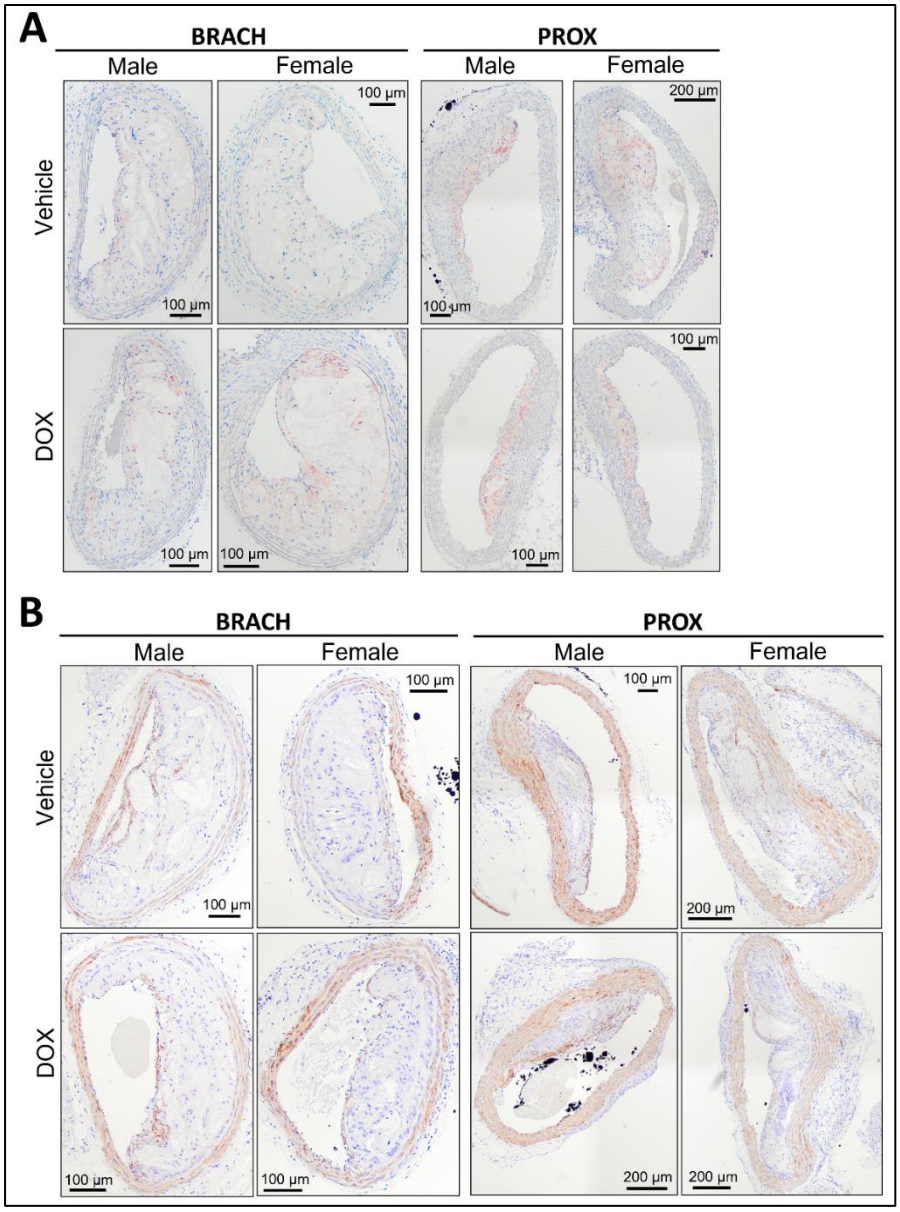

Figure 7.3: Representative images for Mac3 (A) and α-SMA staining (B).

7.4) Discussion

Endothelial dysfunction and arterial stiffness promote atherosclerosis development [59, 184-186]. Since we and others have previously reported that DOX impairs endothelial function, thereby augmenting arterial stiffness [60, 120, 147], the present study investigated whether DOX exacerbates atherosclerotic plaque formation.

DOX increased arterial stiffness after two weeks, which is in line with our previous observations, and thus validates our model [120, 147]. Remarkably, enhanced arterial stiffness continued after therapy discontinuation in DOX-treated male mice. This differs from our previous observations where DOX-treated wild-type male mice exhibited transient arterial stiffness (cf. Chapter VI). While we cannot explain why arterial stiffness did not recover in DOX-treated male ApoE$^{-/-}$ mice, our data suggest that pre-existing or concomitant signs of vascular toxicity induced by, for example, fat-rich diet may influence reversibility of DOX-induced arterial stiffness. It is also worth noting that female DOX-treated ApoE$^{-/-}$ mice, in contrast to the male ApoE$^{-/-}$ mice, exhibited transient arterial stiffness. Sex may therefore be an important determinant in recovery of DOX-induced arterial stiffness as well.

Overall, DOX did not increase plaque amount or size, which is in contrast to epidemiological data reporting a higher incidence of coronary artery disease in anthracycline-treated childhood cancer survivors [26]. On the other hand, our findings are in line with a preclinical study by Ko et al. In DOX-treated animals (3 mg/kg/week for three weeks), the authors observed a trend towards lower plaque burden in the carotid artery after four weeks of HF diet [189]. Although the findings of Ko et al. diverge from the present study in terms of the location of lower plaque burden, the sex where smaller plaques were found and the

experimental duration, these data highlight that DOX may not directly exacerbate atherosclerotic plaque formation. To the best of our knowledge, the current work and the work by Ko et al. are the only studies that investigated the role of DOX in atherosclerosis, and additional research is required to further confirm or refute these findings.

In the proximal aorta, sex and treatment differences in plaque amount were observed. Specifically, vehicle-treated female mice exhibited a higher plaque amount compared to vehicle-treated male mice, which can be explained by the fact that female sex has been demonstrated to represent a risk factor for atherosclerosis development [190-192].

Paradoxically, plaque area in the proximal aorta was lower in DOX-treated female mice in comparison to vehicle-treated female mice. Initially, we hypothesised that DOX possibly impairs macrophage and VSMC proliferation in the same way as it halts cancer cell division. However, macrophage and VSMC content were similar in the proximal aorta, indicating that DOX did not influence macrophage and VSMC proliferation. Alternatively, following DOX therapy, endothelial dysfunction may not last long enough to actively promote plaque formation as we have previously shown that DOX-induced endothelial dysfunction seems reversible after therapy cessation (cf. Chapter VI). Further study is required to understand why DOX does not seem to exacerbate atherosclerotic plaque formation.

The present study has two limitations. First, the HF diet used in the current work provokes endothelial dysfunction as well. Maybe the HF diet is too aggressive for the endothelium, although previous studies have been able to show accelerated plaque formation in the (proximal) aorta of female compared to male mice [190-192], which was also observed in the current work. Second, the duration of the HF diet was 17 weeks in total, a

time point where normal ApoE$^{-/-}$ mice exhibit stable plaques [193, 194]. The long duration of the study may therefore have adversely impacted the time frame to detect possible effects of DOX on plaque growth, although sex differences were observed in line with literature [190-192], providing an acceptable level of confidence in the present study. Collectively, it may be relevant to investigate the impact of DOX on atherosclerosis progression under experimental conditions where DOX is administered prior to starting the HF diet and in a shorter time frame.

In conclusion, while epidemiological report a higher incidence of atherosclerosis in anthracycline-treated childhood cancer survivors, our data reveal that DOX does not seem to accelerate atherosclerotic plaque formation. Importantly, these findings need to be confirmed in a treatment study with shorter follow-up.

Supplementary Figures

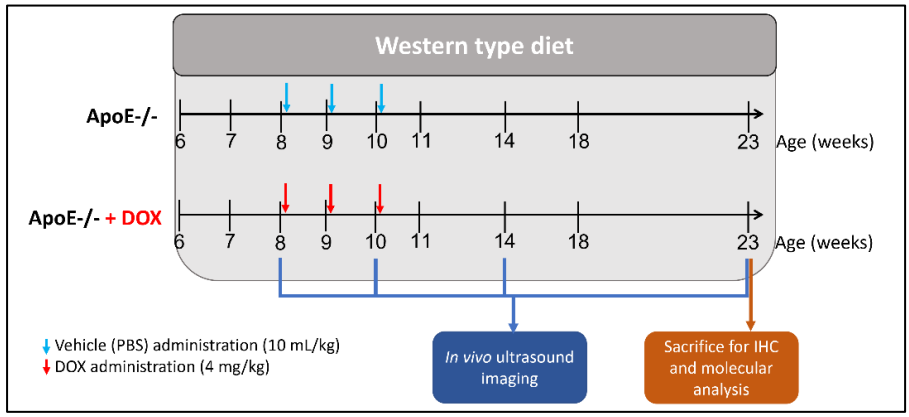

Supplementary Figure 7.1: Schematic overview of the experimental design.

CHAPTER VIII

General discussion

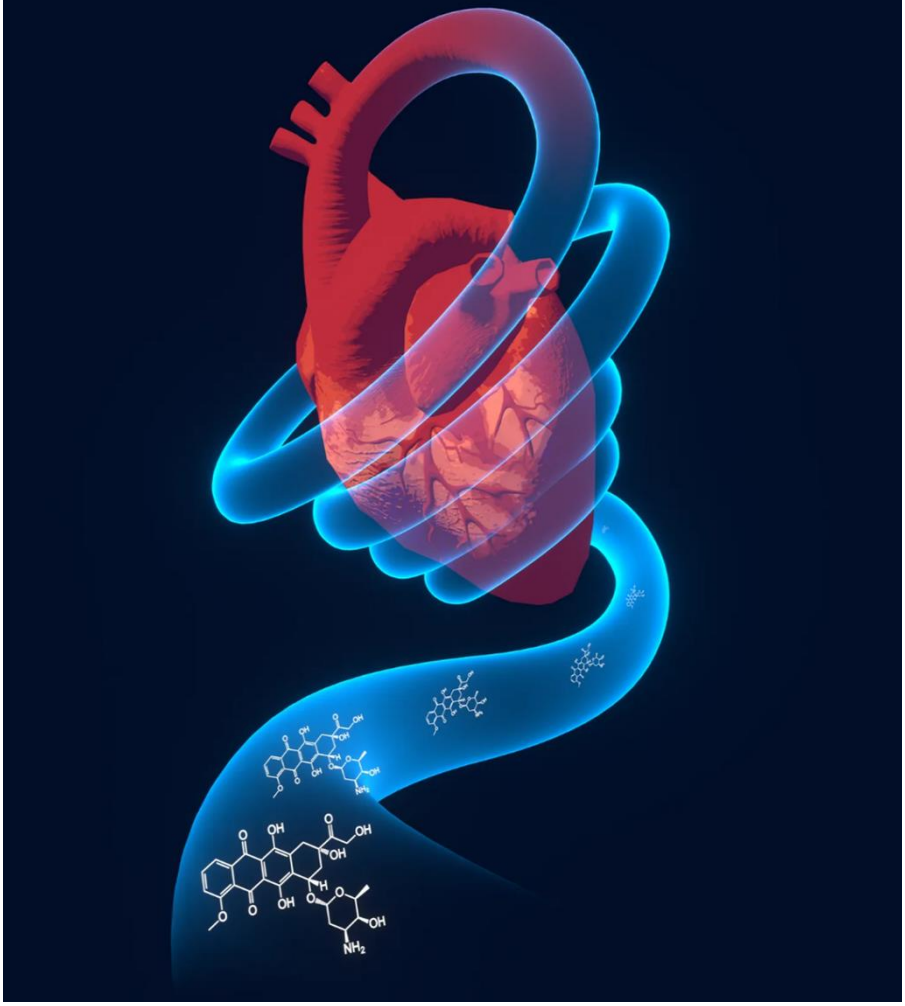

Despite cardiotoxic side effects, the anthracycline doxorubicin (DOX) remains a first-line chemotherapeutic agent for the treatment of breast cancer, leukaemia and lymphoma. While DOX-induced cardiotoxicity has been extensively investigated [14, 152], DOX also adversely impacts the vasculature, as evidenced by a higher incidence of systemic hypertension and coronary artery disease in anthracycline-treated patients [26]. Moreover, DOX increases arterial stiffness and impairs endothelial function in patients [27-32].

Since arterial stiffness and endothelial dysfunction have been shown to predict future cardiovascular events in the general population [47-52], the present doctoral dissertation hypothesised that, in patients receiving DOX, arterial stiffness and endothelial dysfunction precede cardiotoxicity and potentiate cardiac dysfunction, systemic hypertension and atherosclerosis later in life.

In an experimental mouse model, the current doctoral dissertation first investigated the mechanisms involved in DOX-induced arterial stiffness and endothelial dysfunction. In a second part, the time-course of vascular and cardiotoxicity was characterised by evaluating cardiovascular function before, during and after DOX therapy to discern whether arterial stiffness and endothelial dysfunction precede impairment of cardiac function. Continuing on this, we ascertained whether DOX-induced arterial stiffness and endothelial dysfunction contribute to cardiotoxicity, hypertension and atherosclerosis.

8.1) Doxorubicin-induced arterial stiffness displays a transient and dynamic profile that is determined by a complex interplay of altered active and passive components over time

Longitudinal evaluation of DOX-induced vascular toxicity reveals a sequential alteration of both active and passive components that collectively modulate arterial stiffness over time, which is as follows:

1. Early after administration (16 hours), DOX impairs endothelial function (i.e. impaired eNOS-dependent vasodilation) and simultaneously attenuates VSMC contraction (cf. Chapter IV). The coinciding manifestation of endothelial dysfunction and impaired contraction exerted opposing effects, which resulted in unaltered arterial stiffness. Although the mechanisms underlying the attenuated VSMC contraction remain elusive, DOX may block NSCC channels, thereby decreasing Ca^{2+} influx (cf. Chapter IV).

2. Days after DOX administration, arterial stiffness increases (cf. Chapter III). The hypocontraction from the early treatment phase restores, presumably due to clearance of DOX from VSMCs over time. However, since endothelial dysfunction continues, vascular tone increases, which ultimately augments arterial stiffness.

3. Remarkably, continued DOX treatment results in reversal of arterial stiffness to baseline values despite sustained endothelial dysfunction (cf. Chapter VI). Although it remains unclear how arterial stiffness reverses, DOX provoked extracellular matrix remodelling by altering the expression of several extracellular glycoproteins including, but not limited to, SERPINA3 and THBS1 (cf.

Chapter VI), which may improve arterial compliance as a compensating response. In this perspective, further study is required as the exact role of SERPINA3 and THBS1 in overall cardiovascular (patho)physiology remains poorly understood.

4. After therapy cessation, endothelial dysfunction recovers as well, but SERPINA3 and THBS1 levels remain higher.

The different phases of DOX-induced vascular toxicity are schematically illustrated in Figure 8.1.

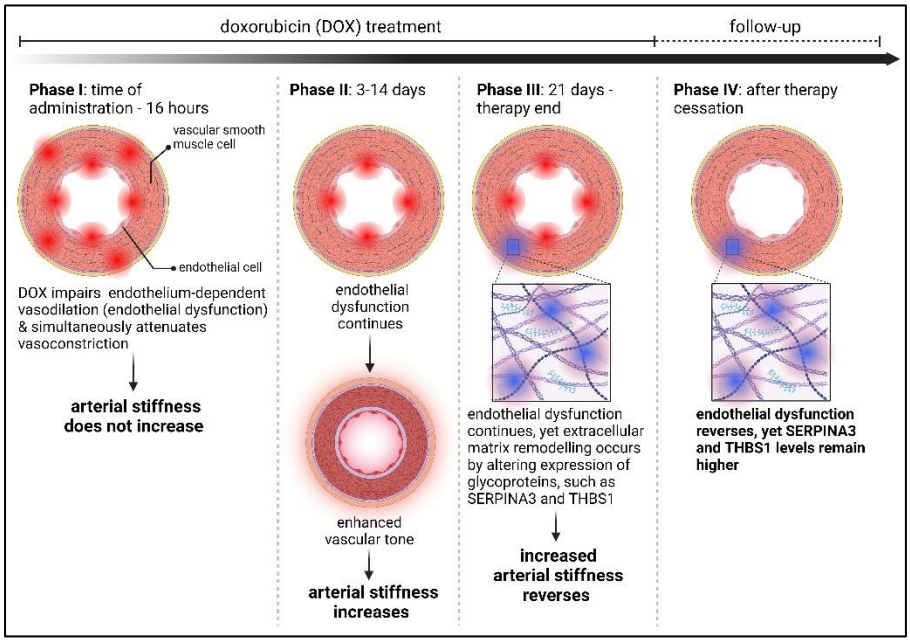

Figure 8.1: Schematic overview of the sequential DOX-induced alterations in active and passive components that collectively modulate arterial stiffness over time.

Our data also reveal that DOX-induced vascular toxicity and cardiotoxicity exhibit, at least in part, distinct underlying mechanisms. More specifically, since DOX impaired endothelial function irrespective of the TOP-IIβ depletor DEXRA, it appears that DOX provokes endothelial dysfunction in a TOP-IIβ-independent way. This differs from the situation in cardiomyocytes where DOX induces cardiotoxicity by inhibiting TOP-IIβ [23]. Furthermore, while it has been proposed that DOX impairs endothelial function through ROS-mediated conversion of NO into peroxynitrite [108], this is not supported by the DEANO-stimulated vasodilation curves which were identical between the vehicle- and DOX-treated groups at all time points, implying that exogenous addition of NO (under the form of DEANO) was not captured and transformed by DOX-induced ROS. This deviates from DOX-induced cardiotoxicity where ROS formation represents an important underlying mechanism [19, 20], although this ROS hypothesis has been increasingly challenged over the past decade [21-23]. Collectively, our data indicate that DOX impairs endothelial function not by targeting TOP-IIβ or by ROS-mediated depletion of NO. Instead, we found that DOX provokes endothelial dysfunction by decreasing eNOS expression.

In summary, DOX-induced arterial stiffness displays a transient and dynamic profile that is modulated by a complex interplay of successively altered active and passive components. While arterial stiffness recovers rapidly during therapy, endothelial dysfunction persists as long as treatment continues. Importantly, unlike cardiotoxicity, DOX appears to induce vascular toxicity in a TOP-IIβ-independent way.

8.2) The transient nature of doxorubicin-induced arterial stiffness and endothelial dysfunction may depend on vascular co-morbidities and sex

The temporary nature of DOX-induced arterial stiffness is in line with the findings of Novo et al. [30]. Specifically, in breast cancer patients (mean age: 56 ± 12 years) without prior history of cardiovascular disease, Novo et al. observed that DOX increased arterial stiffness within 3 months of therapy, followed by a return to baseline values during follow-up (at 6 and 9 months after the final dose) [30]. To the best of our knowledge, no other study has prospectively investigated arterial stiffness or endothelial function in adult patients during and at several time points after DOX therapy. Pending further confirmation, the current work and the study by Novo et al. suggest that DOX-induced arterial stiffness and endothelial dysfunction seem to be transient in patients.

Remarkably, in contrast to (rapid) recovery of arterial stiffness during DOX therapy in wild-type male mice, DOX-treated $ApoE^{-/-}$ male mice on high-fat diet exhibited prolonged arterial stiffness after therapy cessation. While it remains unclear why arterial stiffness did not reverse in DOX-treated $ApoE^{-/-}$ male mice as it did in wild-type male mice, these results raise awareness that other concomitant signs of vascular damage, induced by fat-rich diet for example, can influence reversibility of DOX-induced vascular toxicity. Hence, further study is warranted that investigates how vascular co-morbidities could impact the reversibility of DOX-induced vascular toxicity.

It is important to mention that our work focussed on investigating DOX-induced vascular toxicity in male mice. Male mice were chosen as they are more sensitive to DOX-induced cardiotoxicity [177-179], and to avoid the influence of cyclic changes in female hormones as confounding factors.

Interestingly, in DOX-treated ApoE$^{-/-}$ mice on high-fat diet, female animals showed reversibility of arterial stiffness after therapy cessation whereas male mice exhibited sustained arterial stiffness. Given that DOX-induced cardiotoxicity exhibits sexual dimorphism [177], it is possible that sex similarly influences reversibility of DOX-induced vascular toxicity, yet this requires further exploration.

While the acute and short-term follow-up effects of DOX on arterial stiffness and endothelial dysfunction appear to be transient, long-term vascular toxicity needs further study. This is particularly relevant in the context of paediatric cancer patients who seem to exhibit enhanced arterial stiffness and endothelial dysfunction years to decades after the final anthracycline dose [31, 32, 195, 196]. It remains unclear why these patients develop arterial stiffness and endothelial dysfunction as later-term or longer-term adverse vascular effects.

8.3) Arterial stiffness and endothelial dysfunction represent potential early, but time-sensitive, predictors of future cardiotoxicity in doxorubicin-treated patients

DOX-induced arterial stiffness and endothelial dysfunction manifested prior to and showed a strong correlation with decline in left ventricular systolic function (as schematically illustrated in Figure 8.2). Importantly, both arterial stiffness and endothelial dysfunction were transient whereas impaired systolic function persisted after DOX therapy cessation. From a clinical perspective, these findings place arterial stiffness and endothelial dysfunction as potential early, but time-sensitive, markers of future cardiotoxicity.

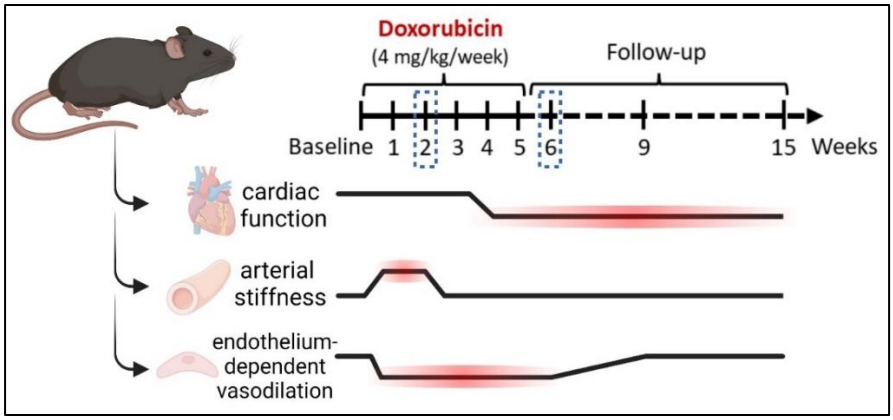

Figure 8.2: Schematic representation of the time-course of DOX-induced cardiovascular toxicity.

For further clinical validation, there are some important aspects that need to be taken into account. First, the time-sensitive window to measure arterial stiffness and endothelial dysfunction makes it challenging to routinely evaluate both parameters in patients. It is therefore recommended to measure arterial stiffness and endothelial dysfunction on well-defined time points. We recommend to measure these parameters at baseline, before each treatment cycle, at the end of therapy and each year thereafter. Second, since arterial stiffness recovered rapidly in DOX-treated wild-type male mice but remained elevated in ApoE$^{-/-}$ male mice on high-fat diet, the time-sensitive window to measure these parameters could differ between patients with and without cardiovascular co-morbidities. Finally, when measuring arterial stiffness, it is recommended to take into account that stiffness values represent a collective "average" of active and passive components and different blood vessels with a gradient along the arterial tree [197].

8.4) SERPINA3 and THBS1 may be useful early markers for future cardiotoxicity in doxorubicin-treated patients

Compared to time-sensitive arterial stiffness and endothelial dysfunction, SERPINA3 and THBS1 may represent more consistent and easy-to-use markers for assessment of cardiotoxicity risk in patients receiving DOX. Specifically, in the current work, circulating SERPINA3 and THBS1 were upregulated in cancer patients with anthracycline-induced severe cardiotoxicity, years after therapy completion. In addition, both SERPINA3 and THBS1 showed an inverse correlation with LVEF in these patients. Moreover, upon therapy completion, SERPINA3 and THBS1 were upregulated in DOX-treated patients with mild cardiotoxicity compared to values prior to DOX-treatment (internal data; not shown). Finally, others have found enhanced circulating levels of SERPINA3 and THBS1 to be associated with future or worsening of cardiovascular disease, as discussed in Chapter VI. Collectively, pending further clinical validation, SERPINA3 and THBS1 hold diagnostic promise in patients during and after DOX therapy. Since SERPINA3 and THBS1 can be measured in blood plasma, these proteins can be easily and routinely assessed as blood is collected during almost every medical check-up.

8.5) Does doxorubicin-induced vascular toxicity contribute to cardiotoxicity and cardiovascular disease?

Despite being a contributor to cardiac dysfunction in the general population [47-52], our data suggest that arterial stiffness and endothelial dysfunction do not potentiate cardiotoxicity during DOX therapy and short-term follow-up. For instance, although we did observe a strong correlation between arterial stiffness and impaired left ventricular systolic function in wild-type mice, LVEF was decreased only to a modest degree. Moreover, in DOX-treated ApoE$^{-/-}$ male mice exhibiting sustained

arterial stiffness after therapy cessation, left ventricular systolic function remained intact. Furthermore, while epidemiological data have reported a higher incidence of atherosclerosis and systemic hypertension [26], our data do not support this either. For example, in ApoE$^{-/-}$ mice on a HF diet, DOX did not change overall atherosclerotic plaque amount nor content. In female DOX-treated ApoE$^{-/-}$ mice, plaque size was surprisingly even lower in the proximal aorta. Finally, systemic hypertension did not develop in DOX-treated wild-type mice as blood pressure remained unaffected following therapy, although it should be noted that, compared to the tail-cuff system, there are more reliable alternatives to measure blood pressure in mice, such as telemetry.

It is important to emphasise that, in the present doctoral thesis, cardiac function, blood pressure and atherosclerotic plaque formation were only investigated in the acute and short-term follow-up phases of DOX treatment, and arterial stiffness and endothelial dysfunction represent only a limited aspect of vascular toxicity. Systemic hypertension, coronary artery disease and heart failure typically manifest in the long-term, years after anthracycline therapy [26]. Investigating the lasting effects of DOX on the vasculature is therefore of major importance to determine how vascular toxicity possibly contributes to cardiovascular disease. Since we have shown that SERPINA3 and THBS1 remain upregulated after DOX therapy cessation, it is of high priority to further investigate the role of these glycoproteins in cardiovascular (patho)physiology, especially given their association with adverse cardiovascular outcome later in life [162-166, 169-171, 173].

Interestingly, while their (patho)physiological role remains poorly understood, the glycoproteins SERPINA3 and THBS1 have been proposed to play an important part in inflammatory responses [159, 198-200]. Since vascular inflammation is considered a key initiator of endothelial dysfunction and arterial stiffness [201, 202], it is possible that sustained high levels of SERPINA3 and THBS1 enhance arterial stiffness and impair endothelial function by inducing gradual, chronic inflammation. Although speculative at present, this would imply that arterial stiffness and endothelial dysfunction recover shortly after DOX therapy cessation, but redevelop in the late-term as a result of chronic SERPINA3- and THBS1-mediated vascular inflammation. Such "redevelopment" of arterial stiffness and endothelial dysfunction could potentiate future cardiovascular disease in DOX-treated patients when persistent in nature. Interestingly, this hypothesis is strengthened by the fact that (partial) alteration of the glycoproteome during childhood (in cancer-free subjects) has been associated with inflammation-mediated endothelial dysfunction and cardiovascular disease later in early- and mid-adult life [203]. Large prospective studies should investigate how vascular function changes in the long-term after DOX therapy cessation with a focus on the possible mediating role of (SERPINA3- and THBS1-induced) chronic inflammation.

In the current work, DOX-induced vascular toxicity was only investigated in the central aorta, which may differ from the peripheral and (coronary) microvascular arteries as cellular composition and function differs substantially along the arterial tree [204]. To understand how cardiovascular disease develops in DOX-treated patients, it is crucial to comprehend how DOX affects vascular function in both central and peripheral blood vessels and their mutual interplay.

8.6) Do doxorubicin-induced SERPINA3 and THBS1 represent new therapeutic targets?

If long-term prospective studies confirm that DOX-induced SERPINA3 and THBS1 contribute to cardiovascular disease by inducing chronic and sustained inflammation, (early) targeting of these proteins may represent a possible therapeutic approach. Although more and extensive additional work is required in this field, several therapeutic avenues could be further explored. For instance, exercise training has proven effective in mitigating anthracycline-induced cardiotoxicity (reviewed elsewhere [205]). Similarly, a growing body of evidence suggests a beneficial role for exercise in improving endothelial function and arterial compliance, and overall vascular function, by reducing inflammatory signalling (reviewed elsewhere [206]). Also food supplementation with anti-oxidant and anti-inflammatory properties has proven successful in this regard [207]. Furthermore, the type II diabetes drug empaglifozin and the antioxidant mitoquinone (also called MitoQ) have been shown to effectively mitigate endothelial inflammation [208, 209]. Finally, also angiotensin-converting enzyme inhibitors and statins, which have been shown to attenuate cardiovascular disease-related mortality [210, 211], may represent promising anti-vascular toxicity candidate drugs for DOX-treated patients.

8.7) Vascular toxicity in the broader cardio-oncology context

Today, there is a wide selection of anticancer drugs. Since DOX-induced vascular toxicity displays a dynamic profile where multiple successive alterations in active and passive elements modulate arterial stiffness, the following questions arise: Should there be an active screening for vascular toxicity during and after anticancer therapy for cardiovascular risk assessment in patients? Should vascular toxicity be monitored in preclinical models as part of safety profiling during novel anticancer agent development?

A growing body of evidence suggests that anticancer drugs other than DOX increase arterial stiffness and impair endothelial function in patients (Table 8.1 and 8.2), raising awareness that anticancer therapy in general poses adverse risk for the entire cardiovascular system. Although still in its "infancy", a continued and collective preclinical and clinical endeavour in the field of cardio-oncology is paramount to elucidate whether an anticancer drug, be it existing or in development, exerts long-lasting adverse effects on cardiovascular health. Large, prospective studies with long-term follow-up are crucial to answer this question. Only by doing so can an anticancer therapy be provided to patients with maximal efficacy and minimal cardiovascular risk.

Table 8.1: Anticancer drugs associated with arterial stiffness

Class of anticancer drug	Study	Anticancer drug (dose)	Cancer type	Population sample size	Modality	Time of Assessment	Results
Taxanes	Florescu et al., 2013 [212]	Paclitaxel (cumulative dose of 417 ± 154 g/m^2)	Breast cancer	n=20 (mean age: 51 years)	β-index	After completion of therapy (exact time frame not specified)	1.3-fold increase in stiffness index (8.1 ± 3 at baseline vs. 10.2 ± 3 at therapy completion)
Platinum-based compounds	Stelwagen et al., 2020 [213]	Cisplatin (dose not specified)	Testicular cancer	n=67 controls, n=69 treated patients (median age: 28 years)	PWV over carotid-femoral artery region	28 years (median) after therapy completion	1.1 fold difference (7.58 m/s [95% CI: 7.24-7.94] in controls vs. 8.07 m/s [7.82-8.37] in cisplatin group)
VEGF inhibitors	Veronese et al., 2006 [214]	Sorafenib (400 mg twice daily)	Solid tumours	n=20 (median age: 59 years)	PWV over carotid-femoral artery region	After 34 days of treatment	1.2 fold increase (8.9 ± 0.5 m/s at baseline vs. 9.7 ± 0.7

							m/s after 34 days)
	Mäki-Petäjä et al., 2021 [215]	Pazopanib (800 mg daily)	Carcinoma, sarcoma, melanoma, cervical and ovarian cancer	n=27 (mean age: 60 years)	PWV in brachial artery	After 12 weeks of treatment	1.2 fold increase (8.0 ± 2.1 m/s at baseline vs. +1.3 m/s [95% CI: 0.3, 2.2] after 12 weeks [=9.3 m/s])
Antiandrogens	Dockery et al., 2013 [216]	Bicalutamide (150 mg once daily) Goserelin (10.8 mg 3 times monthly)	Prostate cancer	n=21 in gosererlin group and n=21 in bicalutamide group	PWV over carotid-femoral artery region	After 12 weeks of treatment	Goserelin: 1.1 fold increase (11.7 ± 1.7 m/s at baseline vs. +1.4 ± 0.4 m/s [=13.1 m/s] after 12 weeks of treatment) Bicalutamide: 1.1 fold increase at 12 weeks after therapy completion

							(12.6 ± 1.3 m/s at baseline vs. +0.8 ± 0.3 m/s [=13.4 m/s] after 12 weeks of treatment)

* IQR: Interquartile range; CI: confidence interval

Table 8.2: Endothelial dysfunction associated with anticancer therapy

Class of anticancer drug	Study	Anticancer drug (dose)	Cancer type	Population sample size	Modality	Time of Assessment	Results
Taxanes	Vassilakopoulou et al., 2010 [217]	Paclitaxel (80 mg/m^2/week for 12 weeks)	Breast cancer	n=5 (mean age: 65 years)	FMD in brachial artery	1 month after therapy completion	3.2 fold decrease compared to baseline (3.8 ± 5.5% at baseline vs. 1.2 ± 1.7% at 1 month after therapy completion)
Platinum-based compounds	Cameron et al., 2020 [218]	Cisplatin (cumulative dose of 100 mg/m^2/cycle for 3-4 cycles)	Testicular cancer	n=10 (age: 34 years)	FMD in brachial artery	24 hours, 6 weeks, and 3, 6 and 9 months after initial cisplatin administration	1.5 fold decrease compared to baseline (16.7 ± 1.6% at baseline vs. 10.9 ± 0.9% at 24 hours after cisplatin administration; no changes at other time points)

VEGF inhibitors	Steeghs et al., 2008 [219]	Telatinib (20-1800 mg; continuously once or twice daily)	Carcinoma and sarcoma	n=18 (age: 55 years)	FMD in brachial artery	After 5 weeks of treatment	1.5 fold decrease compared to baseline (6.0% at baseline vs. 3.9% after 5 weeks of treatment)
	Steeghs et al., 2010 [220]	Bevacizumab (7.5 mg/kg/3 weeks or 10 mg/kg/2 weeks)	Colorectal and breast cancer	n=8 (age: 59 years)	FMD in brachial artery	After 6 weeks of treatment (T1), and 3 months after discontinuation (T2)	2 fold decrease compared to baseline (7.0% at baseline vs. 3.5% at T1 and 3.8% at T2)
	Sen et al., 2013 [221]	Sunitinib (37.5 mg daily for 4 to 36 months)	Carcinoma	n=27 controls (mean age: 43 years), N=18 treated patients (mean age: 53 years)	CFR in coronary artery	When treated with Sunitinib for at least 3 months	1.5-fold difference in CFR (2.5 ± 0.8% in controls vs. 1.7 ± 0.4% in sunitinib group)

CHAPTER IX

Conclusions & Future perspectives

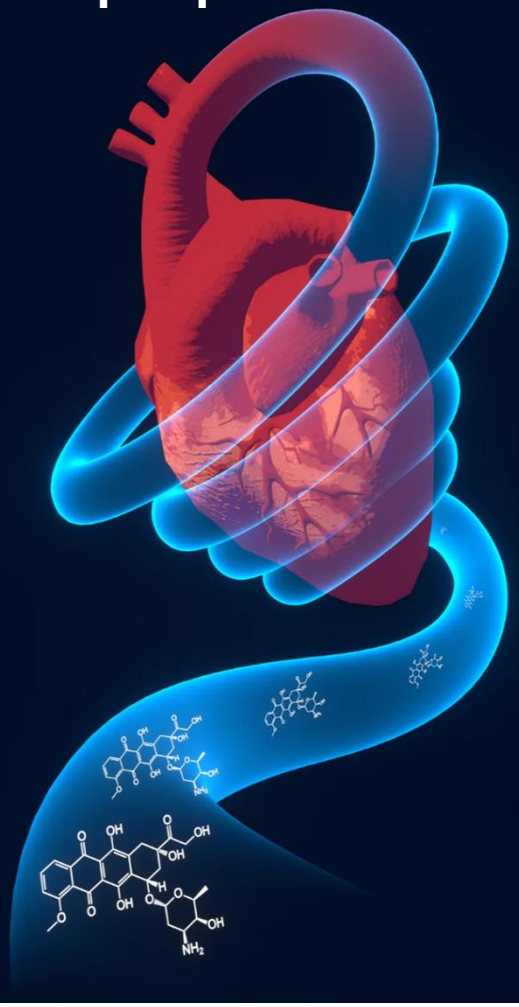

While the cardiotoxic side effects of the chemotherapeutic agent doxorubicin (DOX) have been well-recognised, DOX also induces vascular toxicity, represented mainly by arterial stiffness and endothelial dysfunction. Arterial stiffness and endothelial dysfunction are independent predictors of and important contributors to cardiovascular disease in the general population. In an experimental murine model, the present doctoral dissertation aimed to elucidate the mechanisms underlying DOX-induced arterial stiffness and endothelial dysfunction, to evaluate whether both parameters could be used as possible early markers of future DOX-induced cardiotoxicity, and to delineate whether DOX-induced arterial stiffness and endothelial dysfunction contribute to cardiac dysfunction, systemic hypertension and atherosclerosis.

Our data reveal that DOX-induced vascular toxicity is characterised by a complex, successive alteration of both active and passive components that collectively modulate arterial stiffness over time. DOX-induced arterial stiffness is driven by endothelial dysfunction-mediated enhancement of vascular tone. DOX provokes endothelial dysfunction, not by targeting the TOP-IIβ pathway, but by decreasing eNOS expression. Remarkably, during DOX therapy, arterial stiffness reverses while endothelial dysfunction is present. The exact mechanisms underlying recovery of DOX-induced arterial stiffness remain unclear, yet may relate to DOX altering expression of the glycoproteins, SERPINA3, THBS1, MBL2 and LGALS3BP, indicative of possible compensatory extracellular matrix remodelling. Endothelial dysfunction recovers eventually as well, but after therapy cessation.

Although transient, arterial stiffness and endothelial dysfunction both preceded sustained decline in left ventricular systolic function. From a clinical perspective, arterial stiffness and endothelial dysfunction hold potential as early, but time-sensitive, functional markers of future cardiotoxicity in patients receiving DOX. For further clinical validation, it is recommended to evaluate arterial stiffness and endothelial function at well-defined time points, at least at baseline, prior to each treatment cycle, at therapy completion and each year thereafter. Assessment of arterial stiffness can be performed by measuring carotid-femoral or brachial-ankle PWV while endothelial function can be evaluated with flow-mediated dilation in the brachial artery or with a proprietary device called "EndoPAT®" in the microvasculature of the index finger.

Importantly, the time-sensitive window to measure arterial stiffness and endothelial dysfunction during DOX therapy appears to depend on vascular co-morbidities as DOX-induced arterial stiffness did not recover in male mice when concomitant vascular toxicity induced by high-fat diet was present. On the other hand, female mice on high-fat diet did show recovery of DOX-induced arterial stiffness, highlighting that sex may also be an important determinant of vascular toxicity reversibility. Further study is required that investigates whether DOX-induced arterial stiffness and endothelial dysfunction are transient in patients of all ages by taking the possible influence of vascular co-morbidities and sex hereto into account.

While DOX-induced arterial stiffness and endothelial dysfunction were transient, SERPINA3 and THBS1 levels remained higher after therapy cessation. This was further confirmed in cancer patients with anthracycline-induced severe cardiotoxicity exhibiting increased SERPINA3 and THBS1, years after therapy completion. Since both SERPINA3 and THBS1 showed an inverse correlation with LVEF in these patients,

SERPINA3 and THBS1 hold potential as molecular markers of cardiotoxicity following DOX therapy. However, large-scale prospective studies need to confirm whether these glycoproteins can actually predict cardiovascular events. A major advantage is that SERPINA3 and THBS1 can be easily measured in plasma as blood is collected during almost every routine medical check-up.

Despite potentiating cardiotoxicity in the general population, our data suggest that arterial stiffness and endothelial dysfunction do not contribute to cardiotoxicity following DOX therapy as only a modest decline in left ventricular systolic function was observed. Furthermore, in contrast to epidemiological data reporting a higher incidence of systemic hypertension and atherosclerosis in anthracycline-treated cancer survivors, no changes in blood pressure nor plaque amount/content were observed. However, it is important to emphasise that these findings only apply to the acute and short-term follow-up phases, and, as such, it can only be concluded that DOX-induced vascular toxicity does not contribute to cardiotoxicity, hypertension or atherosclerosis in the short-term. As cardiovascular disease predominantly manifests years after DOX therapy completion, more work is required to delineate the long-lasting adverse effects of DOX treatment on the vasculature and how this could potentiate cardiovascular disease. Since SERPINA3 and THBS1 showed sustained higher levels following DOX therapy, elucidating the exact role of these glycoproteins in cardiovascular (patho)physiology is of high priority, especially given the association between SERPINA3 and THBS1 and cardiovascular disease later in life of cancer-free individuals. Preclinical models with SERPINA3- or THBS1-deficiency, either in the entire organism or selective to ECs and/or VSMCs, could aid in that regard.

Finally, emerging evidence suggests that, not only DOX, but also other anticancer agents increase arterial stiffness and impair endothelial function. Although still in a preliminary stage, a continuing collective endeavour in both the clinical and preclinical fields investigating all aspects of anticancer therapy-associated cardiovascular toxicity is warranted. Only by doing so can anticancer therapy be provided with minimal cardiovascular risk without compromising antitumour treatment efficacy.

CHAPTER X

Summary/Samenvatting

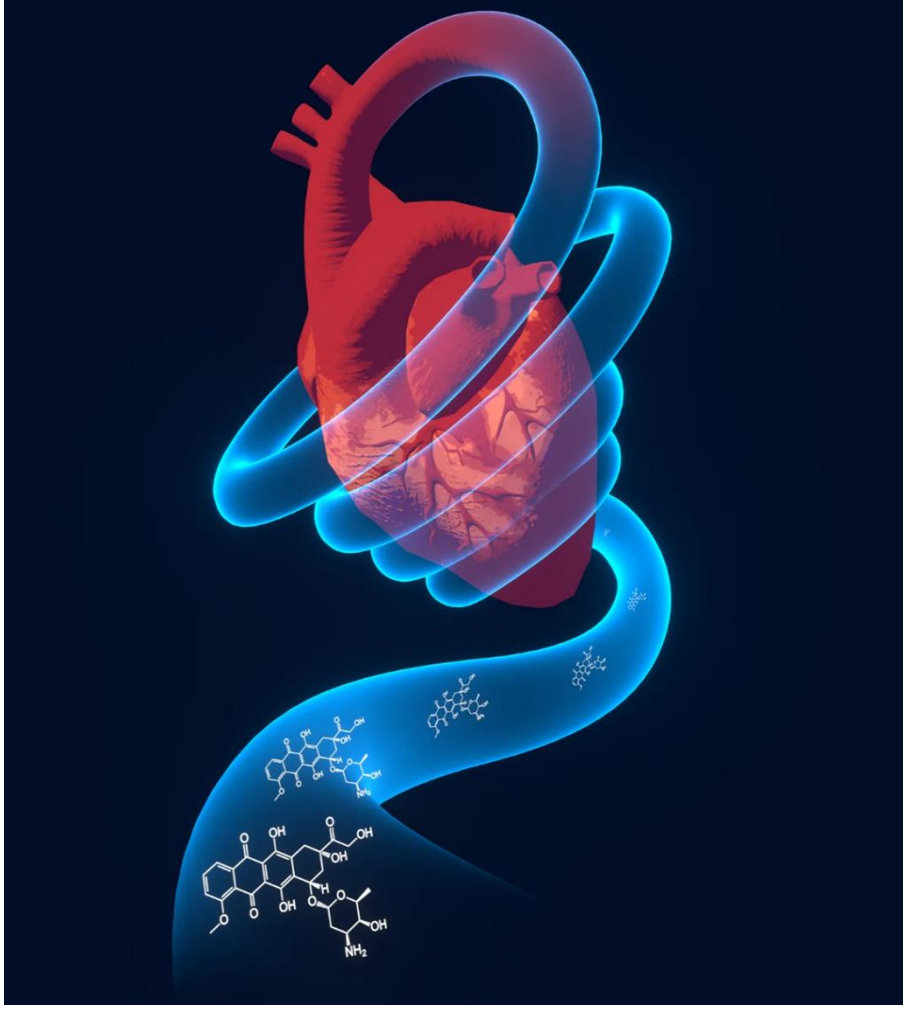

Summary

Apart from cardiotoxicity, the anthracycline chemotherapeutic agent doxorubicin (DOX) induces vascular toxicity, represented mainly by arterial stiffness and endothelial dysfunction. Arterial stiffness and endothelial dysfunction are independent predictors of and important contributors to cardiovascular disease in the general population. Here, in an experimental murine model, we aimed to elucidate the mechanisms underlying DOX-induced arterial stiffness and endothelial dysfunction, to evaluate whether both parameters could be used as possible early markers of future DOX-induced cardiotoxicity, and to delineate whether DOX-induced arterial stiffness and endothelial dysfunction contribute to cardiac dysfunction, systemic hypertension and atherosclerosis.

Our data show that DOX-induced vascular toxicity is characterised by a complex, successive alteration of both active and passive components that collectively modulate arterial stiffness over time. In a first phase of DOX therapy, arterial stiffness increases as a result of endothelial dysfunction-mediated enhancement of vascular tone. Remarkably, arterial stiffness reverses soon thereafter whereas endothelial dysfunction continues. Interestingly, DOX alters the expression of several extracellular glycoproteins, particularly SERPINA3 and THBS1, indicative of extracellular matrix remodelling. This remodelling possibly compensates the early augmentation of DOX-induced arterial stiffness, yet further study is required to understand the role of these glycoproteins in cardiovascular (patho)physiology. Endothelial dysfunction recovers eventually as well, but after DOX therapy cessation.

Although transient, arterial stiffness and endothelial dysfunction preceded impairment of left ventricular systolic function during DOX therapy. This places arterial stiffness and

endothelial dysfunction as potential early, but time-sensitive, markers of future cardiotoxicity in patients receiving DOX. Interestingly, plasma SERPINA3 and THBS1 levels were higher in cancer survivors with anthracycline-induced cardiotoxicity and showed an inverse correlation with cardiac systolic function. As such, SERPINA3 and THBS1 hold diagnostic potential within the context of cardiotoxicity risk assessment in DOX-treated patients. Further clinical validation is required to delineate the marker potential of arterial stiffness, endothelial dysfunction, SERPINA3 and THBS1 in prediction of future cardiovascular events.

The current work suggests that arterial stiffness and endothelial dysfunction do not seem to potentiate cardiovascular disease in DOX-treated mice, despite their contributory role to cardiotoxicity in the general population and reports of a higher incidence of systemic hypertension and atherosclerosis in anthracycline-treated cancer survivors. Importantly, our findings only apply to the acute and short-term follow-up phases. As cardiovascular disease predominantly manifests years after DOX therapy completion, more work is required to delineate the long-lasting adverse effects of DOX treatment on the vasculature and how this could potentiate cardiovascular disease. Since SERPINA3 and THBS1 showed sustained higher levels following DOX therapy, elucidating the exact role of these glycoproteins in cardiovascular (patho)physiology is of high priority, especially given the association between SERPINA3 and THBS1 and cardiovascular disease later in life of cancer-free individuals.

Apart from DOX, emerging and compelling evidence has also implicated other anticancer drugs in cardiovascular disease. Hence, a continuing collective endeavour in both the clinical and preclinical fields investigating all aspects of anticancer therapy-associated cardiovascular toxicity is warranted. Only by doing so can anticancer therapy be provided with minimal cardiovascular risk without compromising antitumour treatment efficacy.

Samenvatting

Naast cardiotoxiciteit induceert het anthracycline chemotherapeuticum doxorubicine (DOX) vasculaire toxiciteit, voornamelijk gekenmerkt door arteriële stijfheid en endotheeldysfunctie. Arteriële stijfheid en endotheeldysfunctie zijn onafhankelijke voorspellers van en belangrijke bijdragers tot cardiovasculaire ziektes in de algemene bevolking. Hier, in een experimenteel muis model, onderzochten wij de onderliggende mechanismen van DOX-geïnduceerde arteriële stijfheid en endotheeldysfunctie, of deze parameters konden gebruikt worden als mogelijke vroege merkers van toekomstige DOX-geïnduceerde cardiotoxiciteit en of arteriële stijfheid en endotheeldysfunctie bijdragen tot cardiale dysfunctie, systemische hypertensie en atherosclerose.

Onze data toont dat DOX-geïnduceerde vasculaire toxiciteit gekenmerkt wordt door een complexe, sequentiële verandering van zowel actieve als passieve elementen die gezamenlijk arteriële stijfheid beïnvloeden doorheen de tijd. In een eerste fase van DOX behandeling verhoogt arteriële stijfheid als gevolg van endotheeldysfunctie-gemedieerde versterking van vasculaire tonus. Opmerkelijk is dat arteriële stijfheid snel daarna herstelt terwijl endotheeldysfunctie aanhoudt. Interessant is dat DOX de expressie van verschillende extracellulaire glycoproteïnes verandert, voornamelijk SERPINA3 en THBS1, wat wijst op extracellulaire matrix hermodellering. Deze hermodellering compenseert mogelijks voor de eerdere DOX-geïnduceerde verhoging in arteriële stijfheid, maar meer onderzoek is noodzakelijk om de rol van deze glycoproteïnes in cardiovasculaire (patho)fysiologie te begrijpen. Endotheeldysfunctie herstelt uiteindelijk ook, maar pas na het stoppen van DOX behandeling.

Ondanks het transiënte karakter gingen arteriële stijfheid en endotheeldysfunctie vooraf aan verminderde linker ventrikel systolische functie. Dit plaatst arteriële stijfheid en endotheeldysfunctie als mogelijke vroege, maar tijdsgevoelige, merkers van toekomstige cardiotoxiciteit in patiënten die DOX krijgen. Interessant is dat plasma SERPINA3 en THBS1 concentraties hoger bleven in kanker overlevers met anthracycline-geïnduceerde cardiotoxiciteit en een omgekeerde correlatie vertoonden met cardiale systolische functie. SERPINA3 en THBS1 houden daarom diagnostisch potentieel voor evaluatie van cardiotoxiciteitsrisico in DOX-behandelde patiënten. Verdere klinische validatie is nodig om het merker potentieel van arteriële stijfheid, endotheeldysfunctie, SERPINA3 en THBS1 te bevestigen.

Wij observeerden geen significante bijdrage van arteriële stijfheid en endotheeldysfunctie tot cardiovasculaire ziektes in DOX-behandelde muizen, ondanks hun bijdrage tot cardiotoxiciteit in de algemene bevolking en gerapporteerde hogere incidentie van systemische hypertensie en atherosclerose in anthracycline-behandelde patiënten. Belangrijk is wel dat onze bevindingen enkel van toepassing zijn op de acute en korte termijn opvolgingsfases. Aangezien cardiovasculaire complicaties voornamelijk ontwikkelen jaren na DOX behandeling is het belangrijk om de lange termijn effecten van DOX op het vasculaire systeem te onderzoeken en hoe dit bijdraagt tot cardiovasculaire ziektes. De aanhoudende verhoogde levels van SERPINA3 en THBS1 onderlijnt het belang van het verder onderzoeken van de rol van deze glycoproteïnes in cardiovasculaire (patho)fysiologie, zeker omwille van de associatie tussen SERPINA3 en THBS1 en cardiovasculaire aandoeningen in het latere leven van kanker-vrije individuen.

Naast DOX is er groeiend en overtuigend bewijs dat andere antikanker geneesmiddelen betrokken zijn in cardiovasculaire complicaties. Een verdere en gezamenlijke streven in zowel de klinische als preklinische gebieden die alle aspecten van antikankerbehandeling-geassocieerde cardiovasculaire toxiciteit onderzoekt is van groot belang. Alleen op deze manier kan antikanker behandeling aangeboden worden met minimaal cardiovasculair risico zonder antitumor efficiëntie aan te tasten.

List of abbrevations

ACh	acetylcholine
aaPWV	abdominal aorta pulse wave velocity
cfPWV	carotid-femoral pulse wave velocity
DEANO	diethylamine NONOate
DEXRA	dexrazoxane
DOX	doxorubicin
EC(s)	endothelial cell(s)
eNOS	endothelial nitric oxide synthase
L-NAME	Nω-nitro-L-arginine methyl ester
LVAW	left ventricular anterior wall
LVEF	left ventricular ejection fraction
LVID	left ventricular internal diameter
LVPW	left ventricular posterior wall
NO	nitric oxide
NSCC(s)	non-selective cation channel(s)
PE	phenylephrine
PWV	pulse wave velocity
ROTSAC	Rodent Oscillatory Tension Set-up to assess Arterial Compliance
SERPINA3	α-1-antichymotrypsin
THBS1	thrombospondin-1
TOP-IIα/TOP-IIβ	topoisomerase-IIα/topoisomerase-IIβ
VGCC(s)	voltage-gated calcium channel(s)
VSMC(s)	vascular smooth muscle cell(s)
2-APB	2-aminoethoxydiphenyl borinate

Scientific *curriculum vitae*

Name BOSMAN, Matthias

Date/Place of birth October 17th, 1995; Rumst

Nationality Belgian

e-mail matthias.bosman1@gmail.com

Education

Master, University of Antwerp, Wilrijk (Antwerp)
September 2017 — July 2019

Graduated as a **Master of Biochemistry & Biotechnology: Molecular and Cellular Gene Biotechnology** with the mention **great distinction**.

Bachelor, University of Antwerp, Wilrijk (Antwerp)
September 2014 — July 2017

Graduated as a **Bachelor of Biochemistry & Biotechnology** with the mention **distinction**.

Additional Educational Courses

FELASA category C to work with laboratory animals in Europe, obtained at University of Antwerp
September 2018 — February 2019

Scientific Career

PhD in Medical Sciences, Laboratory of Physiopharmacology University of Antwerp, Wilrijk (Antwerp)
November 2019 — October 2023

PhD thesis: *Doxorubicin-induced vascular toxicity: Investigating the underlying mechanisms and its temporal relationship to cardiotoxicity*

Supervisors: Prof. Dr. Pieter-Jan Guns & Prof. Dr. Emeline Van Craenenbroeck

Master dissertation in Biochemistry & Biotechnology, Laboratory of Proteinchemistry, Proteomics & Epigenetic Signalling (PPES), University of Antwerp, Wilrijk (Antwerp)
February 2019 — July 2019

Master thesis: *Cytoglobin expression increases in response to a hypoxic environment and has a cytoprotective function in A375 and Malme3M melanoma cells*

Supervisors: Prof. Dr. Sylvia Dewilde, Dr. Eva Geuens & Joey De Backer

---

Scientific Publications

As 1st author

1. ***Dexrazoxane does not mitigate doxorubicin-induced endothelial dysfunction in an ex vivo model of acute vascular toxicity*** - Matthias Bosman, Dustin Krüger, Kasper Favere, Guido De Meyer, Constantijn Franssen, Emeline Van Craenenbroeck and Pieter-Jan Guns – Original Research Article, in revision at *PLOS ONE*
2. ***Doxorubicin-Induced Cardiovascular Toxicity: A Longitudinal Evaluation of Functional and Molecular Markers*** – Matthias Bosman, Dustin Krüger, Charles Van Assche, Hanne Boen, Cédric Neutel, Kasper Favere, Constantijn Franssen, Wim Martinet, Lynn Roth, Guido De Meyer, Berta Cillero-Pastor, Leen Delrue, Ward Heggermont, Emeline Van Craenenbroeck and Pieter-Jan Guns – Original Research Article, accepted for publication in *Cardiovascular Research*
3. ***Doxorubicin Impairs Smooth Muscle Cell Contraction: Novel Insights in Vascular Toxicity*** - Matthias Bosman, Dustin N. Krüger, Kasper Favere, Callan D. Wesley, Cédric H.G. Neutel, Birgit Van Asbroeck, Owen R. Diebels, Bart Faes, Timen J. Schenk, Wim Martinet, Guido R.Y. De Meyer, Emeline M. Van Craenenbroeck and Pieter-Jan D.F. Guns - Original Research article, published on November 26th 2021 in *International Journal of Molecular Sciences* [147]; DOI: https://doi.org/10.3390/ijms222312812

4. ***Doxorubicin induces arterial stiffness: a comprehensive in vivo and ex vivo evaluation of vascular toxicity in mice*** - Matthias Bosman, Kasper Favere, Cédric H.G. Neutel, Griet Jacobs, Guido R.Y. De Meyer, Wim Martinet, Emeline M. Van Craenenbroeck and Pieter-Jan D.F. Guns – Original Research Article, published on April 22nd 2021 in *Toxicology Letters* [120]; DOI: https://doi.org/10.1016/j.toxlet.2021.04.015

As co-author

1. ***Cardiac electrophysiology studies in mice via the transjugular route: comprehensive practical guide –*** Kasper Favere, Jens Van Fraeyenhove, Griet Jacobs, Matthias Bosman, Sander Eens, Johan De Sutter, Hielko Miljoen, Pieter-Jan Guns, Gilles De Keulenaer, Vincent Segers, Hein Heidbuchel – Research Methodology Article, published on August 26th 2022 in *American Journal of Phsyiology: Heart and Circulatory Physiology* [222]; DOI: https://doi.org/10.1152/ajpheart.00337.2022
2. ***Exercise and toll-like receptors: a systematic review*** – Kasper Favere, Matthias Bosman, Peter L. Delputte, Herman W. Favoreel, Emeline M. Van Craenenbroeck, Johan De Sutter, Isabel Witvrouwen, Guido R.Y. De Meyer, Hein Heidbuchel and Pieter-Jan D.F. Guns – Systematic Review, published in May 2021 in *Exercise Immunology Review* [223]; PMID: 33965901
3. ***Toll-like receptors: are they taking a toll on the heart in viral myocarditis?*** - Kasper Favere, Matthias Bosman, Karin Klingel, Stephane Heymans, Sophie Van Linthout, Peter L. Delputte, Johan De Sutter, Hein Heidbuchel and Pieter-Jan D.F. Guns – Review, published on May 27th 2021 in *Viruses* [224]; DOI: 10.3390/v13061003
4. ***A reliable set of reference genes to normalize oxygen-dependent cytoglobin gene expression levels in melanoma*** - Joey De Backer, Darko Maric, Matthias Bosman, Sylvia Dewilde and David Hoogewijs – Original Research Article from master thesis, published on May 25th 2021 in *Scientific Reports* [225]; DOI: 10.1038/s41598-021-90284-6

Poster and Oral Presentations

1. ***Investigating the Impact of Doxorubicin on Plaque Formation in a Mouse Model of Atherosclerosis*** **–** Matthias Bosman, Dustin Krüger, Lynn Roth, Guido De Meyer, Emeline Van Craenenbroeck and Pieter-Jan Guns – Poster Presentation at EAS, Mannheim, Germany, May 2023
2. ***Arterial Stiffness Is Transient During Doxorubicin Treatment Despite Persistent Endothelial Dysfunction: a Longitudinal Study in Mice*** **-** Matthias Bosman, Dustin Krüger, Charles Van Assche, Cédric Neutel, Kasper Favere, Constantijn Franssen, Wim Martinet, Lynn Roth, Guido De Meyer, Berta Cillero-Pastor, Emeline Van Craenenbroeck and Pieter-Jan Guns – Oral Presentation at Spearhead of Oncology (cluster meeting), Antwerp, Belgium, March 2023.
3. ***Arterial Stiffness Is Transient During Doxorubicin Treatment Despite Persistent Endothelial Dysfunction: a Longitudinal Study in Mice*** **-** Matthias Bosman, Dustin Krüger, Charles Van Assche, Cédric Neutel, Kasper Favere, Constantijn Franssen, Wim Martinet, Lynn Roth, Guido De Meyer, Berta Cillero-Pastor, Emeline Van Craenenbroeck and Pieter-Jan Guns – Oral Presentation at Autumn meeting of the Belgian Society of Physiology and Pharmacology, Brussels, Belgium, November 2022.
4. ***Doxorubicin induces measurable vascular toxicity: assessment in a clinical and preclinical study*** **–** Matthias Bosman, Hanne Boen, Constantijn Franssen Dustin Krüger, Cédric Neutel, Kasper Favere, Birgit Van Asbroeck, Inge Goovaerts, Guido De Meyer, Emeline Van Craenenbroeck and Pieter-Jan Guns – Oral Presentation at Frontiers in Cardiovascular Biomedicine, Budapest, Hungary, April 2022
5. ***Doxorubicin Impairs Smooth Muscle Cell Contraction: Novel Insights in Vascular Toxicity*** - Matthias Bosman, Dustin N. Krüger, Kasper Favere, Callan D. Wesley, Cédric H.G. Neutel, Birgit Van Asbroeck, Owen R. Diebels, Bart Faes, Timen J. Schenk, Wim Martinet, Guido R.Y. De Meyer, Emeline M. Van Craenenbroeck and Pieter-Jan D.F. Guns - Oral Presentation at Autumn meeting of the

Belgian Society of Physiology and Pharmacology, Brussels, Belgium, November 2021.

6. ***Doxorubicin induces arterial stiffness: a comprehensive in vivo and ex vivo evaluation of vascular toxicity in mice*** - Matthias Bosman, Kasper Favere, Cédric H.G. Neutel, Griet Jacobs, Guido R.Y. De Meyer, Wim Martinet, Emeline M. Van Craenenbroeck and Pieter-Jan D.F. Guns – Oral Presentation at Spring meeting of the Belgian Society of Physiology and Pharmacology, Brussels, Belgium, April 2021.

Acknowledgements (Dankwoord)

Het begon allemaal tijdens de FELASA opleiding in mijn laatste masterjaar biochemie en biotechnologie, een gastlezing door Pieter-Jan over het gebruik van muizen in cardiovasculair onderzoek. Ik was al geruime tijd aan het denken om een doctoraat te beginnen en op dat moment wist ik het onmiddellijk: mijn doctoraat ga ik in het labo Fysiofarmacologie doen. In de eerste plaats wou ik een doctoraat hier doen uit de wetenschappelijke interesse, maar anderzijds leek me dit labo ook de geschikte plek om meer zelfvertrouwen te ontwikkelen in mijn wetenschappelijk kunnen. Een e-mail van interesse naar Pieter-Jan, een sollicitatie en vier jaar van onderzoek later zijn we hier belandt… Een meer zelfzekere wetenschapper met nieuwe skills, zowel op professioneel als persoonlijk vlak, een kritische ingesteldheid, academisch schrijftalent en nu met de titel van doctor in de medische wetenschappen. Daarom wil ik in de allereerste plek mijn promotoren Prof. Dr. **Pieter-Jan Guns** en Prof. Dr. **Emeline Van Craenenbroeck** bedanken om mij de kans te geven mijn doctoraat te behalen.

Pieter-Jan, jouw deur (en raam 😉) stond altijd wagenwijd open waardoor je altijd bereikbaar was om experimenteel advies of bevestiging te geven wanneer dat nodig was. Die toegankelijkheid siert u, want op die manier had ik steeds het gevoel dat u niet mijn “baas” was maar een collega waar ik ten allen tijde kon op rekenen. Daarnaast heeft u een enorm schrijverstalent en dit heeft mij geleerd hoe je op een duidelijke, beknopte manier een wetenschappelijke boodschap overbrengt. Manuscript feedback kwam ook altijd héél snel wat voor mij het toeliet om telkens zo tijdsefficiënt mogelijk te schrijven. Bedankt dus om van mij een uitstekend schrijver te maken! Tot slot kon u zeer goed vanuit een andere hoek naar data kijken, een manier waarop ik zelf ook anders leerde denken. Dit heeft mijn kritische en creatieve geest aangewakkerd, dus ook bedankt daarvoor.

Emeline, een arts zijn en co-promotor tegelijkertijd is zeker een uitdaging qua tijdsmanagement. Toch slaagde u er altijd in om bij mijn onderzoek betrokken te zijn en te blijven, hetzij in persoon, online of gewoon via e-mail. Bedankt dus om op al die

manieren die bereikbaar- en toegankelijkheid te tonen. Voor iemand die geen geneeskunde heeft gestudeerd heeft u vooral mijn klinische geest versterkt. Denken hoe data relevant (of net niet is) voor patiënten heb ik van u geleerd. Dat uitte zich ook in feedback op manuscripten, waardoor ik steeds het translationeel perspectief tijdens het schrijven nooit uit het oog verloor. Dank voor dat! De keren dat we elkaar zagen vroeg u ook altijd hoe ik me voelde of gaf je een complimentje. Bedankt voor dat menselijke (en niet altijd het wetenschappelijke) aspect.

Een doctoraat loopt ook niet altijd van een leien dakje… Soms mislukken er experimenten, maar de voornaamste hindernis was de coronapandemie. Verschillende rondes van quarantaines, thuiswerk, social engagement beperkingen hebben het zeker niet makkelijk gemaakt om onderzoek te doen, maar beïnvloeden tevens het mentaal welzijn. **Pieter-Jan** en **Emeline**, ik wil jullie bedanken voor jullie steun, zowel op onderzoeksgebied als mentaal vlak.

Wetenschap is teamwerk en ik zou mijn doctoraat ook niet hebben kunnen voltooien zonder de hulp van anderen. **Guido**, bedankt voor uw ongelimiteerd enthousiasme ten allen tijde. U was steeds het zonnetje in het lab en kon me altijd blij maken als het wat minder ging, zowel op wetenschappelijk als privé vlak. **Wim**, ik wil u bedanken voor al het moleculaire werk advies dat u heeft gegeven en de rust dat u uitstraalt. U zorgt ervoor dat mensen direct op hun gemak worden gesteld. **Lynn**, ik denk dat ik voor iedereen hier op het lab spreek dat u naast professor ook een uitstekend therapeut bent. U was de persoon waar ik altijd een gewone, goeie babbel mee kon hebben over van alles en nog wat. Dat maakt u ook een uitstekende manager van ons lab, en ik wil u bedanken dat ik ook altijd bij jou terecht kon (sorry voor de vertragingen met werken haha). **Hans**, bedankt voor je vragen tijdens de Tuesday-meetings. **Gilles** en **Vincent**, jullie zijn een onafscheidelijk duo en, ondanks dat jullie niet rechtsreeks betrokken waren bij mijn onderzoek, stond de deur altijd open voor vragen of experimentele feedback. Bedankt daarvoor.

Naast alle professoren wil ik ook mijn collega-PhD-studenten bedanken. Een dikke merci aan **Paula**, **Besa**, **Dorien**, **Jhana**, **Sofie**, **Isabelle, Bieke** en **Lindsey** om mij welkom te laten voelen op het lab toen ik net begon. Het is jammer dat ik niet langer met jullie hebben kunnen samenwerken. **Farnaz** en **Pauline**, jullie waren bij de start van mijn doctoraat ook van de partij en waren een kompas om mij wegwijs te maken op T2. Bedankt daarvoor! @**Farnaz**, onze babbeltjes over Marvel waren altijd een leuke afwisseling tussen de experimenten door.

Uiteraard een speciale dank aan mijn bureaugenoten. **Kasper**, we zijn samen begonnen en het is ongelofelijk dat ik vier jaar geleden je nog niet kende... Bedankt om steeds mijn manuscripten van klinische feedback te voorzien en ook advies te geven omtrent de verschillende (soms ook vreemde) medische kwaaltjes die ik tijdens mijn doctoraat had. Het voelt raar aan dat ik nog blijf en jij weggaat. Hopelijk blijven we in contact. **Benji**, als jij lacht dan hoort het hele lab dat, en dat is zeker niet negatief bedoeld. In onze bureau, bracht je altijd ambiance (dat is Frans voor "sfeer" en ik weet hoe slecht je bent in deze taal dus vandaar de vertaling haha). We hebben veel gelachen en plezier gemaakt. Bedankt voor die leuke en hilarische momenten. Lachen terzijde, konden we ook bij elkaar onze harten luchten als het wat minder ging; bedankt dus ook om een goede vriend te zijn in de moeilijkere tijden. **Dustin**, *guten Tag mein Freund*, how can I forget my favourite German colleague? Not only were we partners in doxorubicin crime, we also went to Maastricht together for the proteomics experiments. You are a genuinely great, fun and compassionate guy! Thank you for that! Also, your vegan cooking is amazing, so I would get a food truck if I were you and hit the road after your PhD. **Céline**, *buongiorno il mio Italiano preferito*, from Erasmus master student to fellow PhD colleague, you can be very proud of the work you have done and are doing right now. You are an amazing person and I always enjoyed our conversations in the office, especially because you are an exceptionally caring person. I really admire that in you. Thank you! Your Dutch is getting very good as well. Keep up that eagerness to learn.

Naast onze bureau, wil ik ook de andere bureaus nog bedanken. **Cédric**, the experimental T2 *consigliere*, ik ben tijdens mijn doctoraat vaak bij jou langsgekomen voor advies omtrent data en hoe iets zou verklaard kunnen worden. Telkens opnieuw was je meer dan bereidwillig om samen te brainstormen over mogelijke andere onderzoekpistes. Ik heb hier altijd nieuwe inspiratie uitgehaald. Bedankt daarvoor! Daarnaast was je ook gewoon echt *ne plezante kerel* om mee rond te hangen. Of het nu ging over Netflix series, films of games, we vonden wel iets om over te praten en even aan het werk te ontsnappen. Dikke merci daarvoor! Jouw airsoft verhalen waren ook steeds héél boeiend… Ideaal voor de volgende T2 teambuilding toch? Ik kijk al uit naar waar de post-doc ons samen gaat brengen. **Melissa**, niemand op T2 is zo ordelijk als mij buiten jij! Het was telkens een groot plezier om samen met jou experimenten uit te voeren. Je bent bovendien een grote hulp hier op T2 (eerlijk, ik weet niet wat er met ons lab zou gebeuren moest jij niet mee een oogje in het zeil houden). Nog eens bedankt voor jouw onmisbare hulp met mijn atherosclerose studie. **Michelle**, wat moet er nog meer gezegd worden dan dat jij gewoon een top madam bent! Je bent telkens druk bezig met experimenten, maar een echte pilaar van het lab waar iedereen op kan steunen, zowel voor experimentele hulp/advies als plezier en een goede babbel. Bedankt voor de leuke gesprekken en altijd een deugddoende en dag-makende goeiemorgen. **Freke**, net zoals Michelle, ben jij altijd goedgezind, ook als het even wat tegenzit met experimenten. Je blijft optimistisch en dat straalt over op anderen, inclusief mij. Merci!

Birgit en **Dorien**, het onafscheidelijke kinesistenduo op T2, jullie waren echt een plezier om mee samen te werken. Ik weet niet of je het nog kan herinneren, maar ik zeker nog wel, **Dorien**, jij was een enorme hulp bij mijn allereerste badjes experimenten en dat waren héél lange dagen. Bedankt voor die 100+ keer om in de badjes te pipeteren! **Birgit**, we hebben héél vaak héél hard gelachen. Ik denk dat mijn lachklier voor de rest van mijn leven in deze toestand blijft, maar dat was het dubbel en dik waard. Even goed kunnen *zwanzen* en lachen was tussen de experimentjes toch af en toe echt nodig. Merci daarvoor! **Sander**, de opvolger

van Kasper, en meer dan waardig. Je bent een enorme harde werker en dat siert jou. Houd die ingesteldheid vast voor je verdere PhD. **Callan**, my man, you are one of the most empathetic and easy-going guys I have ever met. The way you love and would do anything for your family is impressive and a real source of inspiration. When my grandfather was in the hospital, I always had to think about you and you helped me realise how important the smaller, family things are in life as it can change rapidly. Thank you for that!

There would be no Pharmaco without Physio. **Eline**, het zonnetje van T2, je was altijd supergoed gezind (ook als het wat minder ging). Die positieve houding straalde op iedereen hier op het lab en ik werd altijd goed gezind als we een babbeltje deden. Bedankt daarvoor! **Jens**, voor jou was ik niet Matthias maar Matty. Onze begroetingen in de gang en onze gesprekken waren meestal kort maar zeker altijd plezant. Je bent een ongelofelijke wetenschapper. Ik denk dat niemand hier op T2 ooit jouw operatie skills in muisjes kan evenaren. **Michiel**, de varkentjesexpert en arts. Hoe je dat allemaal hebt kunnen combineren, blijft een raadsel voor mij. Indrukwekkend! Naast dat was je ook een echte comedian en ik kon altijd goed met jouw mopjes lachen. **Jente**, ondanks een moeilijke periode stond je er altijd. Je bent een top madam en wetenschapper! Een groot applaus van mij voor jou en jouw doorzettingsvermogen 😉. **Bo**, mijn fellow Star Wars geek, je bent een fitnessende PhD-doende dierenarts waar ik enorm veel respect voor heb. Naast dit indrukwekkend palmares, genoot ik echt van onze gesprekjes over van alles en nog wat dat met Star Wars te maken had. Binnenkort zullen we het wel uitgebreid over die nieuwe Ashoka serie hebben (hyped!). **Siel**, ik bewonder je ingesteldheid om altijd direct anderen te helpen. Bedankt voor jouw advies bij mijn qPCR experimenten. **Julie**, iemand die net zoals ik niet zonder muziek kan leven. Ik denk dat wij de mensen op het lab waren die altijd koptelefoon/oortjes op hadden met (soms luide) muziek. Wat was het fijn om met jou over van alles en nog wat te babbelen.

There would also be no Pharmaco without Gastro. **Benedicte**, full-time professor en thuis nog voor 4 zonen zorgen… De energie waarmee u dit elke dag doet en naar het lab meebrengt is onuitputtelijk. Ik heb steeds van onze gesprekjes in het meer casual Antwerpse dialect genoten. **Joris**, ondanks dat je niet rechtstreeks bij mijn onderzoek betrokken was, was je wel altijd bereid te helpen. Ik kan je niet genoeg bedanken om de gasflessen voor de badjes mee te helpen vervangen en de microscoop te herstellen wanneer ik deze dringend nodig had. **Shivani**, crazy en nog meer dan dat, maar zo fijn om jou altijd bezig te zien. Merci voor de leuke momenten. **Nikita, Axelle, Arno, Philip** en **Dénise**, ik heb jullie iets minder gezien of niet lang genoeg gekend, maar ik wens jullie nog veel succes met jullie verdere PhD en carrière.

Een lab is meer dan alleen maar doctoraatsstudenten en professoren… **Paul**, de badjesgoeroe, jij bent degene die me alles heeft geleerd van de badjes en hoe je deze data analyseert. Ik heb veel badjesexperimenten gedaan tijdens mijn doctoraat en zonder jouw lessen had ik dit niet gekund. Bedankt om mij altijd te helpen en advies te geven omtrent data interpretatie en verdere experimenten. Jouw pensioen is dubbel en dik verdiend! Geniet ervan 😊! **Marc**, naast de badjes, heb ik veel VEVO experimenten gedaan. Merci om te helpen wanneer er iets misliep met het toestel. **Rita**, voor mij heb je nooit kleuringen gedaan, maar wij waren wel altijd degenen die het lab openden 's ochtends héél vroeg. Onze koffiekletsjes tijdens deze vroege uurtjes waren telkens een goed begin van de dag. Veel plezier met je reizen in Schotland! **Mandy**, een waardige opvolger van Rita, zonder jou had ik nooit histologie geleerd. Dankzij jou kan ik nu coupes kleuren voor mijn data analyses en deze belangrijke labtechniek aan mijn CV toevoegen. Om eerlijk te zijn, ik kan dit goed, maar jij blijft hier toch wel de meester in en coupes van jou zijn toch steeds dat tikkeltje beter. Misschien is het dat vleugje "Mandy" dat een coupe een coupe maakt… Daarnaast was onze Monday en Friday talk elke week een gevestigde waarde om te horen wat we in het weekend gingen doen en vervolgens hoe het weekend was. Dit vond ik elke keer superleuk en dat gaan we blijven doen

tijdens mijn post-doc hè 😉. **Min** en **Abby**, zonder jullie wist ik nooit welke muizen ik had of was ik aan het sukkelen met Anibio. Bedankt voor de genotyperingen, **Min**, en bedankt voor de technische ondersteuning met Anibio, **Abby**. **Maya**, jij zorgt ervoor dat de onderzoeksprojecten worden binnengehaald, merci daarvoor! Ik zal naar aanloop van mijn post-doc project nog wel eens bij jou langskomen voor wat advies. **Griet** en **Kathleen**, héél fijn om te weten dat er op T2 mensen rondlopen die liefst zo ordelijk en gestructureerd werken als ik. Als er ergens weer een boeltje was gemaakt in één van de labs, dan kon ik altijd bij jullie mijn beklag doen en konden we samen actie ondernemen. **Griet**, zonder jou zou het lab niet kunnen draaien. Je bent een steunpilaar voor zowel werk- als privé-gerelateerde zaken en we mogen allemaal wat meer danku zeggen voor wat jij voor ons allemaal doet. Bij deze dus, een ongelofelijke dikke merci! **Kathleen**, bedankt om telkens voor mij te bellen naar een bedrijf als er weeral eens een pakketje vertraging opliep of kwijt was. Zonder jou zouden er geen bestellingen zijn en dus ook geen producten om de experimenten te doen. Jij vormt op deze manier één van de belangrijke schakels in het lab. Merci om ons werk mogelijk te maken! **Lotte**, bij jou kwam ik telkens wanneer de gasflessen voor de badjes weeral eens vergeten besteld waren. Bedankt om dit altijd op te lossen en veel succes/plezier met je nieuwe job. **Evy**, jou ken ik nog niet zo lang, maar dat zal de komende jaren wel veranderen tijdens mijn post-doc. Welkom op T2! **Tine**, net zoals Griet, Kathleen, Mandy, Min en Abby onmisbare schakels zijn voor het lab, ben jij dat voor Fysio en ook voor ons. Bedankt daarvoor!

Ik had nog graag het OLV ziekenhuis in Aalst met **Leen** en **Ward** en de M4I onderzoeksgroep in Maastricht met **Berta**, **Charles** en **Ronny** bedankt voor de mooie samenwerkingen. Zonder jullie had ik die mooie patiënten en proteomics data nooit bekomen. Bedankt om de mogelijkheid te bieden voor deze samenwerking.

Dit doctoraat was nooit mogelijk geweest zonder de onvoorwaardelijke steun van mijn familie, schoonfamilie en vrienden.

Mama en **Papa**, of hoe ik ze noem *Moepie* en *Pips*, ik heb het geluk gehad dat ik bij de beste ouders op deze planeet ben terechtgekomen. Van kleins af aan hebben jullie altijd in mij geloofd en mij altijd verteld dat ik mijn dromen moest volgen. Oorspronkelijk wou ik kanker genezen… Dat was een beetje te hoog gegrepen, maar dankzij jullie onuitputtelijke aanmoedigingen ben ik een lichtjes andere onderzoekspiste ingeslagen, en kijk ik dankzij jullie geloof in mij met trots op dit afgelegde traject terug. Soms waren er moeilijkere momenten en wat putten in mijn weg, maar dat was ook het geval bij jullie. Jullie hebben ondanks tegenslag en stress, denk maar aan alle problemen bij jullie verhuis naar het nieuwe appartement, veel teleurstelling en frustratie ondervonden. Echter, jullie doorzettingsvermogen heeft ervoor gezorgd dat uiteindelijk alles is goedgekomen. Dat licht aan het einde van de lange doorzettingstunnel heeft ook op mij gestraald. Dankzij jullie heb ik de obstakels op mijn doctoraatstraject kunnen overwinnen. Vanuit de grond van het hart van jullie *dropke*, een dikke merci om altijd de hoopvolle en liefdevolle *Moepie* en *Pips* en zoveel meer te zijn voor mij.

Verdere steun was er altijd te vinden bij de rest van mijn familie. Merci aan mijn ***noenkel,*** **tante**, mijn twee **bompa's, moeke, Anita, tante Rita en Sylvie en Bart**.

Yannick, de man van mijn leven, *quelle bibiche mijn gedacht*. De tweede helft van mijn doctoraat was nooit mogelijk geweest zonder jouw onvoorwaardelijke steun en liefde. Het onderzoek, het schrijven en het publiceren van artikels ging op een bepaald moment héél moeizaam, maar toch gaf je mij de kracht om altijd in mezelf te blijven geloven. Net zoals Freddie die zei: *"The show must go on."* en zoals ABBA die zong: *"You can dance, you can jive, having the time of your life"*, zo wist jij net altijd die dingen te zeggen waardoor ik de kracht en de moed vond om door te blijven gaan, maar ook niet vergat om van het

leven te genieten. Vaak zorgde je er voor dat we iets leuks konden gaan doen zodat ik even mijn hoofdje kon leegmaken. Die kleine momenten waren voor mij van onschatbare waarden en zijn steunpilaren geworden waar ik dit doctoraat op heb kunnen bouwen. Door jou ben ik tevens als mens enorm verandert, alleen maar ten goede. Mijn zelfvertrouwen en zelfkennis zijn gegroeid en ben ik ook mentaal veel rustiger geworden. Vanuit het diepste van mijn hartje, een superdikke merci en mijn doctoraat is nu klaar, of zoals Balthasar Boma het zei: *"'t Is in de sacoche."* I love you for infinity and beyond, *boeboe*.

Tot slot, wil ik ook nog mijn schoonfamilie bedanken. Ondanks dat mijn doctoraat en onderzoek niet altijd helemaal te volgen waren, luisterden jullie altijd naar wat ik had te vertellen. **Karin, Dominique, Raymond** en **Rita**, merci daarvoor en bedankt om altijd te luisteren. **Bijoux** en **Lato**, jullie zullen dit niet kunnen lezen als huisdieren maar toch hier vereeuwigd voor de vele tussendoor leuke knuffel en speelmomenten die van groot belang waren voor mij.

Brent, my brother from another mother en mijn beste kameraad, het was geen simpel sociaal leven tijdens corona. Tijdens de pandemie waren wij de enigen die elkaar zagen en daardoor was je dus ook de enige kameraad van mij die kon luisteren naar mijn onderzoek met alle ups en downs. Merci om samen de ups te vieren en mij uit de downmomenten te trekken met o.a. *Just Dance*. En ja, ik schrijf hier *Just Dance* zodat iedereen weet da wij daar echt *mega stars* in zijn (pun intended). Uiteraard ook een dikke merci aan jouw mama, **Helga**, jouw papa **Mark**, jouw zus, **Samantha** en jouw vriendin, **Lara**, die samen met jou een tweede familie vormden voor mij en er voor mij ten allen tijde waren tijdens corona en daarbuiten. Onze trips naar Disneyland waren altijd dé moment om de batterijtjes weer op te laden. En dat was vaak nodig tijdens mijn doctoraat. Merci daarvoor! Tot slot, wil ik ook nog even **Dante, Evelien, Joachim, Manou, Dieter, Rik, Dorien, Willem, *Krikke*, de Jonassen, Jonathan, Roy, Nico, Jorgen en Niels** bedanken voor de superplezante momenten, zowel online als in het echte leven.

References

1. Quaresma, M., M.P. Coleman, and B. Rachet, *40-year trends in an index of survival for all cancers combined and survival adjusted for age and sex for each cancer in England and Wales, 1971-2011: a population-based study.* Lancet, 2015. **385**(9974): p. 1206-18.
2. Miller, K.D., et al., *Cancer treatment and survivorship statistics, 2019.* CA Cancer J Clin, 2019. **69**(5): p. 363-385.
3. Chuquin, D., A. Abbate, and W. Bottinor, *Hypertension in Cancer Survivors: A Review of the Literature and Suggested Approach to Diagnosis and Treatment.* J Cardiovasc Pharmacol, 2022. **80**(4): p. 522-530.
4. Florido, R., et al., *Cardiovascular Disease Risk Among Cancer Survivors: The Atherosclerosis Risk In Communities (ARIC) Study.* J Am Coll Cardiol, 2022. **80**(1): p. 22-32.
5. Zhang, F., et al., *Risk of Stroke in Cancer Survivors: A Meta-analysis of Population-Based Cohort Studies.* Neurology, 2021. **96**(4): p. e513-e526.
6. Whittaker, A.L., R.P. George, and L. O'Malley, *Prevalence of cognitive impairment following chemotherapy treatment for breast cancer: a systematic review and meta-analysis.* Sci Rep, 2022. **12**(1): p. 2135.
7. Dieffenbach, B.V., et al., *Late-onset kidney failure in survivors of childhood cancer: a report from the Childhood Cancer Survivor Study.* Eur J Cancer, 2021. **155**: p. 216-226.
8. Mertens, A.C., et al., *Cause-specific late mortality among 5-year survivors of childhood cancer: the Childhood Cancer Survivor Study.* J Natl Cancer Inst, 2008. **100**(19): p. 1368-79.
9. Patnaik, J.L., et al., *Cardiovascular disease competes with breast cancer as the leading cause of death for older females diagnosed with breast cancer: a retrospective cohort study.* Breast Cancer Res, 2011. **13**(3): p. R64.
10. Morelli, M.B., et al., *Cardiotoxicity of Anticancer Drugs: Molecular Mechanisms and Strategies for Cardioprotection.* Front Cardiovasc Med, 2022. **9**: p. 847012.
11. Cohen, J.B., et al., *Cancer Therapy-Related Hypertension: A Scientific Statement From the American Heart Association.* Hypertension, 2023. **80**(3): p. e46-e57.

12. Lenneman, C.G. and D.B. Sawyer, *Cardio-Oncology: An Update on Cardiotoxicity of Cancer-Related Treatment.* Circ Res, 2016. **118**(6): p. 1008-20.
13. Lyon, A.R., et al., *2022 ESC Guidelines on cardio-oncology developed in collaboration with the European Hematology Association (EHA), the European Society for Therapeutic Radiology and Oncology (ESTRO) and the International Cardio-Oncology Society (IC-OS).* Eur Heart J, 2022. **43**(41): p. 4229-4361.
14. McGowan, J.V., et al., *Anthracycline Chemotherapy and Cardiotoxicity.* Cardiovasc Drugs Ther, 2017. **31**(1): p. 63-75.
15. Zamorano, J.L., et al., *2016 ESC Position Paper on cancer treatments and cardiovascular toxicity developed under the auspices of the ESC Committee for Practice Guidelines: The Task Force for cancer treatments and cardiovascular toxicity of the European Society of Cardiology (ESC).* Eur Heart J, 2016. **37**(36): p. 2768-2801.
16. Hequet, O., et al., *Subclinical late cardiomyopathy after doxorubicin therapy for lymphoma in adults.* J Clin Oncol, 2004. **22**(10): p. 1864-71.
17. Leger, K., et al., *Subclinical cardiotoxicity in childhood cancer survivors exposed to very low dose anthracycline therapy.* Pediatr Blood Cancer, 2015. **62**(1): p. 123-7.
18. Thorn, C.F., et al., *Doxorubicin pathways: pharmacodynamics and adverse effects.* Pharmacogenet Genomics, 2011. **21**(7): p. 440-6.
19. Doroshow, J.H., *Effect of anthracycline antibiotics on oxygen radical formation in rat heart.* Cancer Res, 1983. **43**(2): p. 460-72.
20. Sterba, M., et al., *Oxidative stress, redox signaling, and metal chelation in anthracycline cardiotoxicity and pharmacological cardioprotection.* Antioxid Redox Signal, 2013. **18**(8): p. 899-929.
21. Lyu, Y.L., et al., *Topoisomerase IIbeta mediated DNA double-strand breaks: implications in doxorubicin cardiotoxicity and prevention by dexrazoxane.* Cancer Res, 2007. **67**(18): p. 8839-46.
22. Zhang, S., et al., *Identification of the molecular basis of doxorubicin-induced cardiotoxicity.* Nat Med, 2012. **18**(11): p. 1639-42.

23. Jirkovsky, E., et al., *Clinically Translatable Prevention of Anthracycline Cardiotoxicity by Dexrazoxane Is Mediated by Topoisomerase II Beta and Not Metal Chelation.* Circ Heart Fail, 2021. **14**(11): p. e008209.
24. Maejima, Y., et al., *Induction of premature senescence in cardiomyocytes by doxorubicin as a novel mechanism of myocardial damage.* Aging Cell, 2008. **7**(2): p. 125-36.
25. Altieri, P., et al., *Inhibition of doxorubicin-induced senescence by PPARdelta activation agonists in cardiac muscle cells: cooperation between PPARdelta and Bcl6.* PLoS One, 2012. **7**(9): p. e46126.
26. Armstrong, G.T., et al., *Modifiable risk factors and major cardiac events among adult survivors of childhood cancer.* J Clin Oncol, 2013. **31**(29): p. 3673-80.
27. Chaosuwannakit, N., et al., *Aortic stiffness increases upon receipt of anthracycline chemotherapy.* J Clin Oncol, 2010. **28**(1): p. 166-72.
28. Drafts, B.C., et al., *Low to moderate dose anthracycline-based chemotherapy is associated with early noninvasive imaging evidence of subclinical cardiovascular disease.* JACC Cardiovasc Imaging, 2013. **6**(8): p. 877-85.
29. Mihalcea, D., et al., *3D echocardiography, arterial stiffness, and biomarkers in early diagnosis and prediction of CHOP-induced cardiotoxicity in non-Hodgkin's lymphoma.* Sci Rep, 2020. **10**(1): p. 18473.
30. Novo, G., et al., *Arterial Stiffness: Effects of Anticancer Drugs Used for Breast Cancer Women.* Front Physiol, 2021. **12**: p. 661464.
31. Chow, A.Y., et al., *Anthracyclines cause endothelial injury in pediatric cancer patients: a pilot study.* J Clin Oncol, 2006. **24**(6): p. 925-8.
32. Jang, W.J., D.Y. Choi, and I.S. Jeon, *Vascular endothelial dysfunction after anthracyclines treatment in children with acute lymphoblastic leukemia.* Korean J Pediatr, 2013. **56**(3): p. 130-4.
33. Shirwany, N.A. and M.H. Zou, *Arterial stiffness: a brief review.* Acta Pharmacol Sin, 2010. **31**(10): p. 1267-76.
34. O'Rourke, M.F. and J. Hashimoto, *Mechanical factors in arterial aging: a clinical perspective.* J Am Coll Cardiol, 2007. **50**(1): p. 1-13.

35. Liu, R.M. and L.P. Desai, *Reciprocal regulation of TGF-beta and reactive oxygen species: A perverse cycle for fibrosis.* Redox Biol, 2015. **6**: p. 565-577.
36. Nelson, K.K. and J.A. Melendez, *Mitochondrial redox control of matrix metalloproteinases.* Free Radic Biol Med, 2004. **37**(6): p. 768-84.
37. Rossman, M.J., et al., *Targeting mitochondrial fitness as a strategy for healthy vascular aging.* Clin Sci (Lond), 2020. **134**(12): p. 1491-1519.
38. Mittal, M., et al., *Reactive oxygen species in inflammation and tissue injury.* Antioxid Redox Signal, 2014. **20**(7): p. 1126-67.
39. De Moudt, S., et al., *Progressive aortic stiffness in aging C57Bl/6 mice displays altered contractile behaviour and extracellular matrix changes.* Commun Biol, 2022. **5**(1): p. 605.
40. Safar, M.E., et al., *Pulse pressure, arterial stiffness, and end-organ damage.* Curr Hypertens Rep, 2012. **14**(4): p. 339-44.
41. Vatner, S.F., et al., *Vascular Stiffness in Aging and Disease.* Front Physiol, 2021. **12**: p. 762437.
42. Leloup, A.J.A., et al., *Vascular smooth muscle cell contraction and relaxation in the isolated aorta: a critical regulator of large artery compliance.* Physiol Rep, 2019. **7**(4): p. e13934.
43. Leloup, A.J.A., et al., *Ex vivo aortic stiffness in mice with different eNOS activity.* Am J Physiol Heart Circ Physiol, 2020. **318**(5): p. H1233-H1244.
44. Herrera, M.D., et al., *Endothelial dysfunction and aging: an update.* Ageing Res Rev, 2010. **9**(2): p. 142-52.
45. Sharma, J.N., A. Al-Omran, and S.S. Parvathy, *Role of nitric oxide in inflammatory diseases.* Inflammopharmacology, 2007. **15**(6): p. 252-9.
46. Hadi, H.A., C.S. Carr, and J. Al Suwaidi, *Endothelial dysfunction: cardiovascular risk factors, therapy, and outcome.* Vasc Health Risk Manag, 2005. **1**(3): p. 183-98.
47. Mitchell, G.F., et al., *Arterial stiffness and cardiovascular events: the Framingham Heart Study.* Circulation, 2010. **121**(4): p. 505-11.
48. Lerman, A. and A.M. Zeiher, *Endothelial function: cardiac events.* Circulation, 2005. **111**(3): p. 363-8.

49. Sun, H.J., et al., *Role of Endothelial Dysfunction in Cardiovascular Diseases: The Link Between Inflammation and Hydrogen Sulfide.* Front Pharmacol, 2019. **10**: p. 1568.
50. Maruhashi, T., et al., *Endothelial Dysfunction, Increased Arterial Stiffness, and Cardiovascular Risk Prediction in Patients With Coronary Artery Disease: FMD-J (Flow-Mediated Dilation Japan) Study A.* J Am Heart Assoc, 2018. **7**(14).
51. Bonarjee, V.V.S., *Arterial Stiffness: A Prognostic Marker in Coronary Heart Disease. Available Methods and Clinical Application.* Front Cardiovasc Med, 2018. **5**: p. 64.
52. Boutouyrie, P., et al., *Aortic stiffness is an independent predictor of primary coronary events in hypertensive patients: a longitudinal study.* Hypertension, 2002. **39**(1): p. 10-5.
53. Vasan, R.S., et al., *Interrelations Between Arterial Stiffness, Target Organ Damage, and Cardiovascular Disease Outcomes.* J Am Heart Assoc, 2019. **8**(14): p. e012141.
54. Blacher, J., et al., *Impact of aortic stiffness on survival in end-stage renal disease.* Circulation, 1999. **99**(18): p. 2434-9.
55. Palta, P., et al., *Central Arterial Stiffness Is Associated With Structural Brain Damage and Poorer Cognitive Performance: The ARIC Study.* J Am Heart Assoc, 2019. **8**(2): p. e011045.
56. Heagerty, A.M., E.H. Heerkens, and A.S. Izzard, *Small artery structure and function in hypertension.* J Cell Mol Med, 2010. **14**(5): p. 1037-43.
57. Brandes, R.P., *Endothelial dysfunction and hypertension.* Hypertension, 2014. **64**(5): p. 924-8.
58. Oh, G.C. and H.J. Cho, *Blood pressure and heart failure.* Clin Hypertens, 2020. **26**: p. 1.
59. Davignon, J. and P. Ganz, *Role of endothelial dysfunction in atherosclerosis.* Circulation, 2004. **109**(23 Suppl 1): p. III27-32.
60. He, H., et al., *Doxorubicin Induces Endotheliotoxicity and Mitochondrial Dysfunction via ROS/eNOS/NO Pathway.* Front Pharmacol, 2019. **10**: p. 1531.
61. Clayton, Z.S., et al., *Tumor Necrosis Factor Alpha-Mediated Inflammation and Remodeling of the Extracellular Matrix Underlies Aortic Stiffening Induced by*

the Common Chemotherapeutic Agent Doxorubicin. Hypertension, 2021. **77**(5): p. 1581-1590.
62. Shen, B., et al., *Doxorubicin-induced vasomotion and [Ca(2+)](i) elevation in vascular smooth muscle cells from C57BL/6 mice.* Acta Pharmacol Sin, 2009. **30**(11): p. 1488-95.
63. Gibson, N.M., et al., *Doxorubicin-induced vascular dysfunction and its attenuation by exercise preconditioning.* J Cardiovasc Pharmacol, 2013. **62**(4): p. 355-60.
64. Olukman, M., et al., *Reversal of doxorubicin-induced vascular dysfunction by resveratrol in rat thoracic aorta: Is there a possible role of nitric oxide synthase inhibition?* Anadolu Kardiyol Derg, 2009. **9**(4): p. 260-6.
65. Hayward, R. and D.S. Hydock, *Doxorubicin cardiotoxicity in the rat: an in vivo characterization.* J Am Assoc Lab Anim Sci, 2007. **46**(4): p. 20-32.
66. Olson, L.E., et al., *Protection from doxorubicin-induced cardiac toxicity in mice with a null allele of carbonyl reductase 1.* Cancer Res, 2003. **63**(20): p. 6602-6.
67. Armenian, S.H., et al., *Screening for cardiac dysfunction in anthracycline-exposed childhood cancer survivors.* Clin Cancer Res, 2014. **20**(24): p. 6314-23.
68. Sawaya, H., et al., *Early detection and prediction of cardiotoxicity in chemotherapy-treated patients.* Am J Cardiol, 2011. **107**(9): p. 1375-80.
69. Benetos, A., et al., *Pulse pressure: a predictor of long-term cardiovascular mortality in a French male population.* Hypertension, 1997. **30**(6): p. 1410-5.
70. Said, M.A., et al., *Relationship of Arterial Stiffness Index and Pulse Pressure With Cardiovascular Disease and Mortality.* J Am Heart Assoc, 2018. **7**(2).
71. Lyle, A.N. and U. Raaz, *Killing Me Unsoftly: Causes and Mechanisms of Arterial Stiffness.* Arterioscler Thromb Vasc Biol, 2017. **37**(2): p. e1-e11.
72. Chae, C.U., et al., *Increased pulse pressure and risk of heart failure in the elderly.* JAMA, 1999. **281**(7): p. 634-9.
73. Sutton-Tyrrell, K., et al., *Elevated aortic pulse wave velocity, a marker of arterial stiffness, predicts cardiovascular events in well-functioning older adults.* Circulation, 2005. **111**(25): p. 3384-90.

74. Mitchell, G.F., et al., *Pulse pressure and risk of new-onset atrial fibrillation.* JAMA, 2007. **297**(7): p. 709-15.
75. Mitchell, G.F., et al., *Sphygmomanometrically determined pulse pressure is a powerful independent predictor of recurrent events after myocardial infarction in patients with impaired left ventricular function. SAVE investigators. Survival and Ventricular Enlargement.* Circulation, 1997. **96**(12): p. 4254-60.
76. Zieman, S.J., V. Melenovsky, and D.A. Kass, *Mechanisms, pathophysiology, and therapy of arterial stiffness.* Arterioscler Thromb Vasc Biol, 2005. **25**(5): p. 932-43.
77. Johnson, C.P., et al., *Age related changes in the tunica media of the vertebral artery: implications for the assessment of vessels injured by trauma.* J Clin Pathol, 2001. **54**(2): p. 139-45.
78. Greenwald, S.E., *Ageing of the conduit arteries.* J Pathol, 2007. **211**(2): p. 157-72.
79. Sehgel, N.L., et al., *Increased vascular smooth muscle cell stiffness: a novel mechanism for aortic stiffness in hypertension.* Am J Physiol Heart Circ Physiol, 2013. **305**(9): p. H1281-7.
80. Bellien, J., et al., *Arterial stiffness is regulated by nitric oxide and endothelium-derived hyperpolarizing factor during changes in blood flow in humans.* Hypertension, 2010. **55**(3): p. 674-80.
81. Fitch, R.M., et al., *Nitric oxide synthase inhibition increases aortic stiffness measured by pulse wave velocity in rats.* Cardiovasc Res, 2001. **51**(2): p. 351-8.
82. Laurent, S., et al., *Expert consensus document on arterial stiffness: methodological issues and clinical applications.* Eur Heart J, 2006. **27**(21): p. 2588-605.
83. Hartley, C.J., et al., *Noninvasive determination of pulse-wave velocity in mice.* Am J Physiol, 1997. **273**(1 Pt 2): p. H494-500.
84. Di Lascio, N., et al., *Non-invasive assessment of pulse wave velocity in mice by means of ultrasound images.* Atherosclerosis, 2014. **237**(1): p. 31-7.
85. Leloup, A.J., et al., *Applanation tonometry in mice: a novel noninvasive technique to assess pulse wave velocity and arterial stiffness.* Hypertension, 2014. **64**(1): p. 195-200.

86. Tan, I., et al., *Heart rate dependence of aortic pulse wave velocity at different arterial pressures in rats.* Hypertension, 2012. **60**(2): p. 528-33.
87. Leloup, A.J., et al., *A novel set-up for the ex vivo analysis of mechanical properties of mouse aortic segments stretched at physiological pressure and frequency.* J Physiol, 2016. **594**(21): p. 6105-6115.
88. De Munck, D.G., et al., *Defective autophagy in vascular smooth muscle cells increases passive stiffness of the mouse aortic vessel wall.* Pflugers Arch, 2020. **472**(8): p. 1031-1040.
89. Renu, K., et al., *Molecular mechanism of doxorubicin-induced cardiomyopathy - An update.* Eur J Pharmacol, 2018. **818**: p. 241-253.
90. Parr, S.K., et al., *Anticancer Therapy-Related Increases in Arterial Stiffness: A Systematic Review and Meta-Analysis.* J Am Heart Assoc, 2020. **9**(14): p. e015598.
91. Mozos, I., et al., *Arterial stiffness in hematologic malignancies.* Onco Targets Ther, 2017. **10**: p. 1381-1388.
92. Clayton, Z.S., et al., *Doxorubicin-Induced Oxidative Stress and Endothelial Dysfunction in Conduit Arteries Is Prevented by Mitochondrial-Specific Antioxidant Treatment.* JACC CardioOncol, 2020. **2**(3): p. 475-488.
93. Hodjat, M., et al., *Urokinase receptor mediates doxorubicin-induced vascular smooth muscle cell senescence via proteasomal degradation of TRF2.* J Vasc Res, 2013. **50**(2): p. 109-23.
94. van Langen, J., et al., *Selective loss of basal but not receptor-stimulated relaxation by endothelial nitric oxide synthase after isolation of the mouse aorta.* Eur J Pharmacol, 2012. **696**(1-3): p. 111-9.
95. Niiranen, T.J., et al., *Relative Contributions of Pulse Pressure and Arterial Stiffness to Cardiovascular Disease.* Hypertension, 2019. **73**(3): p. 712-717.
96. Swain, S.M., F.S. Whaley, and M.S. Ewer, *Congestive heart failure in patients treated with doxorubicin: a retrospective analysis of three trials.* Cancer, 2003. **97**(11): p. 2869-79.
97. Bull, J.M., et al., *A randomized comparative trial of adriamycin versus methotrexate in combination drug therapy.* Cancer, 1978. **41**(5): p. 1649-57.

98. Geisler, C.H., et al., *Long-term progression-free survival of mantle cell lymphoma after intensive front-line immunochemotherapy with in vivo-purged stem cell rescue: a nonrandomized phase 2 multicenter study by the Nordic Lymphoma Group.* Blood, 2008. **112**(7): p. 2687-93.
99. von Pawel, J., et al., *Topotecan versus cyclophosphamide, doxorubicin, and vincristine for the treatment of recurrent small-cell lung cancer.* J Clin Oncol, 1999. **17**(2): p. 658-67.
100. Nichols, W.W. and D.A. McDonald, *Wave-velocity in the proximal aorta.* Med Biol Eng, 1972. **10**(3): p. 327-35.
101. Latham, R.D., et al., *Regional wave travel and reflections along the human aorta: a study with six simultaneous micromanometric pressures.* Circulation, 1985. **72**(6): p. 1257-69.
102. Murata, T., et al., *Chronic effect of doxorubicin on vascular endothelium assessed by organ culture study.* Life Sci, 2001. **69**(22): p. 2685-95.
103. Sung, J.Y., et al., *Interaction between mTOR pathway inhibition and autophagy induction attenuates adriamycin-induced vascular smooth muscle cell senescence through decreased expressions of p53/p21/p16.* Exp Gerontol, 2018. **109**: p. 51-58.
104. Hong, Z., et al., *Vascular smooth muscle cell stiffness and adhesion to collagen I modified by vasoactive agonists.* PLoS One, 2015. **10**(3): p. e0119533.
105. Carvajal, J.A., et al., *Molecular mechanism of cGMP-mediated smooth muscle relaxation.* J Cell Physiol, 2000. **184**(3): p. 409-20.
106. Fransen, P., et al., *Dissecting out the complex Ca2+-mediated phenylephrine-induced contractions of mouse aortic segments.* PLoS One, 2015. **10**(3): p. e0121634.
107. Luscher, T.F. and F.C. Tanner, *Endothelial regulation of vascular tone and growth.* Am J Hypertens, 1993. **6**(7 Pt 2): p. 283S-293S.
108. Vasquez-Vivar, J., et al., *Endothelial nitric oxide synthase-dependent superoxide generation from adriamycin.* Biochemistry, 1997. **36**(38): p. 11293-7.
109. Kalivendi, S.V., et al., *Doxorubicin-induced apoptosis is associated with increased transcription of endothelial nitric-oxide synthase. Effect of antiapoptotic antioxidants and calcium.* J Biol Chem, 2001. **276**(50): p. 47266-76.

110. Vaziri, N.D., K. Liang, and Y. Ding, *Increased nitric oxide inactivation by reactive oxygen species in lead-induced hypertension.* Kidney Int, 1999. **56**(4): p. 1492-8.
111. Mitry, M.A. and J.G. Edwards, *Doxorubicin induced heart failure: Phenotype and molecular mechanisms.* Int J Cardiol Heart Vasc, 2016. **10**: p. 17-24.
112. Bryant, J., et al., *Clinical and cost-effectiveness of cardioprotection against the toxic effects of anthracyclines given to children with cancer: a systematic review.* Br J Cancer, 2007. **96**(2): p. 226-30.
113. Kremer, L.C., et al., *Frequency and risk factors of anthracycline-induced clinical heart failure in children: a systematic review.* Ann Oncol, 2002. **13**(4): p. 503-12.
114. Schlitt, A., et al., *Cardiotoxicity and oncological treatments.* Dtsch Arztebl Int, 2014. **111**(10): p. 161-8.
115. Floyd, J.D., et al., *Cardiotoxicity of cancer therapy.* J Clin Oncol, 2005. **23**(30): p. 7685-96.
116. Luu, A.Z., et al., *Role of Endothelium in Doxorubicin-Induced Cardiomyopathy.* JACC Basic Transl Sci, 2018. **3**(6): p. 861-870.
117. Bar-Joseph, H., et al., *In vivo bioimaging as a novel strategy to detect doxorubicin-induced damage to gonadal blood vessels.* PLoS One, 2011. **6**(9): p. e23492.
118. Yersal, O., et al., *Arterial Stiffness in Breast Cancer Patients Treated with Anthracycline and Trastuzumab-Based Regimens.* Cardiol Res Pract, 2018. **2018**: p. 5352914.
119. Nagy, L., et al., *A method for detection of doxorubicin-induced cardiotoxicity: Flow-mediated vasodilation of the brachial artery.* Exp Clin Cardiol, 2001. **6**(2): p. 87-92.
120. Bosman, M., et al., *Doxorubicin induces arterial stiffness: A comprehensive in vivo and ex vivo evaluation of vascular toxicity in mice.* Toxicol Lett, 2021. **346**: p. 23-33.
121. Duquaine, D., et al., *Rapid-onset endothelial dysfunction with adriamycin: evidence for a dysfunctional nitric oxide synthase.* Vasc Med, 2003. **8**(2): p. 101-7.
122. Catterall, W.A., *Voltage-gated calcium channels.* Cold Spring Harb Perspect Biol, 2011. **3**(8): p. a003947.
123. Fransen, P., et al., *Contribution of transient and sustained calcium influx, and sensitization to depolarization-induced contractions of the intact mouse aorta.* BMC Physiol, 2012. **12**: p. 9.

124. Brozovich, F.V., et al., *Mechanisms of Vascular Smooth Muscle Contraction and the Basis for Pharmacologic Treatment of Smooth Muscle Disorders.* Pharmacol Rev, 2016. **68**(2): p. 476-532.
125. Neumann-Raizel, H., et al., *2-APB and CBD-Mediated Targeting of Charged Cytotoxic Compounds Into Tumor Cells Suggests the Involvement of TRPV2 Channels.* Front Pharmacol, 2019. **10**: p. 1198.
126. Ghosh, D., et al., *Calcium Channels in Vascular Smooth Muscle.* Adv Pharmacol, 2017. **78**: p. 49-87.
127. Prevarskaya, N., L. Zhang, and G. Barritt, *TRP channels in cancer.* Biochim Biophys Acta, 2007. **1772**(8): p. 937-46.
128. Santoni, G. and V. Farfariello, *TRP channels and cancer: new targets for diagnosis and chemotherapy.* Endocr Metab Immune Disord Drug Targets, 2011. **11**(1): p. 54-67.
129. Fiorio Pla, A. and D. Gkika, *Emerging role of TRP channels in cell migration: from tumor vascularization to metastasis.* Front Physiol, 2013. **4**: p. 311.
130. Chen, J., et al., *Transient receptor potential (TRP) channels, promising potential diagnostic and therapeutic tools for cancer.* Biosci Trends, 2014. **8**(1): p. 1-10.
131. Azimi, I., S.J. Roberts-Thomson, and G.R. Monteith, *Calcium influx pathways in breast cancer: opportunities for pharmacological intervention.* Br J Pharmacol, 2014. **171**(4): p. 945-60.
132. Kosar, P.A., et al., *Synergic Effects of Doxorubicin and Melatonin on Apoptosis and Mitochondrial Oxidative Stress in MCF-7 Breast Cancer Cells: Involvement of TRPV1 Channels.* J Membr Biol, 2016. **249**(1-2): p. 129-40.
133. Earley, S. and J.E. Brayden, *Transient receptor potential channels in the vasculature.* Physiol Rev, 2015. **95**(2): p. 645-90.
134. Iwata, Y., et al., *Novel inhibitor candidates of TRPV2 prevent damage of dystrophic myocytes and ameliorate against dilated cardiomyopathy in a hamster model.* Oncotarget, 2018. **9**(18): p. 14042-14057.
135. Iwata, Y. and T. Matsumura, *Blockade of TRPV2 is a Novel Therapy for Cardiomyopathy in Muscular Dystrophy.* Int J Mol Sci, 2019. **20**(16).

136. Verigos, J., et al., *Transcriptional Profiling of Tumorspheres Reveals TRPM4 as a Novel Stemness Regulator in Breast Cancer.* Biomedicines, 2021. **9**(10).
137. Wynne, B.M., C.W. Chiao, and R.C. Webb, *Vascular Smooth Muscle Cell Signaling Mechanisms for Contraction to Angiotensin II and Endothelin-1.* J Am Soc Hypertens, 2009. **3**(2): p. 84-95.
138. Bhaskaran, S., J. Zaluski, and A. Banes-Berceli, *Molecular interactions of serotonin (5-HT) and endothelin-1 in vascular smooth muscle cells: in vitro and ex vivo analyses.* Am J Physiol Cell Physiol, 2014. **306**(2): p. C143-51.
139. Kotamraju, S., et al., *Doxorubicin-induced apoptosis in endothelial cells and cardiomyocytes is ameliorated by nitrone spin traps and ebselen. Role of reactive oxygen and nitrogen species.* J Biol Chem, 2000. **275**(43): p. 33585-92.
140. Kannan, K. and S.K. Jain, *Oxidative stress and apoptosis.* Pathophysiology, 2000. **7**(3): p. 153-163.
141. Li, J., et al., *Intracellular superoxide induces apoptosis in VSMCs: role of mitochondrial membrane potential, cytochrome C and caspases.* Apoptosis, 2002. **7**(6): p. 511-7.
142. Numaga-Tomita, T., et al., *TRPC6 regulates phenotypic switching of vascular smooth muscle cells through plasma membrane potential-dependent coupling with PTEN.* FASEB J, 2019. **33**(9): p. 9785-9796.
143. Petsophonsakul, P., et al., *Role of Vascular Smooth Muscle Cell Phenotypic Switching and Calcification in Aortic Aneurysm Formation.* Arterioscler Thromb Vasc Biol, 2019. **39**(7): p. 1351-1368.
144. Aston, W.J., et al., *A systematic investigation of the maximum tolerated dose of cytotoxic chemotherapy with and without supportive care in mice.* BMC Cancer, 2017. **17**(1): p. 684.
145. Young, R.C., R.F. Ozols, and C.E. Myers, *The anthracycline antineoplastic drugs.* N Engl J Med, 1981. **305**(3): p. 139-53.
146. Schneider, C., et al., *Time-Dependent Effect of Anthracycline-Based Chemotherapy on Central Arterial*

Stiffness: A Systematic Review and Meta-Analysis. Front Cardiovasc Med, 2022. **9**: p. 873898.
147. Bosman, M., et al., *Doxorubicin Impairs Smooth Muscle Cell Contraction: Novel Insights in Vascular Toxicity.* Int J Mol Sci, 2021. **22**(23).
148. Langer, S.W., *Dexrazoxane for the treatment of chemotherapy-related side effects.* Cancer Manag Res, 2014. **6**: p. 357-63.
149. Capranico, G., et al., *Different patterns of gene expression of topoisomerase II isoforms in differentiated tissues during murine development.* Biochim Biophys Acta, 1992. **1132**(1): p. 43-8.
150. Barpe, D.R., D.D. Rosa, and P.E. Froehlich, *Pharmacokinetic evaluation of doxorubicin plasma levels in normal and overweight patients with breast cancer and simulation of dose adjustment by different indexes of body mass.* Eur J Pharm Sci, 2010. **41**(3-4): p. 458-63.
151. Jirkovsky, E., et al., *Pharmacokinetics of the Cardioprotective Drug Dexrazoxane and Its Active Metabolite ADR-925 with Focus on Cardiomyocytes and the Heart.* J Pharmacol Exp Ther, 2018. **364**(3): p. 433-446.
152. Johnson-Arbor, K. and R. Dubey, *Doxorubicin*, in *StatPearls*. 2022: Treasure Island (FL).
153. Neutel, C.H.G., et al., *High Pulsatile Load Decreases Arterial Stiffness: An ex vivo Study.* Front Physiol, 2021. **12**: p. 741346.
154. Navarro, P., et al., *General statistical framework for quantitative proteomics by stable isotope labeling.* J Proteome Res, 2014. **13**(3): p. 1234-47.
155. Obata, Y., et al., *The Effects of Hemodynamic Changes on Pulse Wave Velocity in Cardiothoracic Surgical Patients.* Biomed Res Int, 2016. **2016**: p. 9640457.
156. Engwall, M.J., et al., *The Effects of Repeat-Dose Doxorubicin on Cardiovascular Functional Endpoints and Biomarkers in the Telemetry-Equipped Cynomolgus Monkey.* Front Cardiovasc Med, 2021. **8**: p. 587149.
157. Fransen, P., et al., *Endothelial function in aorta segments of apolipoprotein E-deficient mice before development of atherosclerotic lesions.* Pflugers Arch, 2008. **455**(5): p. 811-8.

158. Kauser, K., et al., *Role of endogenous nitric oxide in progression of atherosclerosis in apolipoprotein E-deficient mice.* Am J Physiol Heart Circ Physiol, 2000. **278**(5): p. H1679-85.
159. de Mezer, M., et al., *SERPINA3: Stimulator or Inhibitor of Pathological Changes.* Biomedicines, 2023. **11**(1).
160. Hurlimann, J. and G. van Melle, *Prognostic value of serum proteins synthesized by breast carcinoma cells.* Am J Clin Pathol, 1991. **95**(6): p. 835-43.
161. Han, Y., et al., *Combination of plasma biomarkers and clinical data for the detection of sporadic Alzheimer's disease.* Neurosci Lett, 2012. **516**(2): p. 232-6.
162. Boyang, C., et al., *Construction and analysis of heart failure diagnosis model based on random forest and artificial neural network.* Medicine (Baltimore), 2022. **101**(41): p. e31097.
163. Delrue, L., et al., *Circulating SERPINA3 improves prognostic stratification in patients with a de novo or worsened heart failure.* ESC Heart Fail, 2021. **8**(6): p. 4780-4790.
164. Jiang, Y., Y. Zhang, and C. Zhao, *Integrated gene expression pro fi ling analysis reveals SERPINA3, FCN3, FREM1, MNS1 as candidate biomarkers in heart failure and their correlation with immune in fi ltration.* J Thorac Dis, 2022. **14**(4): p. 1106-1119.
165. Li, B., et al., *The Association and Pathogenesis of SERPINA3 in Coronary Artery Disease.* Front Cardiovasc Med, 2021. **8**: p. 756889.
166. Zhao, L., et al., *Circulating Serpina3 levels predict the major adverse cardiac events in patients with myocardial infarction.* Int J Cardiol, 2020. **300**: p. 34-38.
167. Kaur, S., et al., *Thrombospondin-1 inhibits VEGF receptor-2 signaling by disrupting its association with CD47.* J Biol Chem, 2010. **285**(50): p. 38923-32.
168. Chistiakov, D.A., et al., *Thrombospondins: A Role in Cardiovascular Disease.* Int J Mol Sci, 2017. **18**(7).
169. Xia, Y., et al., *Endogenous thrombospondin 1 protects the pressure-overloaded myocardium by modulating fibroblast phenotype and matrix metabolism.* Hypertension, 2011. **58**(5): p. 902-11.

170. Frangogiannis, N.G., et al., *Critical role of endogenous thrombospondin-1 in preventing expansion of healing myocardial infarcts.* Circulation, 2005. **111**(22): p. 2935-42.
171. Moura, R., et al., *Thrombospondin-1 deficiency accelerates atherosclerotic plaque maturation in ApoE-/- mice.* Circ Res, 2008. **103**(10): p. 1181-9.
172. Munoz-Pacheco, P., et al., *Eplerenone enhances cardioprotective effects of standard heart failure therapy through matricellular proteins in hypertensive heart failure.* J Hypertens, 2013. **31**(11): p. 2309-18; discussion 2319.
173. van Almen, G.C., et al., *MicroRNA-18 and microRNA-19 regulate CTGF and TSP-1 expression in age-related heart failure.* Aging Cell, 2011. **10**(5): p. 769-79.
174. Fahndrich, S., et al., *Cardiovascular risk in patients with alpha-1-antitrypsin deficiency.* Respir Res, 2017. **18**(1): p. 171.
175. Mehri, H., et al., *Evaluation of the serum levels of Mannose binding lectin-2, tenascin-C, and total antioxidant capacity in patients with coronary artery disease.* J Clin Lab Anal, 2021. **35**(10): p. e23967.
176. Suthahar, N., et al., *Galectin-3 Activation and Inhibition in Heart Failure and Cardiovascular Disease: An Update.* Theranostics, 2018. **8**(3): p. 593-609.
177. Meiners, B., C. Shenoy, and B.N. Zordoky, *Clinical and preclinical evidence of sex-related differences in anthracycline-induced cardiotoxicity.* Biol Sex Differ, 2018. **9**(1): p. 38.
178. Norton, N., et al., *Trpc6 Promotes Doxorubicin-Induced Cardiomyopathy in Male Mice With Pleiotropic Differences Between Males and Females.* Front Cardiovasc Med, 2021. **8**: p. 757784.
179. Moulin, M., et al., *Sexual dimorphism of doxorubicin-mediated cardiotoxicity: potential role of energy metabolism remodeling.* Circ Heart Fail, 2015. **8**(1): p. 98-108.
180. Nebigil, C.G. and L. Desaubry, *Updates in Anthracycline-Mediated Cardiotoxicity.* Front Pharmacol, 2018. **9**: p. 1262.
181. Sawyer, D.B., *Anthracyclines and heart failure.* N Engl J Med, 2013. **368**(12): p. 1154-6.

182. Lusis, A.J., *Atherosclerosis.* Nature, 2000. **407**(6801): p. 233-41.
183. Hansson, G.K., *Inflammation, atherosclerosis, and coronary artery disease.* N Engl J Med, 2005. **352**(16): p. 1685-95.
184. Rubbo, H., et al., *Interactions of nitric oxide and peroxynitrite with low-density lipoprotein.* Biol Chem, 2002. **383**(3-4): p. 547-52.
185. Endres, M., et al., *Stroke protection by 3-hydroxy-3-methylglutaryl (HMG)-CoA reductase inhibitors mediated by endothelial nitric oxide synthase.* Proc Natl Acad Sci U S A, 1998. **95**(15): p. 8880-5.
186. Steinberg, D. and J.L. Witztum, *Is the oxidative modification hypothesis relevant to human atherosclerosis? Do the antioxidant trials conducted to date refute the hypothesis?* Circulation, 2002. **105**(17): p. 2107-11.
187. Palombo, C. and M. Kozakova, *Arterial stiffness, atherosclerosis and cardiovascular risk: Pathophysiologic mechanisms and emerging clinical indications.* Vascul Pharmacol, 2016. **77**: p. 1-7.
188. van Popele, N.M., et al., *Association between arterial stiffness and atherosclerosis: the Rotterdam Study.* Stroke, 2001. **32**(2): p. 454-60.
189. Ko, K.A., et al., *Developing a Reliable Mouse Model for Cancer Therapy-Induced Cardiovascular Toxicity in Cancer Patients and Survivors.* Front Cardiovasc Med, 2018. **5**: p. 26.
190. Marek, I., et al., *Sex differences in the development of vascular and renal lesions in mice with a simultaneous deficiency of Apoe and the integrin chain Itga8.* Biol Sex Differ, 2017. **8**: p. 19.
191. Caligiuri, G., et al., *Effects of sex and age on atherosclerosis and autoimmunity in apoE-deficient mice.* Atherosclerosis, 1999. **145**(2): p. 301-8.
192. Man, J.J., J.A. Beckman, and I.Z. Jaffe, *Sex as a Biological Variable in Atherosclerosis.* Circ Res, 2020. **126**(9): p. 1297-1319.
193. Roth, L., et al., *Acetylsalicylic Acid Reduces Passive Aortic Wall Stiffness and Cardiovascular Remodelling in a Mouse*

Model of Advanced Atherosclerosis. Int J Mol Sci, 2021. **23**(1).
194. Roth, L., et al., *Cholesterol-independent effects of atorvastatin prevent cardiovascular morbidity and mortality in a mouse model of atherosclerotic plaque rupture.* Vascul Pharmacol, 2016. **80**: p. 50-8.
195. Budinskaya, K., et al., *Non-invasive assessment of vascular system function and damage induced by anthracycline treatment in the pediatric cancer survivors.* Physiol Res, 2017. **66**(Suppl 4): p. S553-S560.
196. Jenei, Z., et al., *Anthracycline causes impaired vascular endothelial function and aortic stiffness in long term survivors of childhood cancer.* Pathol Oncol Res, 2013. **19**(3): p. 375-83.
197. Fortier, C. and M. Agharazii, *Arterial Stiffness Gradient.* Pulse (Basel), 2016. **3**(3-4): p. 159-66.
198. Lopez-Dee, Z., K. Pidcock, and L.S. Gutierrez, *Thrombospondin-1: multiple paths to inflammation.* Mediators Inflamm, 2011. **2011**: p. 296069.
199. Tabary, M., et al., *The matricellular protein thrombospondin-1 in lung inflammation and injury.* Am J Physiol Cell Physiol, 2022. **323**(3): p. C857-C865.
200. Soman, A. and S. Asha Nair, *Unfolding the cascade of SERPINA3: Inflammation to cancer.* Biochim Biophys Acta Rev Cancer, 2022. **1877**(5): p. 188760.
201. Castellon, X. and V. Bogdanova, *Chronic Inflammatory Diseases and Endothelial Dysfunction.* Aging Dis, 2016. **7**(1): p. 81-9.
202. Mozos, I., et al., *Inflammatory Markers for Arterial Stiffness in Cardiovascular Diseases.* Front Immunol, 2017. **8**: p. 1058.
203. Chiesa, S.T., et al., *Glycoprotein Acetyls: A Novel Inflammatory Biomarker of Early Cardiovascular Risk in the Young.* J Am Heart Assoc, 2022. **11**(4): p. e024380.
204. Yu, S. and C.M. McEniery, *Central Versus Peripheral Artery Stiffening and Cardiovascular Risk.* Arterioscler Thromb Vasc Biol, 2020. **40**(5): p. 1028-1033.
205. Scott, J.M., et al., *Exercise Therapy and Cardiovascular Toxicity in Cancer.* Circulation, 2018. **137**(11): p. 1176-1191.

206. El Assar, M., et al., *Effect of Physical Activity/Exercise on Oxidative Stress and Inflammation in Muscle and Vascular Aging.* Int J Mol Sci, 2022. **23**(15).
207. Kozakova, M. and C. Palombo, *Vascular Ageing and Aerobic Exercise.* Int J Environ Res Public Health, 2021. **18**(20).
208. Campeau, M.A. and R.L. Leask, *Empagliflozin mitigates endothelial inflammation and attenuates endoplasmic reticulum stress signaling caused by sustained glycocalyx disruption.* Sci Rep, 2022. **12**(1): p. 12681.
209. Rossman, M.J., et al., *Chronic Supplementation With a Mitochondrial Antioxidant (MitoQ) Improves Vascular Function in Healthy Older Adults.* Hypertension, 2018. **71**(6): p. 1056-1063.
210. Brown, N.J. and D.E. Vaughan, *Angiotensin-converting enzyme inhibitors.* Circulation, 1998. **97**(14): p. 1411-20.
211. Ward, N.C., G.F. Watts, and R.H. Eckel, *Statin Toxicity.* Circ Res, 2019. **124**(2): p. 328-350.
212. Florescu, M., et al., *Taxanes-induced cardiotoxicity is related to increased arterial stiffness and oxidative stress.* European Heart Journal, 2013. **34**(suppl_1).
213. Stelwagen, J., et al., *Vascular aging in long-term survivors of testicular cancer more than 20 years after treatment with cisplatin-based chemotherapy.* Br J Cancer, 2020. **123**(11): p. 1599-1607.
214. Veronese, M.L., et al., *Mechanisms of hypertension associated with BAY 43-9006.* J Clin Oncol, 2006. **24**(9): p. 1363-9.
215. Maki-Petaja, K.M., et al., *Mechanisms Underlying Vascular Endothelial Growth Factor Receptor Inhibition-Induced Hypertension: The HYPAZ Trial.* Hypertension, 2021. **77**(5): p. 1591-1599.
216. Dockery, F., et al., *Effect of androgen suppression compared with androgen receptor blockade on arterial stiffness in men with prostate cancer.* J Androl, 2009. **30**(4): p. 410-5.
217. Vassilakopoulou, M., et al., *Paclitaxel chemotherapy and vascular toxicity as assessed by flow-mediated and nitrate-mediated vasodilatation.* Vascul Pharmacol, 2010. **53**(3-4): p. 115-21.

218. Cameron, A.C., et al., *Comprehensive Characterization of the Vascular Effects of Cisplatin-Based Chemotherapy in Patients With Testicular Cancer.* JACC CardioOncol, 2020. **2**(3): p. 443-455.
219. Steeghs, N., et al., *Hypertension and rarefaction during treatment with telatinib, a small molecule angiogenesis inhibitor.* Clin Cancer Res, 2008. **14**(11): p. 3470-6.
220. Steeghs, N., et al., *Reversibility of capillary density after discontinuation of bevacizumab treatment.* Ann Oncol, 2010. **21**(5): p. 1100-5.
221. Sen, F., et al., *Impaired coronary flow reserve in metastatic cancer patients treated with sunitinib.* J BUON, 2013. **18**(3): p. 775-81.
222. Favere, K., et al., *Cardiac electrophysiology studies in mice via the transjugular route: a comprehensive practical guide.* Am J Physiol Heart Circ Physiol, 2022. **323**(4): p. H763-H773.
223. Favere, K., et al., *A systematic literature review on the effects of exercise on human Toll-like receptor expression.* Exerc Immunol Rev, 2021. **27**: p. 84-124.
224. Favere, K., et al., *Toll-Like Receptors: Are They Taking a Toll on the Heart in Viral Myocarditis?* Viruses, 2021. **13**(6).
225. De Backer, J., et al., *A reliable set of reference genes to normalize oxygen-dependent cytoglobin gene expression levels in melanoma.* Sci Rep, 2021. **11**(1): p. 10879.